

KU Leuven
Biomedical Sciences Group
Faculty of Medicine
Department of Imaging and Pathology



Joint PhD with the University of Milano Bicocca
Faculty of medicine
DIMET



THE LOCAL IMMUNE RESPONSE IN MELANOMA

IN SITU ANALYSIS OF THE MICRO-ENVIRONMENTAL IMMUNE
SIGNATURE OF PRIMARY MELANOMA

Francesca Maria Bosisio

Jury:

Promotor: Prof. Dr. Joost van den Oord

Co-promotor: Dr. Nicolas van Baren

Co-promotor: Prof. Dr. Cattoretti Giorgio

Co-promotor: Dr. Jasper Wouters

Chair: Prof. Dr. Tania Roskams

Secretary: Prof. Patrick Matthys

Jury members: Prof. Dr. Lorenzo Cerroni

Prof. Dr. Biagio Eugenio Leone

Prof. Patrizia Agostinis

Prof. Dr. Fulvio Magni

Dissertation presented in
partial fulfilment of the
requirements for the
degree of Doctor in
Biomedical Sciences

To Marco,
Because if you didn't let me go
and continuously supported
firmly believeing in me during this years,
I would not have been here today.

Inhoudsopgave

List of abbreviations	5
SUMMARY	9
SAMENVATTING	10
INTRODUCTION - IMMUNOPLASTICITY IN CUTANEOUS MELANOMA: BEYOND PURE MORPHOLOGY	11
.....	12
Tumor Infiltrating Lymphocytes [TILs] and TILs patterns in melanoma	12
Limitations in the assessment of the anti-tumor response in melanoma	17
The “brisk” pattern: evidence of a successful immune response?	20
The “non brisk” pattern: spatial heterogeneity and partial failure of the immune response?	21
The “absent” pattern: ignorance by the immune system and complete failure of the immune response?	23
Conclusion: the need for a refinement of the TILs patterns in melanoma	23
References	24
AIMS	34
CHAPTER I - PLASMA CELLS IN PRIMARY MELANOMA. PROGNOSTIC SIGNIFICANCE AND POSSIBLE ROLE OF IGA	35
.....	36
Abstract	36
Introduction.....	37
Materials and methods	37
Evaluation of cases	37
Immunohistochemistry	38
Gene Scan Analysis	40
Statistical analysis.....	40
Results	40
Clinico-pathological features of PC+ melanomas.....	40
Immunohistochemical features of PC+ melanomas.....	45
Molecular analysis of Ig genes expressed by PC+ melanomas.....	45
Analysis of lymph nodes draining PC+ melanomas	48
Outcome of patients with PC+ melanomas.....	48
Discussion	52
References	55
CHAPTER II – ABERRANT HLA-DR EXPRESSION IN MELANOMA TISSUE: HINTS AT A GERMINAL CENTER- LIKE INFLAMMATORY MICROENVIRONMENT	59
References.....	70

CHAPTER III – TILS HIGH-DIMENSIONAL “IN SITU” SINGLE CELL-ANALYSIS OF TUMOUR INFILTRATING LYMPHOCYTES IN PRIMARY MELANOMA USING MULTIPLEX IMMUNOSTAINING ON TISSUE SECTIONS..	73
Material and methods	76
Patients.....	76
TMA construction	76
Multiplex-Stripping Immunofluorescence.....	76
Image Pre-processing	76
Image Analysis	78
Laser Microdissection.....	79
qPCR of laser microdissected samples	79
Shotgun Proteomics of laser microdissected samples	80
Pathways Analysis.....	81
Results	81
Functional analysis of TILs at tissue-based single cell level.....	81
Association of the TILs activation status with brisk/non-brisk status, regression and other histopathological prognostic parameters.....	84
Study of the inflammatory microenvironment associated with activation and exhaustion: cluster analysis	87
Study of the inflammatory microenvironment associated with activation and exhaustion: neighborhood analysis.....	92
Validation of the functional subclassification of the brisk/non-brisk categories using qPCR and proteomics on microdissected TILs from melanoma metastases.....	96
Discussion	98
References.....	102
Supplementary materials	105
DISCUSSION AND FUTURE PERSPECTIVES.....	111
References.....	117
ACKNOWLEDGEMENT, PERSONAL CONTRIBUTION AND CONFLICT OF INTEREST	120
Personal contribution	120
Conflict of interest statement	120
Scientific acknowledgements	120
Personal acknowledgement	122
CURRICULUM VITAE	125

List of abbreviations

ABC	Ammonium Bicarbonate
AIPL1	Aryl Hydrocarbon Receptor Interacting Protein Like 1
ANOVA	One-way Analysis of Variance
BAFFR	B cell-activating factor receptor
BC	B cells
BCR	B-cell receptor
BDCA	Blood dendritic cell antigen
Blimp1	B lymphocyte-induced maturation protein-1
BTLA	B- and T-lymphocyte attenuator
CCL	chemokine [C-C motif] ligand
CCR	C-C chemokine receptor
CD	cluster of differentiation
cDC	classical dendritic cells
MAF	musculoaponeurotic fibrosarcoma oncogene
CRTAM	MHC I-restricted T cell-associated molecule
CSF	colony stimulating factor
CTLA-4	cytotoxic T lymphocyte antigen 4
CXCL	C-X-C Motif Chemokine Ligand
CORO1A	Coronin-1A
CytoF	cytometry Time Of Flight
DARC	Duffy antigen/chemokine receptor
DAVID	Database for Annotation, Visualization and Integrated Discovery
DC	dendritic cells
DCLAMP	DC-Lysosome-Associated Membrane protein
DTT	dithiothreitol
DENND1C	DENN Domain Containing 1C
DNA	Deoxyribonucleic acid
DNAM-1	DNAX Accessory Molecule-1
ELISA	enzyme-linked immunosorbent assay
ETS	E26 transformation-specific
FAT3	FAT atypical cadherin 3

FBXL21	F-Box And Leucine Rich Repeat Protein 21
FDA	Food and drug administration
FF	Fresh frozen
FFPE	Formalin fixed paraffin embedded
FHT	Follicular helper T cells
FOXP3	forkhead box P3
GBP1	Guanylate Binding Protein 1
GITR	glucocorticoid-induced TNFR-related protein
GSEA	Gene Set Enrichment Analysis
HC	Hierarchical Clustering
HEV	high endothelial venules
HLA	human leucocyte antigen
IAA	Iodoacetamide
ICOS	Inducible T-cell COStimulator
IFN	interferon
Ig	immunoglobulin
IGF2	Insulin-like growth factor 2
IL	interleukin
ILC	Innate Lymphoid Cells
ITK	IL2 Inducible T Cell Kinase
LAG3	lymphocyte-activation gene
Lang	Langerhans cells
LDA	Linear Discriminant Analysis
LILRB2	Leukocyte Immunoglobulin Like Receptor B2
LMM	Lentigo Maligna Melanoma
LT β R	Lymphotoxin Beta Receptor
MAGEA3	melanoma antigen family A, 3
MHC	major histocompatibility complex
MICA/B	Major histocompatibility complex class I-related chain A/B
MITF	microftalmia transcription factor
MMP	matrix metalloproteinasi
MNDA	Myeloid Cell Nuclear Differentiation Antigen
MX1	Interferon-induced GTP-binding protein Mx1

MZB1	Marginal zone B and B1 cell-specific protein
NFIC	Nuclear Factor I C
NFKB	Nuclear Factor K B
NGS	Next Generation Sequencing
NK	Natural Killer
NKG2D	Natural Killer Group 2D
NMM	Nodular Malignant Melanoma
OCM2	Oncomodulin 2
PBS	Phosphate-buffered saline
PC	plasma cells
PCA	Principal Component Analysis
PCDHA9	Protocadherin Alpha 9
PD	programmed death
pDC	plasmacytoid dendritic cells
PD-L	programmed death ligand
PNAD	peripheral nodal addressin
PNPLA1	Patatin Like Phospholipase Domain Containing 1
pSTAT1	Signal Transducer And Activator Of Transcription 1
PTPRCAP	Protein Tyrosine Phosphatase, Receptor Type C Associated Protein
QC	Quality Control
RARRES2	Retinoic Acid Receptor Responder 2
RBP-J	Recombination Signal Binding Protein For Immunoglobulin Kappa J Region
RNA	ribonucleic acid
RT-PCR	real time polymerase chain reaction
SELPLG	Selectin P Ligand
Sema7A	semaphorin 7A
SH2D1A	SH2 domain-containing protein 1A
SLO	secondary lymphoid structures
SOX2	SRY-Box 2
SSMM	Superficial Spreading Malignant Melanoma
STRA6	Stimulated By Retinoic Acid 6
STRING	Search Tool for the Retrieval of Interacting Genes/Proteins
TAMs	tumor-associated macrophages

TCF4	Transcription Factor 4
TCGA	The Cancer Genome Atlas
TCM	T cell memory
TCR	T-cell receptor
Tcy	cytotoxic T cells
TGF	transforming growth factor
Th	T helpers
TKTL1	Transketolase Like 1
TIGIT	T-cell immunoreceptor with Ig and ITIM domains
TILs	tumor infiltrating lymphocytes
TIM3	T-cell immunoglobulin domain and mucin domain
TLO	tertiary lymphoid structures
TMA	Tissue Micro-array
TNF	Tumor necrosis factor
TNFR	Tumor necrosis factor receptor
TNFRSF25	TNF Receptor Superfamily Member 25
Treg	regulatory T cells
TRGC2	T Cell Receptor Gamma Constant 2
tSNE	t-Distributed Stochastic Neighbour Embedding
TUBA4A	Tubulin Alpha 4a
ULBP2	UL16 Binding Protein 2
VISTA	V-Set Immunoregulatory Receptor
Webgestalt	WEB-based GENE SeT Analysis Toolkit
ZNF	Zinc-finger

SUMMARY

In the new landscape of immunotherapies, the local microenvironment of melanoma needs to be explored and clarified in order to identify predictive biomarkers of response. In fact, not all the patients respond to checkpoint inhibition and there is the need to identify those patients that will respond in order to avoid unnecessary treatments and potential adverse effects. In order to lay the basis for a personalized therapy, we need a thorough understanding of the complexity of the local immune response. In this thesis, we first explored singularly determined types of inflammatory populations, and in particular we chose two less known actors of the inflammatory microenvironment, i.e. plasma cells and melanophages. We observed that aggregates of plasma cells in the surroundings of primary melanoma has a negative impact on prognosis and survival. We hypothesize that this effect may be mediated by an isotypeswitch toward an IgA-producing plasma cell type, to which immune-suppressive properties has been ascribed in the literature. Subsequently, we moved from the study of inflammatory subpopulations to the study of the whole microenvironment, in particular the areas of aberrant HLA-DR-expression by melanoma cells. The significance of this feature is controversial in the literature but may be important for the response to immunotherapy. Here we find with a multi-omics approach (expressomics and proteomics) that the microenvironment in HLA-DR-positive areas resembles the milieu of a germinal center, with a possible impairment of the recirculation of the inflammatory cells between the tumoral site and the lymph nodes, thereby favouring exhaustion due to chronic stimulation. Finally, we abandoned bulk-analysis approaches in favour of a single cells-analysis approach which allowed us to obtain a high resolution landscape of the tumor microenvironment in melanoma. We applied a high throughput multiplex immunostaining technique in order to study the activation status of Tumor Infiltrating Lymphocytes (TILs). In this way, we not only performed a functional investigation of the “brisk” and “non-brisk” morphological categories, but we also used neighbourhood analysis in order to highlight meaningful interactions between TILs and other inflammatory cells that may play a role in TILs activation. Moreover, we found that late regression in melanoma is associated with TILs activation. In conclusion, this doctoral work attempts to shed a light on some of the previously less clarified components of the inflammatory microenvironment in melanoma and implements in practice a high throughput single cells-analysis method that allows a multiparametric immunological study on tissue sections, suitable for future applications in the clinic for prediction of response to immunotherapy.

SAMENVATTING

In het perspectief van de nieuwe vormen van immunotherapie, is het van het grootste belang om het lokale micro-milieu van het cutane maligne melanoom te onderzoeken en op te helderen teneinde predictieve biomarkers die wijzen op respons, te identificeren. Inderdaad, lang niet alle patiënten antwoorden op behandeling met “checkpoint” blokkeerders en er is duidelijk behoefte aan de identificatie van patiënten die zullen antwoorden op de therapie, teneinde nodeloze behandeling en mogelijke nevenwerkingen te voorkomen. Om de basis te leggen voor “gepersonaliseerde” therapie moeten we de complexiteit van de lokale immuun respons goed begrijpen. In deze thesis, hebben we eerst enkele welbepaalde inflammatoire types van cellen bestudeerd, met name plasma cellen en melanofagen, twee weinig bestudeerde actoren in het lokale inflammatoire micro-milieu. We zagen dat clusters van plasma cellen in de directe nabijheid van primaire melanomen een negatieve impact hadden op prognose en overleving. We veronderstellen dat dit effect veroorzaakt wordt door een “isotype switch” naar een IgA-producerend plasma cel type, waaraan in de literatuur immuun-suppressieve eigenschappen zijn toegeschreven. Vervolgens verlieten we de studie van inflammatoire subpopulaties, en bestudeerden we het gehele micromilieu, met name de gebieden van aberrante HLA-DR-expressie door melanoma cellen. Met behulp van een multi-omics benadering (expressomics en proteomics) vonden we dat het micro-milieu van HLA-DR positieve tumorgebieden gelijk op het milieu van een germinatief centrum, met een mogelijke belemmering van de recirculatie van ontstekingscellen tussen de oorspronkelijke tumor en de lymfeklieren, hetgeen zou kunnen leiden tot “uitputting” (exhaustion) als gevolg van chronische stimulatie. Tenslotte verlieten we de “bulk” analyse voor een multiplex analyse van afzonderlijke cellen hetgeen ons toeliet een “hoge resolutie overzicht” te verkrijgen van het tumor micromilieu in het primair cutaan maligne melanoom. Hierbij pasten we een “high throughput” multiplex immunohistochemische techniek toe teneinde de activatie status van Tumor Infiltrerende Lymfocyten (TILs) na te gaan. Dit liet ons niet alleen toe de morfologische categorieën “brisk” en “non-brisk” functioneel te onderzoeken, maar we konden via “neighbourhood analysis” ook de betekenisvolle interacties blootleggen tussen TILs enerzijds, en andere inflammatoire cellen die mogelijk een rol spelen in de activatie van TILs. Bovendien konden we aantonen dat late stadia van spontane regressie in melanomen geassocieerd zijn met TILs activatie. Samenvattend poogt dit doctoraatswerk licht te werpen op enkele, voorheen duistere, aspecten van het inflammatoir micro-milieu in melanoom en implementeert een “high throughput” multiplex method voor de analyse van afzonderlijke cellen in weefselcoupes; toepassing van deze methode in de praktijk laat hopelijk toe om via een multiparametrische immunologische study meer nauwgezet de het antwoord op immunotherapie te voorspellen.

PUBLISHED

Immunoplasticity in cutaneous melanoma: beyond pure morphology

Francesca Maria Bosisio^{1,2} · Joost J. van den Oord¹

¹ Laboratory of Translational Cell and Tissue Research, KUL, Minderbroederstraat 19, 3000 Leuven, Belgium

² Università degli studi di Milano-Bicocca, Milan, Italy

Tumor Infiltrating Lymphocytes [TILs] and TILs patterns in melanoma

Melanoma is one of the most antigenic tumors, which is reflected by the occurrence of partial or complete regression and the success of immune-mediated therapies, but on the other hand it also has an enhanced ability to escape the immune response. The high antigenicity is derived from an elevated mutational burden [1], accounting for ~30,000 mutations for melanomas arising in intermittently UV-exposed skin, ~100,000 in chronically UV-exposed areas and <1,000 in melanomas arising at unexposed sites [2]. This high mutational burden favors the genesis of an increased number of neoantigens, a class of antigens strictly produced during tumoral progression. Neoantigens possess higher immunogenic efficacy and can trigger more powerful immune reactions than antigens that are also expressed in non-tumoral tissues, because the latter will interact at low avidity with immune cells due to tolerogenic mechanisms [3]. In spite of this high antigenicity, the phenomenon of immune-mediated complete regression of melanoma is rare [12.4%], whereas partial regression occurs much more frequently [23-58%] suggesting the onset of mechanisms of immune escape that allow the tumor to resist the immune attack [4]. Two of the major mechanisms of immune escape are immune editing and immune modulation [Figure 1]. Immune editing is based on the recognition of highly antigenic tumor proteins and killing of the melanoma cells that bear these antigens by TILs favoring the selection of less antigenic clones that can escape the immune attack. Histologically, this phenomenon will appear as a new clone of melanoma cells without associated lymphocytes that arises within or at the border of a melanoma that does harbor TILs. Immune modulation is the ability of melanoma cells to influence [and downregulate] the anti-tumor response through several mechanisms. These mechanisms can be present already during early tumor progression phases, resulting in a melanoma that is morphologically devoid of inflammatory cells, or arise at some point during tumor progression. In primary cutaneous melanoma, the invasive radial growth phase [which marks the onset of invasion] is usually accompanied by a dense mononuclear infiltrate and many early invasive melanoma cells will presumably be destroyed by the immune system at this stage; however, during the vertical growth phase, a dense, “brisk” infiltrate is rather uncommon and most melanomas present with a focal, “non-brisk” type of response. Hence, immune modulation is a dynamic process that varies during melanoma progression, in part due to the process of immune editing as well. Therefore, even in the presence of inflammatory cells in the tumor environment, their functional status can be altered by the process of immune modulation and result in a melanoma devoid of inflammation during its progression. This dynamical perspective of the tumor-associated inflammatory subpopulations was defined as the “immunome” and explored by Bindea et al in colon cancer [5].

The easiest way to assess the anti-tumor immune response is by evaluating TILs on a simple hematoxylin-eosin staining. In melanoma, not only the presence of TILs is evaluated, but also their pattern of topographical arrangement in and around the tumor. The classical patterns of TILs are: a “brisk” infiltrate, when TILs are present diffusely all over the tumor area [diffuse variant] or all along the periphery of the tumor [peripheral variant] [Figure 2]; a “non brisk” infiltrate, when tumoral areas with associated TILs alternate with tumoral areas without TILs infiltration; and an “absent” infiltrate, when the TILs are totally absent or are present in the peritumoral area, without evident contact with the melanoma cells [6] [Fig3]. It has been known since more than 20 years that these patterns are an independent prognostic factor both in primary and metastatic melanoma [7, 8]. The density and distribution of the TILs infiltration is also an independent predictor of the sentinel lymph node [SLN] status, with a lower number of TILs being associated with the presence of SLN metastasis [9]. In other cancers however, e.g. colon cancer, the distribution of the TILs in addition to their quantifications has been included as a relevant parameter only since 10 years [10].

Although the prognostic value of the patterns and density of TILs is still under debate, the introduction of immunotherapy has renewed the interest in TILs and has coined the question whether the TILs pattern and/or the composition of the tumor-associated inflammatory infiltrate could be an additional piece of information to predict which patient would show response to immunotherapy. First to be approved by the FDA in 2011 for the treatment of stage IV melanoma, ipilimumab targets the cytotoxic T lymphocyte antigen 4 [CTLA-4]. The immune checkpoint CTLA-4 plays a role in the early, afferent phase of the immune response: expressed by the activated T lymphocyte, it delivers an inhibitory signal after interaction with CD80, an inhibitory co-signalling molecule that is expressed by antigen-presenting cells [11]. Second in the timeline of approval for clinical use were the PD-1 inhibitors pembrolizumab and nivolumab. PD-1 is a checkpoint molecule expressed by the activated T lymphocyte in the second, effector phase of the anti-tumor response, when the T cell encounters the melanoma cell in order to eliminate it. The two main ligands are PD-L1 and PD-L2, and they can be expressed both by other inflammatory cells as well as by the melanoma cells themselves. Drugs directed against PD-L1 are available as well and one of these, Atezolizumab [MPDL3280A], recently entered the clinic, but the problem in targeting only PD-L1 is that the signal can still be initiated through PD-L2. [12] The response rates for these drugs are promising: 10-15% for ipilimumab [13], 33% for pembrolizumab [14], and 40% for nivolumab [15]. Since the generation of activated anti-tumor T-cells takes time, immunotherapies in comparison with targeted therapies have a slower onset, but definitely last longer in time and may exceptionally “cure” the patient. Therefore, growing evidence is now supporting the use of immune checkpoint inhibitors in combination with other immunotherapies or targeted therapies to improve the response rate and to keep the patient on a durable remission or on a stable disease [16][17][18]. Though, from an economic point of view these are costly therapies, and moreover they are burdened with serious adverse effects. [13] Therefore, markers to predict which patient will respond to this therapeutical approach are urgently needed. The topographical pattern, density or cellular composition of the immune infiltrate can be one of these markers [19]. In addition, since the “immunome”, as stated above, is a dynamic concept with changes over time and space in melanoma evolution, the changing composition of the infiltrate at different moments and in relation to different schedules and combinations of immunotherapy could explain the eventual onset of loss of effectiveness/resistance. In this review, we will discuss on immune modulation and immune editing in melanoma in relation to the different TILs patterns, and the need for a global evaluation of the immune infiltrate in melanoma.

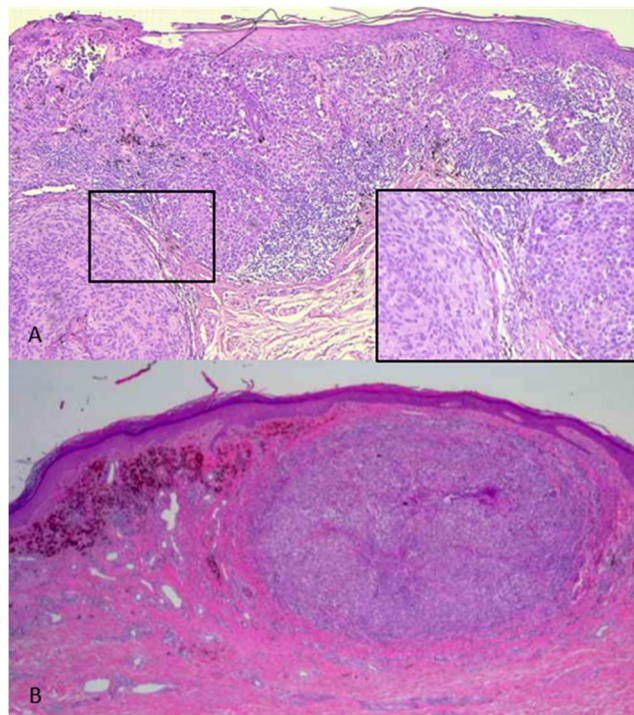
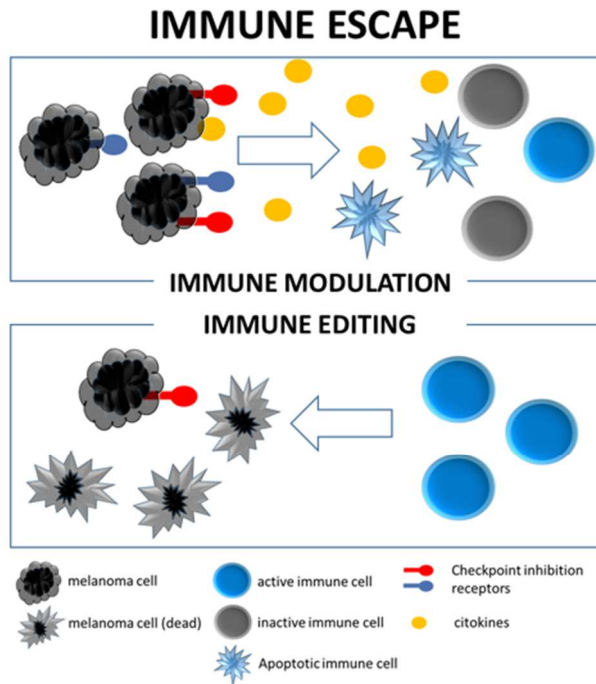


Fig 1 In the schematic image on top, a visual resume of the two main components of immune escape as described in the text, are depicted. The histological figures represent morphologic clues of an ongoing process of “immune modulation” and “immune editing”. A. Coexistence in the same melanoma of nodules with diffuse TILs infiltration (right), undergoing immune attack, and one nodule without TILs (left), escaping the immune surveillance; the rectangle shows a magnification of the two nodules for comparison (H&E, x50). B. Loss of HLA class I molecules (not shown) could have favoured an immune escaping clone, resulting in a solitary expanding nodule next to a superficial area of late regression, suggesting that immune editing of the tumor happened in this case (H&E, x25).

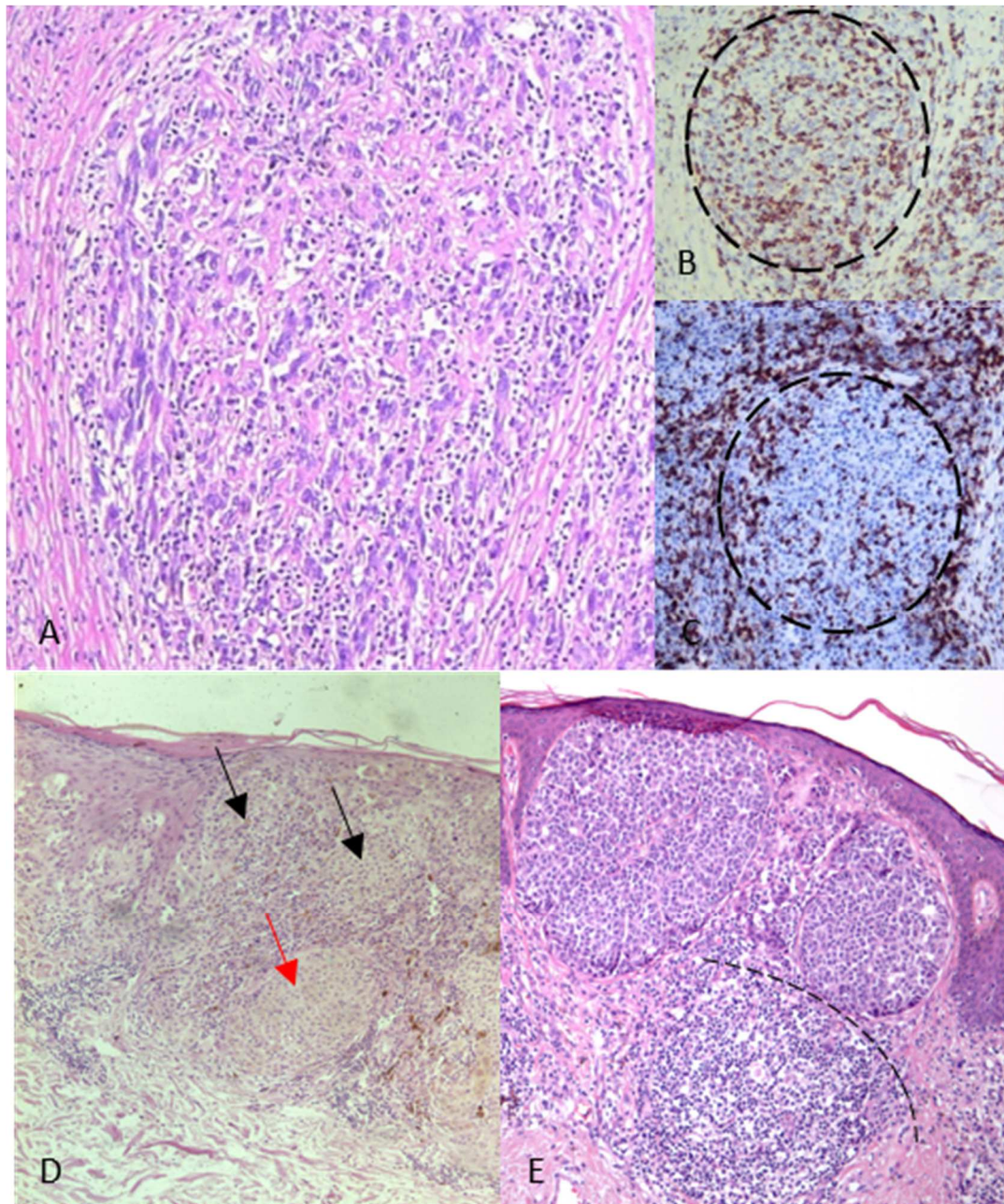


Fig 2 Differences in the “brisk” pattern. A. Melanoma nodule with a diffuse infiltration of TILs, the so-called “diffuse brisk” pattern. (H&E, x100) B-C. Comparison between the “diffuse” and “peripheral” brisk patterns. CD8 stainings on the previously shown nodule (B) with a “diffuse brisk” pattern and on another nodule (C) with a “peripheral brisk” pattern (melanoma nodules bordered by discontinuous line).

The “non-brisk” and the “absent” patterns. D. In this non-brisk primary cutaneous melanoma, two nodules are diffusely infiltrated by TILs (black arrows) while a third nodule is not (red arrow) E. In this case, despite the presence of many lymphocytes in the surrounding stroma, no TILs were found in contact and infiltrating the melanoma nodules, thus defining an “absent” type of TILs infiltration (discontinuous line marking the border between lymphoid nodules and melanoma nodules).

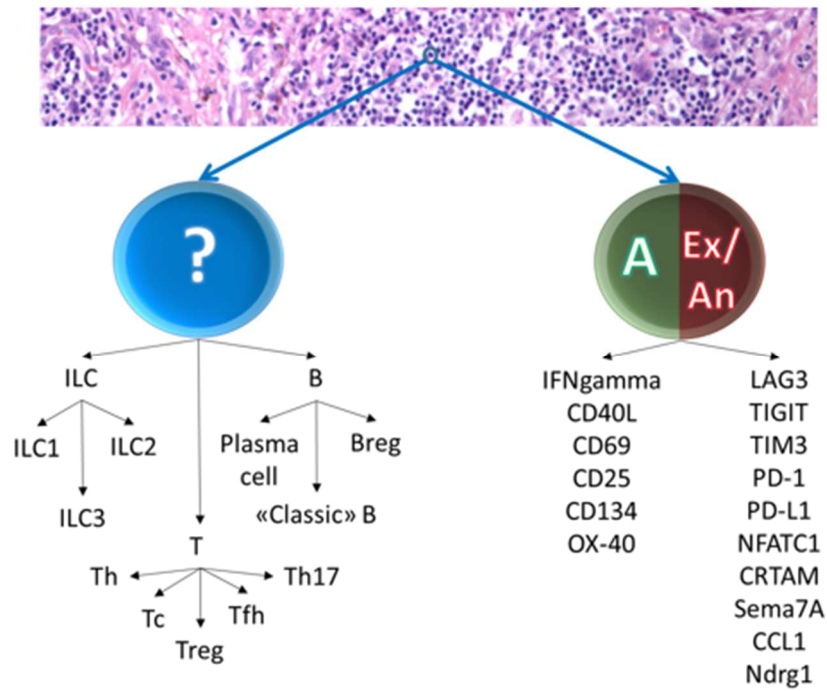


Fig 3 Two major limitations of the morphological evaluation of the TILs. On the left, a small mononuclear cell with scant cytoplasm can belong to various, immunologically different, cell types, each with a particular effect on tumor progression. ILC: innate lymphoid cell; Breg: regulatory B cell; Th: T helper; Tc: T cytotoxic; Treg: regulatory T cell; Tfh: T follicular helper. On the right, lymphocytes in the tumor microenvironment can be in different activation status, ranging from active (left row of markers) to exhausted/anergic (right row of markers), and the balance between markers of exhaustion and activation must be evaluated to define the status of the single lymphocyte.

Limitations in the assessment of the anti-tumor response in melanoma

One major limitation of the morphological evaluation of the inflammatory infiltrate into brisk, non-brisk and absent patterns is the fact that it is focused on small mononuclear cells with rounded nucleus and scant cytoplasm, i.e. lymphocytes. These cells could represent different subtypes of T cells, B cells, or Innate Lymphoid Cells [ILC] [Figure 3]. Despite their morphological similarity, all these subtypes of cells have different impact on the immune response. ILC constitute a subset of lymphocytes derived from the common lymphoid precursor and are characterized by the lack of cell line markers [i.e. they do not express the T-cell receptor or TCR, the rearranged B-cell receptor or BCR, myeloid markers or dendritic cells markers]. Based on the cytokines produced, they are further divided into ILC1, producing IFN-gamma; ILC2, producing IL-5 and IL-13; and ILC3, producing IL-17 or IL-22. ILC1 have a role in stimulating the immune response [20], while the role of ILC3 is still uncertain, with some evidence indicating either a role in immune tolerance [21, 22] or for participation in a successful immune response [23, 24]. Natural Killer [NK] cells belongs to the ILC1 group and they have a positive effect on the immune response. They are able to kill both senescent cancer cells and cancer-initiating cells [25, 26], to induce dendritic cell [DC] maturation through cytokines secretion, thereby stimulating antigen presentation [27], and they also play a role in preventing the development of hematogenous metastasis by eliminating circulating tumor cells [28]. However, NK cells are usually scarce in number and show decreased activity in the microenvironment of solid tumors. Moreover, resistance mechanisms to escape from NK-mediated tumor cell killing have been found: MHC I-negative cancers, particularly susceptible for killing by NK cells, can protect themselves by the release of ligands for the NK receptor NKG2D, thereby reducing its efficacy in recognizing cancer cells. [29, 30] B lymphocytes have a controversial role in tumor biology. On the one hand, they may act as antigen presenting cells, and enhance the T cell and macrophage response through cytokines, chemokines and immunoglobulins [31]. High expression of BCR in melanoma has indeed been found in association with increased numbers of T cells and hence, correlated with good overall survival [32], and B-cells in melanoma have been correlated with good outcome, metastasis free-survival and favorable response to chemotherapy [33, 35]. On the other hand, B cell-deficient mice showed an improved immunological control of their tumor, and in human melanoma patients, more than 15% of B cells in the infiltrate indicated worse prognosis and proved to be an independent marker for local recurrence. [36] In analogy with T cells, this ambiguous role of tumor-associated B-lymphocytes may find an explanation when their functional status will be investigated. In fact, B cells can produce cytokines like IFN γ and IL-4 that may polarize T cells respectively toward a TH1 or TH2 response [31]. Moreover, plasma cells, the terminally differentiated form of the B lymphocyte, have been correlated with an increased risk of lymph node metastasis and poor survival in melanoma, [37, 38] and a possible immune suppressive role for IgA was proposed. [39] Finally, the discovery of an immunosuppressive subtype of B cells, called regulatory B cells [Bregs] shed a new light on the role of B lymphocytes in immune suppression. Bregs decrease the proliferation of CD4 $^{+}$ T cells, recruit Tregs through chemokine [C-C motif] ligand 4 [CCL4], and enhance FOXP3 and CTLA-4 expression by Tregs [31]. In addition, a subset of Bregs expressing high levels of PD-L1 have a critical role in suppressing the PD-1 expressing follicular helper T lymphocytes [FHT]; interestingly, this subset of Bregs is resistant to B-cell depletion through Rituximab [a drug that selectively eliminates B cells by targeting the CD20 molecule]. [40] Furthermore, B cells are able to induce the formation of tertiary lymphoid structures [TLS] at the site of inflammation by secreting lymphotoxin; these TLS mimick secondary lymphoid organs [SLO] where the adaptive immune response has its origin. TLS differ from SLO because they are ectopic, inducible and transient structures, while SLO are constitutive, but they share with SLO the same cytokines involved in their genesis, and the same B and T topography [41]. The criteria that define a TLS are the admixture of T and B cells, with DCLAMP + mature dendritic cells in the T-zone and germinal centers with evidence of B cells switching; the presence of PNAD + high endothelial venules [HEV] allowing extravasation of CD62L $^{+}$ [PNAD ligand] naive T and B cells, memory

T-cells and dendritic cells; and expression of cytokines important for the organization of SLO such as CCL19, CCL21, CXCL13, which attract CCR7 + cells [i.e. naive T cells, TCM cells and T regs] and CXCR5 + cells [i.e. naive B cells, FHT cells, 42]. A peculiar difference with SLO is the lack of NK cells in cancer-associated TLS. Follicular DC, tingible body macrophages and another peculiar subgroup of T cells, follicular helper T cells [FHT], are in contact with B lymphocytes within the B cell zone. FHT cells in peritumoral TLS are attracted by CXCL13 and IL-21 and predict an improved disease outcome in breast cancer and colorectal cancer. [43, 5] TLS could therefore represent clusters of immune cells in an organized structure that is able to escape from tumoral immunosuppression. They are correlated with the induction of humoral immunity and with a good prognosis in several types of cancer [42].

Another weak spot in the morphological evaluation of TILs is that, in addition to small mononuclear cells with scant cytoplasm [i.e. various subpopulations of lymphocytes], the tumoral microenvironment contains other, non-lymphoid cells [Table 1]. The latter cells influence the immune response, but are usually not taken into account during the actual pathological assessment of the stromal cells in melanoma. Cells of myeloid derivation, most often present in the melanoma microenvironment, are tumor-associated macrophages [TAMs], dendritic cells [DCs] and tumor-associated neutrophils TAMs are frequently abundant in melanoma and, in general, are characterized by plasticity: they switch between a proinflammatory M1 status, that determines an antitumor response promoting T helper [Th] 1 responses, and an M2 status, promoting Th2 responses and tissue repair. In immunohistochemistry, a panel to identify a M1 or M2 polarization has been described by Barros: CD163+pSTAT1+, CD68+pSTAT1+, CD163+RBP-J+ and CD68+RBP-J+ macrophages constitute the M1 subset, eliciting Th1 responses and CD163+CMAF+ and CD68+CMAF+ macrophages constitute the M2 subset, associated with Th2 responses. [44] Outside the tumor microenvironment macrophages exert various anti-tumor effects [45] but within the tumoral microenvironment, TAMs are educated to assume an M2 polarization. This results in various effects that facilitate tumor growth: decreased CD8+ T cell recruitment and NK cell activity through IDO secretion, direct inhibition of CD8+ lymphocytes through expression of PD-L1 and B7-H4 and inhibition of CD8+ T cells through recruitment of Tregs and favoring the conversion of lymphocytes in Tregs [46, 28]. TAMs tend to accumulate in hypoxic areas to induce the formation of leaky blood vessels, which in turn secrete CXCL8 [IL-8] and CXCL2 that increase the invasiveness of the neoplastic cells, but they may also accompany malignant cells during their migration to the vessels due to the secretion of CSF1 by malignant cells that induces motility of macrophages [47]. TNF- α secreted by TAMs may favour Epithelial-to-Mesenchymal Transition [EMT], which in turn results in suppression of MITF expression and consequent induction of dedifferentiation of melanoma cells, and in the enhanced production of cytokines and chemokines that attract myeloid cells, such as CCL2. In turn, monocytes, macrophages and neutrophils secrete IL-6, IL -23 and TGFbeta1, that play a role in further inducing EMT [48, 49]. A new hypothetical role for TAMs in EMT and immune escape was suggested by Kemény et al [50], following the observation that in vitro melanoma cells are able to fuse with stromal fibroblasts and macrophages, thereby losing their melanocytic phenotype and acquiring fibroblast- and macrophage-like [mesenchymal] traits.

Dendritic cells [DC] are well known pivotal players in melanoma biology and in melanoma therapy. They are divided into CD11c+ myeloid DC [mDC, further subdivided into BDCA-1+ and BDCA-3+ subsets] and plasmacytoid DC [pDC] carrying the CD123+CD11c-BDC-a2+BDCA-4+ phenotype [51]. Within the tumor microenvironment however, mDCs can lose their MHC class II expression and hence, their ability to stimulate the T lymphocytes, gradually tuning the inflammatory response towards a Th2 type. In fact, it was recently demonstrated that only a small part of DC in the tumor retains the ability to present the antigen in an optimal way, and that these DC are characterized by expression of CD103 and by the secretion of IL-12 [52, 53].

Regarding the pDC subtype, some studies report an inverse correlation between their number and the number of peripheral cytotoxic PD-L1+ T cells [51]. Moreover, the presence of pDC infiltrating the tumor has been shown to correlate with an increased number of Tregs, and a decreased number of CD8+ lymphocytes, and thus with higher risk of metastasis [28]. In particular, pDCs expressing PD-L1 and IDO were identified as tolerogenic [3].

Also tumor-associated neutrophils are able to dampen the T cell immunity [54], but, as stated above, their presence is not taken into account in the assessment of the local immune response in melanoma. Tumor-associated neutrophils are often increased in cancer patients both in the tumor and in the peripheral blood. High neutrophil counts in the blood are associated with higher clinical stage [55] and with poor response to checkpoint inhibitors [56, 57, 58] but the same increase can be observed in melanoma patients due to ulceration [59]. In their activated state, tumor-associated neutrophils produce cytotoxic mediators that can destroy malignant cells, [34] but they can also block the activation of CD8+ T-cells and increase angiogenesis and intravasation of neoplastic cells through MMP9 production [28]. Overall, a neutrophil-related gene-expression signature has been found associated with poor prognosis [60].

The morphology-based evaluation of TILs has a predictive value probably because most melanoma-infiltrating cells are T lymphocytes, in particular of the cytotoxic type [61]. T lymphocytes are subclassified in CD4+ T helper lymphocytes and cytotoxic CD8+ T lymphocytes, the last ones directly killing the tumor cells. Both subsets are generally associated with a good prognosis.. CD4+ T helpers interact with CD8+ T cells stimulating their conversion in CD8+ memory T cells, even if it has recently been observed that CD8+ T cells also have an intrinsic ability to activate the memory programme [62]. On the other hand, based on the recognition of specific tumor antigens, CD4+ cells are also able to directly control tumor growth in an IFN γ -dependent manner [63, 64]. In addition to cytotoxic and helper lymphocytes, there are also other peculiar subgroups of T cells. Among CD4+ T cells, CD4+/FOXP3+/CD25+ regulatory T cells [Tregs] have been associated with poor prognosis and shorter survival [65]. They have a physiological role in preventing autoimmunity, by controlling self-reactive T cells via CTLA-4 and PD-1 [66]. In the peritumoral area however, they facilitate tumor growth through inhibition of DCs, NK cells and B cells via secretion of TGF-beta and IL-10 [67]. Their recruitment depends on CCL2 and CCL5 or galectin1, produced by the tumor, and their number is expanded by TGF- β and TNF produced by other inflammatory cells [68]. Tregs also play a role in immunotherapy, as disease progression during anti-PD-1 treatment has been found associated with an increase of Tregs [69]. T Helper-17 cells constitute another particular subset of T helper cells that produce IL-17. At the tumoral site, T Helper-17 cells are recruited by IL-6, IL-23 and TGF-beta, released by myeloid-derived suppressor cells [MDSC, 70]. Their meaning is still unclear: in contrast to Th1 responses, a Th17 response was associated with bad prognosis in colon cancer [71]. In melanoma and colon cancer, low levels of IL-17 suppress metastasis, whereas in lung carcinoma, metastatic spread is stimulated [28].

Finally, even if only CD8+ cytotoxic T-cells would be present in the tumor microenvironment, their activation status cannot be evaluated by morphology alone and they could be either active or exhausted [Figure 3]. The contact of a lymphocyte with tumor cells, in fact, can lead to the elimination of the tumor cell; however, in the absence of co-stimulatory molecules or in the presence of negative signals, the CD8+ T-cells may become functionally neutralized [“exhausted”] although these cells would still morphologically be similar to other lymphocytes. Hence there is indeed some evidence that the analysis of the activation status of TILs might be more important than we think. First of all, Hillen et al. found that a good prognosis was correlated with CD69+ lymphocytes, defined by the author as a marker of T cell activation [72]. Also the activation markers CD25 and CD134 have been found more expressed in peritumoral than intratumoral lymphocytes and correlate with a better prognosis [35] suggesting inactivation of the lymphocyte upon

contact with the melanoma cell. Moreover, the analysis of the TCR repertoire in different cancers has found an elevated clonotype diversity but only a small fraction of these TCR appear to be directed toward neoantigens, representing mainly sequences most likely directed toward antigens that are common among different people, like the ones related to persistent viral infections [73]. According to Bersen et al however, this clonality of the T cells in melanoma patients is limited, not associated with the type of infiltrate [brisk/non brisk] and does not influence the prognosis, probably because the subtype of T cell clone [T helper vs Treg] and the functional status of the clone might be the determining factors [74].

Activated CD8 lymphocytes secrete IFN-gamma, an immune-stimulatory cytokine. When activated, lymphocytes increase on their surface the expression of inhibitory molecules in order to prevent damage from an exuberant immune response. These inhibitory molecules are PD-1 [programmed death 1], LAG-3 [lymphocyte-activation gene 3], TIGIT [T-cell immunoreceptor with Ig and ITIM domains], and TIM-3 [T-cell immunoglobulin domain and mucin domain 3, 75]. T cells expressing these markers in the tumor microenvironment are potentially exhausted TILs, and their targeting using specific antibodies is the concept on which immunotherapy is based [76]. Several studies have shown that the CD8 + TILs are functionally inert in various cancers [67]. A recent report described PD-1 as a marker identifying the clonally expanded tumor-specific CD8+ T-cell population [77] PD-1 is a molecule expressed on both activated CD4+ and CD8+ TILs, but because of its coinhibitory role in preventing the hyper-activation of lymphocytes, PD-1 expression is considered a sign of T cell exhaustion. [35] Another recent paper has characterized the anergic cells from a molecular point of view, and has shown them to express Lag-3, MHC I-restricted T cell-associated molecule [CRTAM], semaphorin 7A [Sema7A], and chemokine CCL1 [78]. Despite these discrepant findings, PD1 has a prevalent role in the suppression of the immune response since targeting LAG-3, TIM-3, or TIGIT with blocking antibodies has a minimal impact on tumor control, but combination with anti PD1 therapy empowers the response [69]. Given that the markers that induce the exhaustion status in the lymphocyte are expressed upon its activation, it is difficult to define the status of a lymphocyte using the above mentioned markers. By using single cell RNA-sequencing, Tirosh et al. characterized distinct expression signatures for five non malignant cell types. Looking at T cell signatures, the expression of multiple coinhibitory molecules on the same cells was correlated also with expression of cytotoxicity and activation markers [the so-called activation-dependent exhaustion program], making it hard to distinguish activation from exhaustion. Therefore, to define a clear cut activation-independent exhausted state, high expression of five co-inhibitor receptors and exhausted related genes relative to a low expression of cytotoxicity genes were searched for. Using this core exhaustion signature, it was observed that the less exhausted T cells were the ones not clonally expanded, while the T cells that shared the same TCR sequence also expressed the “exhaustion signature” [79]. NFATC1, a transcription marker, was identified among this signature as an effective marker of exhaustion [79], while another group identified Ndr1 as a marker of anergy [80].

The “brisk” pattern: evidence of a successful immune response?

A brisk infiltrate is characterized by the presence of lymphocytes diffusely through the lesion or all along the borders of the vertical growth phase of a melanoma. This pattern suggests a homogeneous expression of antigens by the melanoma cells and/or an excellent and undisrupted traffic of T-cells towards the melanoma. The brisk pattern is associated with a good prognosis, but not in 100% of the cases. [7] It is generally assumed that a brisk infiltrate is composed predominantly of activated cytotoxic T-cells directed to one or more tumor antigens; however, functional studies have been performed on T-cells isolated from melanomas without knowledge of their TILs pattern, and immunophenotypical studies related to the major TILs-patterns are extremely rare. Moreover, actively regressing melanomas are not necessarily accompanied by a brisk infiltrate, suggesting that many T-cells in the brisk infiltrate are bystanders, not directed to tumor-

antigens but contributing [via secretion of cytokines?] to the “activated landscape” [81]. A recent study on 67 primary melanomas revealed upregulation of T-cell activation pathways and inhibition of upstream immune checkpoint regulators suggesting a predominant pattern of T-cell activation in brisk melanomas [82]. Our own data based on an RT-PCR study of microdissected metastatic melanomas indicate an interferon-gamma rich micro-environment in melanomas with a brisk TILs pattern, suggesting an enrichment of activated T-cells in the brisk infiltrate [Bosisio et al. unpublished data]. Despite these findings, notable regression of melanoma with replacement of the tumor by fibrous tissue is not a regular finding in “brisk” melanomas and future research should analyse in depth the cellular composition of the brisk infiltrate and the transcriptome of the melanoma cells in these brisk areas.

The “non brisk” pattern: spatial heterogeneity and partial failure of the immune response?

A non brisk pattern suggests by its own definition the presence of a heterogeneous microenvironment, with areas of immune attack and areas of immune ignorance, possibly as a result of tumor heterogeneity and immunoediting. The areas of immune attack represent small areas of a “brisk” response, and the areas of immune ignorance lack TILs and may reflect the expansion of less immunogenic melanoma cell clones, or a change in the immune microenvironment towards immunosuppression.

Most often, markers with a role in the immune response expressed by melanoma cells are heterogeneously expressed when comparing areas at the periphery of a melanoma with the center of the same area. There is lot of evidence that the inflammatory infiltrate at the border of the tumor plays a pivotal role. In Merkel cell carcinoma, for example, a dense infiltrate in this region is associated with a better prognosis [83]. Differences between the marginal and the central zone of the tumor were found also in colon cancer. In particular, B cells and T cells predominantly localize at the tumor border, but the density of the infiltrate varies over time for the two types of lymphocytes: while T cells decreased with tumor progression, B cells as well as innate immune cells increased. Instead, the center of the tumor harbored predominantly cytotoxic T lymphocytes and occasional FTH, but very few B lymphocytes. [5] Thus, the tumor/stroma interface is a pivotal region for tumor evolution, since various stress stimuli, such as cytokines and chemokines derived from the local immune response, may modify melanoma cells, assuming different characteristics in different areas. For example, at the borders of melanoma nodules, expression of SOX2 and nestin can be found, both associated with epithelial-mesenchymal transition and a shorter survival [84]; similarly, the ligands for NK activating receptors NKG2D and DNAM-1 such as MICA/B and ULBP2, are preferentially expressed at the tumor periphery as a mechanism of defense against innate immunity [27]. Also some markers of response to immune therapy are mainly expressed at the margin of the nodules. In addition to Major Histocompatibility Complex class I [MHC I], the IFN-gamma induced molecules PD-L1 and MHC II are usually found preferentially expressed at the tumor-stroma interface where TILs migrate and secrete. MHC I molecules are lost in 16-50% of solid tumors at least focally [85]. In cases with heterogeneous expression of MHC I, positive areas are rich in TILs. The relationship between the presence of TILs and MHC I expression is easily explained by the fact that the most powerful stimulus for MHC I expression is IFN-gamma, produced by activated T lymphocytes and NK cells [86]. In a minority of melanomas, this irreversible MHC I loss is due to mutation of the $\beta 2$ microglobulin gene [87], but in the majority of MHC I-negative cases, MHC I expression can be rescued by administration of cytokines, in particular of IFN- γ . In these cases, an alternative and yet poorly understood mechanism regulates MHC I expression [88]. For example, the involvement of epigenetic aside of genetic mechanisms were described by Chang et al in one melanoma patient following immunotherapy [89]. Also the mutational status of BRAF influences the immune response not only by upregulating immunomodulatory factors, but also through intracellular internalization of MHC I resulting in loss of expression at the surface [90]. Loss of MHC I has been linked not only with immune escape, but also

with higher oncogenic abilities of melanoma cells; when MHC I was completely downregulated, melanoma cell lines showed increased invasiveness [91]. Though, due to the discovery of mechanisms to overcome MHC I loss by the immune system, the role of MHC molecules in anti-melanoma immunity has recently been re-evaluated [92]. New evidences indicates that MHC I molecules are not essential for the induction of an immune response [93], nevertheless their presence helps to trigger more powerful responses [94, 95].

With respect to PD-L1, its value as a marker for the immune response is well known and long debated [96, 97]. As the immunome is variable in space and time, [5] not only PD-1 expression is highly heterogeneous in tumors, but also with tumor progression the PD-L1 status can change in metastasis compared to primaries [98] and therefore may not be the best predictive marker of response to immunotherapy. Furthermore, different anti PD-L1 antibodies exist and variability in the pre-analytical tissue processing will yield different immunohistochemical staining results. Additionally, the evaluation of this staining is still subjective. Cut-off levels for calling a melanoma positive are highly variable, and the subcellular localization of immunoreactivity may also vary, since it can be expressed both on melanoma and inflammatory cells, and in melanoma, expression on the membrane is relevant, while in inflammatory cells also cytoplasmic expression plays a role [99, 100, 101]. A recent RNA sequencing study described a molecular signature called “innate anti-PD1 resistance signature” [IPRES] that turned out to be linked with resistance to PD1-blocking therapies. That signature in particular showed a “mesenchymal and inflammatory” phenotype, with expression of epithelial-to-mesenchymal transition genes, immunosuppressive genes, and monocyte chemotactic genes, while T-cell related genes did not discriminate between responders and non-responders [102]. Moreover, a classification of tumors according to PD-L1 expression and the presence of TILs has been proposed [76], and divides them into four types, each type having benefits from different therapies. In melanoma, the prevalence of these different types has been quantified. Type I and type II are the most frequent [38% and 41%, respectively], with PD-L1 positivity associated with TILs [adaptive immunity] in the first category and PD-L1 negativity and absence of TILs [immune ignorance] in the second group. At the opposite, melanomas with PD-L1 expression and no TILs are extremely infrequent [1%, type III], while PD-L1 negativity associated with TILs [type IV] represents some 20% of melanomas. In Type I and type IV the chance that immunotherapy will work is higher, since TILs are present but probably prevented from cytotoxicity because of PD-L1 expression in the first group, or due to other immune tolerance mechanisms in the second. Checkpoint blockade is instead unlikely to work by itself in Type II and Type III patients, because of the lack of TILs, but a combination of checkpoints inhibitors with vaccination, targeted therapies, adoptive T-cell transfer, chemotherapy, or radiotherapy that stimulate immunogenic cell death could stimulate the lymphocytes recruitment inside the tumor site and, in addition, prevent them from being inactivated [76, 103, 104].

Regarding the other putative marker to predict the immune response that is expressed at melanoma margins, MHC II expression on melanoma cells can be constitutive in the tumor or can be induced by IFN γ , but its prognostic significance is still unclear. In experiments on cell lines, MHC II expression was associated with lymphocytic activation pathways signatures, and in melanoma patients treated with PD-1 blockade, MHC II expression was associated with the presence of TILs, survival and response to therapy [105]. On the other hand, in a recent paper MHC II expression in melanoma was associated with the presence of CD4+ T lymphocytes specifically directed toward tumor antigens; these CD4+ T-cells produced TNF and prevented the activation of cytotoxic T lymphocytes [106]. Finally, the presence of immune checkpoints molecules expressed on different types of cells [e.g. melanoma cells or macrophages] at the border of the tumor suggests the existence of a “shield effect” held by those cells against effective immunity [107].

The “absent” pattern: ignorance by the immune system and complete failure of the immune response?

Melanomas with an absent TILs patterns are apparently ignored by the immune system. This immune ignorance could be present since the beginning because of low immunogenicity of the melanoma clones or could develop throughout the phases of tumor progression due to immune modulation and immune editing. Alternatively, immune editing may already have eliminated the most immunogenic clones resulting in a melanoma composed of poorly antigenic clones that can escape the immune attack [108]; another possibility is that a tolerogenic mechanism towards the tumor antigens has resulted in a reduced activation of the dendritic cells or the T lymphocytes.

An absent TILs infiltrate can also be caused by an impairment in the attraction or traffic of immune cells towards the tumor. For example, , overexpression of endothelin B receptor and hypoexpression of E-selectin, P selectin or ICAM-1 prevent the vascular exit of TILs at the tumor site [109, 110]. Interesting is the recent finding that in particular Tregs but not other T cells use a specific molecule to extravasate, the lymphotoxin [111]. The lack of entry of lymphocytes in the tumor can also be due to a low level of lymphotactic chemokines, e.g. CCL2-5, CXCL9, CXCL10, that usually are produced by melanoma cells upon stimulation by interferons [110]. Patients with an absent TILs infiltrate may benefit better from a combined therapy, because a combined approached targeting more than one immune checkpoint has more chances to re-activate inflammation in the case of an end stage immune escape [112, 113].

Conclusion: the need for a refinement of the TILs patterns in melanoma

A growing body of evidence resumed in this review points toward the need to characterize the immune landscape as a whole, not only for prognostic but also therapeutic purposes, and not only on H&E sections but also in a functional way. Data on the evaluation of the T cell landscape [114] as well as the interpretation of single stainings for immune check point molecules have already shown utility in predicting the response to therapy [96, 115, 105, 116, 76, 102]. Nevertheless, the different aspects of the tumoral immune response should not be considered separately, but integrated also with molecular melanoma-cell centered information in order to achieve a better prognostic definition and therapy tailoring for every single patient. This process to create an immunoscore has already been initiated for colon cancer, and has already resulted in a grading of the local immune response Galon et al started in 2012 to test a simple evaluation of the immune response applicable in daily routine: a simple immunophenotyping of the TILs using CD45RO, CD3 and CD8 immunostaining on an FFPE section, analyzed with image analysis and given as a score from 0 to 4 in relation to the density of infiltration. This approach has shown correlation with survival and has been proposed as TNM-I [TNM-Immune] to add in the TNM classification [117].

Blank et al propose the use of the “cancer immunogram”, a radar plot taking into account 7 parameters: tumor foreignness, general immune status, immune cells infiltration, absence of checkpoints, absence of soluble inhibitors, absence of tumor inhibitory metabolism and tumor sensitivity to immune effectors [118]. The first studies demonstrating that an immunoscore approach has a beneficial effect on the management of patients are now appearing in the literature [119, 120]. Although the current morphological classification of TILs in melanoma has prognostic significance, we believe that a functional analysis, particularly of the non-brisk pattern [encompassing the majority of primary melanomas] can help to understand this patterns and, probably, to subdivide this pattern into separate subgroups based on the degrees of tumor cell plasticity and immune modulation using extensive phenotypical and molecular tools.

References

1. Alexandrov LB, Nik-Zainal S, Wedge DC, Aparicio SA, Behjati S, Biankin AV, Bignell GR, Bolli N, Borg A, Børresen-Dale AL, Boyault S, Burkhardt B, Butler AP, Caldas C, Davies HR, Desmedt C, Eils R, Eyfjörd JE, Foekens JA, Greaves M, Hosoda F, Hutter B, Ilicic T, Imbeaud S, Imielinski M, Jäger N, Jones DT, Jones D, Knappskog S, Kool M, Lakhani SR, López-Otín C, Martin S, Munshi NC, Nakamura H, Northcott PA, Pajic M, Papaemmanuil E, Paradiso A, Pearson JV, Puente XS, Raine K, Ramakrishna M, Richardson AL, Richter J, Rosenstiel P, Schlesner M, Schumacher TN, Span PN, Teague JW, Totoki Y, Tutt AN, Valdés-Mas R, van Buuren MM, van 't Veer L, Vincent-Salomon A, Waddell N, Yates LR; Australian Pancreatic Cancer Genome Initiative; ICGC Breast Cancer Consortium; ICGC MMML-Seq Consortium; ICGC PedBrain, Zucman-Rossi J, Futreal PA, McDermott U, Lichten P, Meyerson M, Grimmond SM, Siebert R, Campo E, Shibata T, Pfister SM, Campbell PJ, Stratton MR. Signatures of mutational processes in human cancer. *Nature*. 2013 Aug 22;500[7463]:415-21. doi: 10.1038/nature12477. Epub 2013 Aug 14.
2. Bastian BC The molecular pathology of melanoma: an integrated taxonomy of melanocytic neoplasia. *Annu Rev Pathol*. 2014;9:239-71.
3. Gajewski TF, Schreiber H, Fu YX. Innate and adaptive immune cells in the tumor microenvironment. *Nat Immunol*. 2013 October ; 14[10]: 1014–1022.
4. Bae JM, Choi YY, Kim DS, Lee JH, Jang HS, Lee JH, Kim H, Oh BH, Roh MR, Nam KA, Chung KY. Metastatic melanomas of unknown primary show better prognosis than those of known primary: a systematic review and meta-analysis of observational studies. *J Am Acad Dermatol*. 2015 Jan;72[1]:59-70.
5. Bindea G, Mlecnik B, Tosolini M, Kirilovsky A, Waldner M, Obenaus AC, Angell H, Fredriksen T, Lafontaine L, Berger A, Bruneval P, Fridman WH, Becker C, Pagès F, Speicher MR, Trajanoski Z, Galon J. Spatiotemporal dynamics of intratumoral immune cells reveal the immune landscape in human cancer. *Immunity*. 2013 Oct 17;39[4]:782-95.
6. Lee N, Zakka LR, Mihm MC Jr, Schatton T. Tumour-infiltrating lymphocytes in melanoma prognosis and cancer immunotherapy. *Pathology*. 2016 Feb;48[2]:177-87.
7. Clemente CG, Mihm MC Jr, Bufalino R, Zurrida S, Collini P, Cascinelli N. Prognostic value of tumor infiltrating lymphocytes in the vertical growth phase of primary cutaneous melanoma. *Cancer*. 1996 Apr 1;77[7]:1303-10.
8. Mihm MC Jr, Clemente CG, Cascinelli N. Tumor infiltrating lymphocytes in lymph node melanoma metastases: a histopathologic prognostic indicator and an expression of local immune response. *Lab Invest*. 1996 Jan;74[1]:43-7.
9. Azimi F, Scolyer RA, Rumcheva P, Moncrieff M, Murali R, McCarthy SW, Saw RP, Thompson JF. Tumor-infiltrating lymphocyte grade is an independent predictor of sentinel lymph node status and survival in patients with cutaneous melanoma. *J Clin Oncol* 2012 Jul 20;30[21]:2678-83.
10. Galon J, Costes A, Sanchez-Cabo F, Kirilovsky A, Mlecnik B, Lagorce-Pagès C, Tosolini M, Camus M, Berger A, Wind P, Zinzindohoué F, Bruneval P, Cugnenc PH, Trajanoski Z, Fridman WH, Pagès F. Type, density, and location of immune cells within human colorectal tumors predict clinical outcome. *Science*. 2006 Sep 29;313[5795]:1960-4.
11. Schadendorf D, Hodi FS, Robert C, Weber JS, Margolin K, Hamid O, Patt D, Chen TT, Berman DM, Wolchok JD. Pooled Analysis of Long-Term Survival Data From Phase II and Phase III Trials of Ipilimumab in Unresectable or Metastatic Melanoma. *J Clin Oncol*. 2015 Jun 10;33[17]:1889-94.
12. Sullivan RJ and Flaherty KT Anti-PD-1 therapies—a new firstline option in advanced melanoma. *Nat Rev Clin Oncol*. 2015 Nov;12[11]:625-6.
13. Ribas A, Flaherty KT. Gauging the Long-Term Benefits of Ipilimumab in Melanoma. *J Clin Oncol*. 2015 Jun 10;33[17]:1865-6.
14. Ribas A, Hamid O, Daud A, Hodi FS, Wolchok JD, Kefford R, Joshua AM, Patnaik A, Hwu WJ, Weber JS, Gangadhar TC, Hersey P, Dronca R, Joseph RW, Zarour H, Chmielowski B, Lawrence DP, Algazi A, Rizvi NA, Hoffner B, Mateus C7,

Gergich K, Lindia JA, Giannotti M, Li XN, Ebbinghaus S, Kang SP, Robert C. Association of Pembrolizumab With Tumor Response and Survival Among Patients With Advanced Melanoma. *JAMA*. 2016 Apr 19;315[15]:1600-9.

15. Robert C, Long GV, Brady B, Dutriaux C, Maio M, Mortier L, Hassel JC, Rutkowski P, McNeil C, Kalinka-Warzocha E, Savage KJ, Hernberg MM, Lebbé C, Charles J, Mihalciou C, Chiarion-Sileni V, Mauch C, Cognetti F, Arance A, Schmidt H, Schadendorf D, Gogas H, Lundgren-Eriksson L, Horak C, Sharkey B, Waxman IM, Atkinson V, Ascierto PA. Nivolumab in previously untreated melanoma without BRAF mutation. *N Engl J Med*. 2015 Jan 22;372[4]:320-30.

16. Orloff M, Weight R, Valsecchi ME, Sato T. Immune Check Point Inhibitors Combination in Melanoma: Worth the Toxicity? *Rev Recent Clin Trials*. 2016;11[2]:81-6.

17. Spain L, Larkin J. Combination immune checkpoint blockade with ipilimumab and nivolumab in the management of advanced melanoma. *Expert Opin Biol Ther*. 2016;16[3]:389-96. doi: 10.1517/14712598.2016.1141195. Epub 2016 Feb 1.

18. Grimaldi AM, Marincola FM, Ascierto PA. Single versus combination immunotherapy drug treatment in melanoma. *Expert Opin Biol Ther*. 2016 Apr;16[4]:433-41.

19. Teixeira C, Gonzalez-Cao M, Karachaliou N, Rosell R: Predictive factors for immunotherapy in melanoma. *Ann Transl Med* 2015; 3 [15]: 208-218

20. Spits H, Cupedo T. Innate lymphoid cells: emerging insights in development, lineage relationships, and function. *Annu Rev Immunol*. 2012;30:647-75.

21. M. Gomez de Agüero, S. C. Ganai-Vonarburg, T. Fuhrer, S. Rupp, Y. Uchimura, H. Li, A. Steinert, M. Heikenwalder, S. Hapfelmeier, U. Sauer, K. D. McCoy, A. J. Macpherson, The maternal microbiota drives early postnatal innate immune development. *Science* 351, 1296–1302 [2016].

22. R. Duffin, R. A. O'Connor, S. Crittenden, T. Forster, C. Yu, X. Zheng, D. Smyth, C. T. Robb, F. Rossi, C. Skouras, S. Tang, J. Richards, A. Pellicoro, R. B. Weller, R. M. Breyer, D. J. Mole, J. P. Iredale, S. M. Anderton, S. Narumiya, R. M. Maizels, P. Ghazal, S. E. Howie, A. G. Rossi, C. Yao, Prostaglandin E2 constrains systemic inflammation through an innate lymphoid cell–IL-22 axis. *Science* 351, 1333–1338 [2016].

23. Carrega P, Loiacono F, Di Carlo E, Scaramuccia A, Mora M, Conte R, Benelli R, Spaggiari GM, Cantoni C, Campana S, Bonaccorsi I, Morandi B, Truini M, Mingari MC, Moretta L, Ferlazzo G. NCR[+]ILC3 concentrate in human lung cancer and associate with intratumoral lymphoid structures. *Nat Commun*. 2015 Sep 23;6:8280.

24. C. Viant, L. C. Rankin, M. J. H. Girard-Madoux, C. Seillet, W. Shi, M. J. Smyth, L. Bartholin, T. Walzer, N. D. Huntington, E. Vivier, G. T. Belz, Transforming growth factor- β and Notch ligands act as opposing environmental cues in regulating the plasticity of type 3 innate lymphoid cells. *Sci. Signal*. 9, ra46 [2016].

25. Fišerová A, Richter J, Čapková K, Bieblová J, Mikyšková R, Reiniš M, Indrová M. Resistance of novel mouse strains different in MHC class I and the NKC domain to the development of experimental tumors. *Int J Oncol*. 2016 Jun 3.

26. Tallerico R, Garofalo C, Carbone E. A New Biological Feature of Natural Killer Cells: The Recognition of Solid Tumor-Derived Cancer Stem Cells. *Front Immunol*. 2016 May 10;7:179.

27. Tarazona R, Duran E, Solana R. Natural Killer Cell Recognition of Melanoma: New Clues for a More Effective Immunotherapy. *Front Immunol*. 2016 Jan 7;6:649.

28. Kitamura T, Qian BZ, Pollard JW. Immune cell promotion of metastasis. *Nat Rev Immunol*. 2015 Feb;15[2]:73-86

29. Groh V, Wu J, Yee C, Spies T. Tumour-derived soluble MIC ligands impair expression of NKG2D and T-cell activation. *Nature* 2002; 419: 734-738.

30. Waldhauer I, Steinle A. Proteolytic release of soluble UL16-binding protein 2 from tumor cells. *Cancer Res* 2006; 66: 2520-2526.
31. Fremd C, Schuetz F, Sohn C, Beckhove P, Domschke C. B cell-regulated immune responses in tumor models and cancer patients. *Oncoimmunology*. 2013 Jul 1;2[7]:e25443.
32. Iglesia MD, Parker JS, Hoadley KA, Serody JS, Perou CM, Vincent BG. Genomic Analysis of Immune Cell Infiltrates Across 11 Tumor Types. *J Natl Cancer Inst*. 2016 Jun 22;108[11]. pii: djw144. doi: 10.1093/jnci/djw144. Print 2016 Nov.
33. Garg K, Maurer M, Griss J, Brügger MC, Wolf IH, Wagner C, Willi N, Mertz KD, Wagner SN. Tumor associated B cells in cutaneous primary melanoma and improved clinical outcome. *Hum Pathol*. 2016 Apr 20. pii: S0046-8177[16]30043-0.
34. Ladányi A, Kiss J, Mohos A, Somlai B, Liskay G, Gilde K, Fejös Z, Gaudi I, Dobos J, Tímár J. Prognostic impact of B-cell density in cutaneous melanoma. *Cancer Immunol Immunother*. 2011 Dec;60[12]:1729-38.
35. Ladányi A Prognostic and predictive significance of immune cells infiltrating cutaneous melanoma. *Pigment Cell Melanoma Res*. 2015 Mar 26.
36. Martinez-Rodriguez M, Thompson AK, Monteagudo C. A significant percentage of CD20-positive TILs correlates with poor prognosis in patients with primary cutaneous malignant melanoma. *Histopathology*. 2014 Nov;65[5]:726-8.
37. Weissmann A, Roses DF, Harris MN, Dubin N. Prediction of lymph node metastases from the histologic features of primary cutaneous malignant melanomas. *Am J Dermatopathol*. 1984 Summer;6 Suppl:35-41.
38. Mascaro JM, Molgo M, Castel T, Castro J. Plasma cells within the infiltrate of primary cutaneous malignant melanoma of the skin. A confirmation of its histoprognostic value. *Am J Dermatopathol*. 1987 Dec;9[6]:497-9.
39. Bosisio FM, Wilmott JS, Volders N, Mercier M, Wouters J, Stas M, Blokk WA, Massi D, Thompson JF, Scolyer RA, van Baren N, van den Oord JJ. Plasma cells in primary melanoma. Prognostic significance and possible role of IgA. *Mod Pathol*. 2016 Apr;29[4]:347-58.
40. Khan AR, Hams E, Floudas A, Sparwasser T, Weaver CT, Fallon PG. PD-L1hi B cells are critical regulators of humoral immunity. *Nat Commun*. 2015 Jan 22;6:5997.
41. Germain C, Gnjjatic S, Dieu-Nosjean MC. Tertiary Lymphoid Structure-Associated B Cells are Key Players in Anti-Tumor Immunity. *Front Immunol*. 2015 Feb 23;6:67.
42. Dieu-Nosjean MC, Goc J, Giraldo NA, Sautès-Fridman C, Fridman WH. Tertiary lymphoid structures in cancer and beyond. *Trends Immunol*. 2014 Nov;35[11]:571-80.
43. Fridman WH, Pages F, Sautès-Fridman C, Galon J. The immune contexture in human tumours: impact on clinical outcome. *Nat Rev Cancer* 2012; 12:298–306.
44. Barros MH, Hauck F, Dreyer JH, Kempkes B, Niedobitek G. Macrophage polarisation: an immunohistochemical approach for identifying M1 and M2 macrophages. *PLoS One*. 2013 Nov 15;8[11]:e80908. doi: 10.1371/journal.pone.0080908. eCollection 2013.
45. Pucci F, Garris C, Lai CP, Newton A, Pfirschke C, Engblom C, Alvarez D, Sprachman M, Evavold C, Magnuson A, von Andrian UH, Glatz K, Breakefield XO, Mempel TR, Weissleder R, Pittet MJ. SCS macrophages suppress melanoma by restricting tumor-derived vesicle-B cell interactions. *Science*. 2016 Apr 8;352[6282]:242-6.
46. Bulman A, Neagu M, Constantin C. Immunomics in Skin Cancer - Improvement in Diagnosis, Prognosis and Therapy Monitoring. *Curr Proteomics*. 2013 Sep;10[3]:202-217.

47. Fridman WH, Remark R, Goc J, Giraldo NA, Becht E, Hammond SA, Damotte D, Dieu-Nosjean MC, Sautès-Fridman C. The immune microenvironment: a major player in human cancers. *Int Arch Allergy Immunol*. 2014;164[1]:13-26.
48. Riesenberger S, Groetchen A, Siddaway R, Bald T, Reinhardt J, Smorra D, Kohlmeyer J, Renn M, Phung B, Aymans P, Schmidt T, Hornung V, Davidson I, Goding CR, Jönsson G, Landsberg J, Tüting T, Hölzel M. MITF and c-Jun antagonism interconnects melanoma dedifferentiation with pro-inflammatory cytokine responsiveness and myeloid cell recruitment. *Nat Commun*. 2015 Nov 4;6:8755.
49. Smith HA, Kang Y. The metastasis-promoting roles of tumor-associated immune cells. *J Mol Med [Berl]*. 2013 Apr;91[4]:411-29.
50. Kemény LV, Kurgyis Z, Buknicz T, Groma G, Jakab Á, Zänker K, Dittmar T, Kemény L, Németh IB. Melanoma Cells Can Adopt the Phenotype of Stromal Fibroblasts and Macrophages by Spontaneous Cell Fusion in Vitro. *Int J Mol Sci*. 2016 Jun 2;17[6].
51. Chevolet I, Speckaert R, Schreuer M, Neyns B, Krysko O, Bachert C, Van Gele M, van Geel N, Brochez L. Clinical significance of plasmacytoid dendritic cells and myeloid-derived suppressor cells in melanoma. *J Transl Med*. 2015 Jan 16;13[1]:9.
52. Broz ML, Binnewies M, Boldajipour B, Nelson AE, Pollack JL, Erle DJ, Barczak A, Rosenblum MD, Daud A, Barber DL, Amigorena S, Van't Veer LJ, Sperling AI, Wolf DM, Krummel MF. Dissecting the tumor myeloid compartment reveals rare activating antigen-presenting cells critical for T cell immunity. *Cancer Cell*. 2014 Nov 10;26[5]:638-52.
53. Zitvogel L, Kroemer G. CD103+ dendritic cells producing interleukin-12 in anticancer immunosurveillance. *Cancer Cell*. 2014 Nov 10;26[5]:591-3.
54. Coffelt SB, Kersten K, Doornebal CW, Weiden J, Vrijland K, Hau CS, Versteegen NJ, Ciampricotti M, Hawinkels LJ, Jonkers J, de Visser KE. IL-17-producing $\gamma\delta$ T cells and neutrophils conspire to promote breast cancer metastasis. *Nature*. 2015 Jun 18;522[7556]:345-8.
55. Templeton AJ, McNamara MG, Šeruga B, Vera-Badillo FE, Aneja P, Ocaña A, Leibowitz-Amit R, Sonpavde G, Knox JJ, Tran B, Tannock IF, Amir E. Prognostic role of neutrophil-to-lymphocyte ratio in solid tumors: a systematic review and meta-analysis. *J Natl Cancer Inst*. 2014 May 29;106[6]:dju124.
56. Gebhardt C, Sevko A, Jiang H, Lichtenberger R, Reith M, Tarnanidis K, Holland-Letz T, Umansky L, Beckhove P, Sucker A, Schadendorf D, Utikal J, Umansky V. Myeloid Cells and Related Chronic Inflammatory Factors as Novel Predictive Markers in Melanoma Treatment with Ipilimumab. *Clin Cancer Res*. 2015 Dec 15;21[24]:5453-9.
57. Ferrucci PF, Gandini S, Battaglia A, Alfieri S, Di Giacomo AM, Giannarelli D, Cappellini GC, De Galitiis F, Marchetti P, Amato G, Lazzeri A, Pala L, Cocorocchio E, Martinoli C. Baseline neutrophil-to-lymphocyte ratio is associated with outcome of ipilimumab-treated metastatic melanoma patients. *Br J Cancer*. 2015 Jun 9;112[12]:1904-10.
58. Kim K, Skora AD, Li Z, Liu Q, Tam AJ, Blosser RL, Diaz LA Jr, Papadopoulos N, Kinzler KW, Vogelstein B, Zhou S. Eradication of metastatic mouse cancers resistant to immune checkpoint blockade by suppression of myeloid-derived cells. *Proc Natl Acad Sci U S A*. 2014 Aug 12;111[32]:11774-9.
59. Bald T, Quast T, Landsberg J, Rogava M, Glodde N, Lopez-Ramos D, Kohlmeyer J, Riesenberger S, van den Boorn-Konijnenberg D, Hömig-Hölzel C, Reuten R, Schadow B, Weighardt H, Wenzel D, Helfrich I, Schadendorf D, Bloch W, Bianchi ME, Lugassy C, Barnhill RL, Koch M, Fleischmann BK, Förster I, Kastenmüller W, Kolanus W, Hölzel M, Gaffal E, Tüting T. Ultraviolet-radiation-induced inflammation promotes angiogenesis and metastasis in melanoma. *Nature*. 2014 Mar 6;507[7490]:109-13.
60. Gentles AJ, Newman AM, Liu CL, Bratman SV, Feng W, Kim D, Nair VS, Xu Y, Khuong A, Hoang CD, Diehn M, West RB, Plevritis SK, Alizadeh AA. The prognostic landscape of genes and infiltrating immune cells across human cancers. *Nat Med*. 2015 Aug;21[8]:938-45.

61. Hussein, M.R., Elasers, D.A.H., Fadel, S.A., and Omar, A.E.M. [2006] Immunohistological characterization of tumour infiltrating lymphocytes in melanocytic skin lesions. *J. Clin. Pathol.* 59, 316–324
62. Kim J, Ryu SJ, Oh K, Ju JM, Jeon JY, Nam G, Lee DS, Kim HR, Kim JY, Chang J, Sproule T, Choi K, Roopenian D, Choi EY. Memory programming in CD8[+] T-cell differentiation is intrinsic and is not determined by CD4 help. *Nat Commun.* 2015 Aug 14;6:7994.
63. Shklovskaya E, Terry AM, Guy TV, Buckley A, Bolton HA, Zhu E, Holst J, Fazekas de St Groth B. Tumour-specific CD4 T cells eradicate melanoma via indirect recognition of tumour-derived antigen. *Immunol Cell Biol.* 2016 Feb 3.
64. Fonteneau JF, Brilot F, Münz C, Gannagé M. The Tumor Antigen NY-ESO-1 Mediates Direct Recognition of Melanoma Cells by CD4+ T Cells after Intercellular Antigen Transfer. *J Immunol.* 2016 Jan 1;196[1]:64-71.
65. Balkwill FR, Capasso M, Hagemann T. The tumor microenvironment at a glance. *J Cell Sci.* 2012 Dec 1;125 [Pt 23]:5591-6.
66. Feng Y, van der Veeken J, Shugay M, Putintseva EV, Osmanbeyoglu HU, Dikiy S, Hoyos BE, Moltedo B, Hemmers S, Treuting P, Leslie CS, Chudakov DM, Rudensky AY. A mechanism for expansion of regulatory T-cell repertoire and its role in self-tolerance. *Nature.* 2015 Dec 3;528[7580]:132-6.
67. Bruno TC, French JD, Jordan KR, Ramirez O, Sippel TR, Borges VF, Haugen BR, McCarter MD, Waziri A, Slansky JE. Influence of human immune cells on cancer: studies at the University of Colorado. *Immunol Res.* 2013 Mar;55[1-3]:22-33.
68. Bothur E, Raifer H, Haftmann C, Stittrich AB, Brüstle A, Brenner D, Bollig N, Bieringer M, Kang CH, Reinhard K, Camara B, Huber M, Visekruna A, Steinhoff U, Repenning A, Bauer UM, Sexl V, Radbruch A, Sparwasser T, Mashreghi MF, Wah Mak T, Lohoff M. Antigen receptor-mediated depletion of FOXP3 in induced regulatory T-lymphocytes via PTPN2 and FOXO1. *Nat Commun.* 2015 Oct 13;6:8576
69. Kim JM, Chen DS. Immune-escape to PD-L1/PD-1 blockade: 7 steps to success [or failure]. *Ann Oncol.* 2016 May 20.
70. Yoon JH, Sudo K, Kuroda M, Kato M, Lee IK, Han JS, Nakae S, Imamura T, Kim J, Ju JH, Kim DK, Matsuzaki K, Weinstein M, Matsumoto I, Sumida T, Mamura M. Phosphorylation status determines the opposing functions of Smad2/Smad3 as STAT3 cofactors in TH17 differentiation. *Nat Commun.* 2015 Jul 21;6:7600.
71. Tosolini M, Kirilovsky A, Mlecnik B, Fredriksen T, Mauger S, Bindea G, Berger A, Bruneval P, Fridman WH, Pagès F, Galon J. Clinical impact of different classes of infiltrating T cytotoxic and helper cells [Th1, th2, treg, th17] in patients with colorectal cancer. *Cancer Res.* 2011 Feb 15;71[4]:1263-71.
72. Hillen F., Baeten, C.I.M., van de Winkel, A., Creyten, D., van der Schaft, D.W.J., Winnepenninckx, V., and Griffioen, A.W. [2008] Leukocyte infiltration and tumor cell plasticity are parameters of aggressiveness in primary cutaneous melanoma. *Cancer Immunol. Immunother.* 57, 97–106
73. Li B, Li T, Pignon JC, Wang B, Wang J, Shukla SA, Dou R, Chen Q, Hodi FS, Choueiri TK, Wu C, Hacohen N, Signoretti S, Liu JS, Liu XS. Landscape of tumor-infiltrating T cell repertoire of human cancers. *Nat Genet.* 2016 Jul;48[7]:725-32.
74. Bernsen MR, Diepstra JH, van Mil P, Punt CJ, Figdor CG, van Muijen GN, Adema GJ, Ruiter DJ. Presence and localization of T-cell subsets in relation to melanocyte differentiation antigen expression and tumour regression as assessed by immunohistochemistry and molecular analysis of microdissected T cells. *J Pathol.* 2004 Jan;202[1]:70-9.
75. Chen L, Flies DB. Molecular mechanisms of T cell co-stimulation and co-inhibition. *Nat Rev Immunol.* 2013 Apr;13[4]:227-42. doi: 10.1038/nri3405. Epub 2013 Mar 8.
76. Teng MW, Ngio SF, Ribas A, Smyth MJ. Classifying Cancers Based on T-cell Infiltration and PD-L1. *Cancer Res.* 2015 Jun 1;75[11]:2139-45. doi: 10.1158/0008-5472.CAN-15-0255.

77. Gros, A., Robbins, P.F., Yao, X., Li, Y.F., Turcotte, S., Tran, E., Wunderlich, J.R., Mixon, A., Farid, S., Dudley, M.E., et al. [2014] PD-1 identifies the patient-specific CD8+ tumor-reactive repertoire infiltrating human tumors. *J. Clin. Invest.* 124, 2246–2259
78. Zheng Y, Zha Y, Spaapen RM, Mathew R, Barr K, Bendelac A, Gajewski TF. Egr2-dependent gene expression profiling and ChIP-Seq reveal novel biologic targets in T cell anergy. *Mol Immunol.* 2013 Oct;55[3-4]:283-91.
79. Tirosh I, Izar B, Prakadan SM, Wadsworth MH 2nd, Treacy D, Trombetta JJ, Rothenberg ME, Chao A, Li L, Liu X, et al. Dissecting the multicellular ecosystem of metastatic melanoma by single-cell RNA-seq. *Science.* 2016 Apr 8;352[6282]:189-96.
80. Oh YM, Park HB, Shin JH, Lee JE, Park HY, Kho DH, Lee JS, Choi H, Okuda T, Kokame K, Miyata T, Kim IH, Lee SH, Schwartz RH, Choi K. Ndr1 is a T-cell clonal anergy factor negatively regulated by CD28 costimulation and interleukin-2. *Nat Commun.* 2015 Oct 28;6:8698.
81. Cipponi A, Wieers G, van Baren N, Coulie PG. Tumor-infiltrating lymphocytes: apparently good for melanoma patients. But why? *Cancer Immunol Immunother.* 2011 Aug;60[8]:1153-60.
82. Weiss SA, Han SW, Lui K, Tchack J, Shapiro R, Berman R, Zhong J, Krogsaard M, Osman I, Darvishian F. Immunologic heterogeneity of tumor-infiltrating lymphocyte composition in primary melanoma. *Hum Pathol.* 2016; 57: 116-125
83. Feldmeyer L, Hudgens CW, Lyons GR, Nagarajan P, Aung PP, Curry JL, Torres Cabala CA, Mino B, Rodriguez-Canales J, Reuben A, Chen PL, Ko JS, Billings SD, Bassett RL, Wistuba II, Cooper ZA, Prieto VG, Wargo JA, Tetzlaff MT. Density, distribution, and composition of immune infiltrates correlate with survival in Merkel cell carcinoma. *Clin Cancer Res.* 2016 May 10.
84. Laga AC, Zhan Q, Weishaupt C, Ma J, Frank MH, Murphy GF. SOX2 and nestin expression in human melanoma: an immunohistochemical and experimental study. *Exp Dermatol.* 2011 Apr;20[4]:339-45.
85. Kikuchi E, Yamazaki K, Torigoe T, Cho Y, Miyamoto M, Oizumi S, Hommura F, Dosaka-Akita H, Nishimura M. HLA class I antigen expression is associated with a favorable prognosis in early stage non-small cell lung cancer. *Cancer Sci.* 2007 Sep;98[9]:1424-30. Epub 2007 Jul 23.
86. Al-Batran SE, Rafiyan MR, Atmaca A, Neumann A, Karbach J, Bender A, Weidmann E, Altmannsberger HM, Knuth A, Jäger E. Intratumoral T-cell infiltrates and MHC class I expression in patients with stage IV melanoma. *Cancer Res.* 2005 May 1;65[9]:3937-41.
87. del Campo AB, Kyte JA, Carretero J, Zinchenko S, Méndez R, González-Aseguinolaza G, Ruiz-Cabello F, Aamdal S, Gaudernack G, Garrido F, Aptsiauri N. Immune escape of cancer cells with beta2-microglobulin loss over the course of metastatic melanoma. *Int J Cancer.* 2014 Jan 1;134[1]:102-13.
88. Garrido F, Algarra I, García-Lora AM. The escape of cancer from T lymphocytes: immunoselection of MHC class I loss variants harboring structural-irreversible "hard" lesions. *Cancer Immunol Immunother.* 2010 Oct;59[10]:1601-6.
89. Chang CC, Pirozzi G, Wen SH, Chung IH, Chiu BL, Errico S, Luongo M, Lombardi ML, Ferrone S. Multiple structural and epigenetic defects in the human leukocyte antigen class I antigen presentation pathway in a recurrent metastatic melanoma following immunotherapy. *J Biol Chem.* 2015 Oct 30;290[44]:26562-75.
90. Bradley SD, Melendez B, Talukder A, Lizée G. Trouble at the core: BRAF[V600E] drives multiple modes of T-cell suppression in melanoma. *Oncoimmunology.* 2015 Aug 25;5[2]:e1078966.

91. Garrido C, Paco L, Romero I, Berruguilla E, Stefansky J, Collado A, Algarra I, Garrido F, Garcia-Lora AM. MHC class I molecules act as tumor suppressor genes regulating the cell cycle gene expression, invasion and intrinsic tumorigenicity of melanoma cells. *Carcinogenesis*. 2012 Mar;33[3]:687-93.
92. Buferne M, Chasson L, Grange M, Mas A, Arnoux F, Bertuzzi M, Naquet P, Leserman L, Schmitt-Verhulst AM, Auphan-Anezin N. IFN γ producing CD8+ T cells modified to resist major immune checkpoints induce regression of MHC class I-deficient melanomas. *Oncoimmunology*. 2015 Mar 6;4[2]:e974959.
93. Hiltbrunner S, Larssen P, Eldh M, Martinez-Bravo MJ, Wagner AK, Karlsson MC, Gabrielsson S. Exosomal cancer immunotherapy is independent of MHC molecules on exosomes. *Oncotarget*. 2016 May 25.
94. Capasso C, Hirvonen M, Garofalo M, Romaniuk D, Kuryk L, Sarvela T, Vitale A, Antopolsky M, Magarkar A, Viitala T, Suutari T, Bunker A, Yliperttula M, Urtti A, Cerullo V. Oncolytic adenoviruses coated with MHC-I tumor epitopes increase the antitumor immunity and efficacy against melanoma. *Oncoimmunology*. 2015 Oct 29;5[4]:e1105429.
95. Cafri G, Sharbi-Yunger A, Tzehoval E, Alteber Z, Gross T, Vadai E, Margalit A, Gross G, Eisenbach L. mRNA-transfected Dendritic Cells Expressing Polypeptides That Link MHC-I Presentation to Constitutive TLR4 Activation Confer Tumor Immunity. *Mol Ther*. 2015 Aug;23[8]:1391-400.
96. Compton LA, Murphy GF, Lian CG. Diagnostic Immunohistochemistry in Cutaneous Neoplasia: An Update. *Dermatopathology [Basel]*. 2015 Apr 8;2[1]:15-42.
97. Tumei PC, Harview CL, Yearley JH, Shintaku IP, Taylor EJ, Robert L, Chmielowski B, Spasic M, Henry G, Ciobanu V, West AN, Carmona M, Kivork C, Seja E, Cherry G, Gutierrez AJ, Grogan TR, Mateus C, Tomasic G, Glaspy JA, Emerson RO, Robins H, Pierce RH, Elashoff DA, Robert C, Ribas A. PD-1 blockade induces responses by inhibiting adaptive immune resistance. *Nature* 2014 Nov 27;515(7528):568-71
98. Cimino-Mathews A, Thompson E, Taube JM, Ye X, Lu Y, Meeker A, Xu H, Sharma R, Lecksell K, Cornish TC, Cuka N, Argani P, Emens LA. PD-L1 [B7-H1] expression and the immune tumor microenvironment in primary and metastatic breast carcinomas. *Hum Pathol*. 2016 Jan;47[1]:52-63.
99. Herbst RS, Soria JC, Kowanetz M, Fine GD, Hamid O, Gordon MS, et al. Predictive correlates of response to the anti-PD-L1 antibody MPDL3280A in cancer patients. *Nature* 2014;515:563–7.
100. Taube JM, Anders RA, Young GD, Xu H, Sharma R, McMiller TL, Chen S, Klein AP, Pardoll DM, Topalian SL, Chen L. Colocalization of inflammatory response with B7-h1 expression in human melanocytic lesions supports an adaptive resistance mechanism of immune escape. *Sci Transl Med*. 2012 Mar 28;4[127]:127ra37.
101. Thompson E, Taube JM, Elwood H, Sharma R, Meeker A, Warzecha HN, Argani P, Cimino-Mathews A, Emens LA. The immune microenvironment of breast ductal carcinoma in situ. *Mod Pathol*. 2016 Mar;29[3]:249-58.
102. Hugo W, Zaretsky JM, Sun L et al. Genomic and Transcriptomic Features of Response to Anti-PD-1 Therapy in Metastatic Melanoma. *Cell* 2016; 165: 35-44. [2016].
103. Gandhi L BA, Hui R. MK-3475 [anti-PD-1 monoclonal antibody] for non-small cell lung cancer [NSCLC]L Antitumor activity and association with tumor PD-L1 expression. [abstract]. In: Proceedings of the 105th Annual Meeting of the American Association for Cancer Research; 2014 Apr 5–9; San Diego, CA. Philadelphia [PA]: AACR; 2014. Abstract nr CT105.
104. Daud AI HO, Ribas A. Antitumor activity of the anti-PD-1 monoclonal antibody MK-3475 in melanoma: Correlation of tumor PD-L1 expression with outcome[abstract]. In: Proceedings of the 105th Annual Meeting of the American Association for Cancer Research; 2014 Apr 5-9; San Diego, CA. Philadelphia [PA]: AACR; Abstract nr CT104.
105. Johnson DB, Estrada MV, Salgado R, Sanchez V, Doxie DB, Opalenik SR, Vilgelm AE, Feld E, Johnson AS, Greenplate AR, Sanders ME, Lovly CM, Frederick DT, Kelley MC, Richmond A, Irish JM, Shyr Y, Sullivan RJ, Puzanov I,

Sosman JA, Balko JM. Melanoma-specific MHC-II expression represents a tumour-autonomous phenotype and predicts response to anti-PD-1/PD-L1 therapy. *Nat Commun.* 2016 Jan 29;7:10582.

106. Donia M, Kjeldsen JW, Svane IM. The controversial role of TNF in melanoma. *Oncoimmunology.* 2015 Oct 29;5[4]:e1107699.

107. Llosa NJ, Cruise M, Tam A, Wicks EC, Hechenbleikner EM, Taube JM, Blosser RL, Fan H, Wang H, Luber BS, Zhang M, Papadopoulos N, Kinzler KW, Vogelstein B, Sears CL, Anders RA, Pardoll DM, Housseau F. The vigorous immune microenvironment of microsatellite instable colon cancer is balanced by multiple counter-inhibitory checkpoints. *Cancer Discov.* 2015 Jan;5[1]:43-51.

108. Matsushita H, Vesely MD, Koboldt DC, Rickert CG, Uppaluri R, Magrini VJ, Arthur CD, White JM, Chen YS, Shea LK, Hundal J, Wendl MC, Demeter R, Wylie T, Allison JP, Smyth MJ, Old LJ, Mardis ER, Schreiber RD. Cancer exome analysis reveals a T-cell-dependent mechanism of cancer immunoediting. *Nature.* 2012 Feb 8;482[7385]:400-4.

109. Buckanovich RJ, Facciabene A, Kim S, Benencia F, Sasaroli D, Balint K, Katsaros D, O'Brien-Jenkins A, Gimotty PA, Coukos G. Endothelin B receptor mediates the endothelial barrier to T cell homing to tumors and disables immune therapy. *Nat Med.* 2008 Jan;14[1]:28-36.

110. Erdag G, Schaefer JT, Smolkin ME, Deacon DH, Shea SM, Dengel LT, Patterson JW, Slingluff CL Jr. Immunotype and immunohistologic characteristics of tumor-infiltrating immune cells are associated with clinical outcome in metastatic melanoma. *Cancer Res.* 2012 Mar 1;72[5]:1070-80.

111. Brinkman CC, Iwami D, Hritzo MK, Xiong Y, Ahmad S, Simon T, Hippen KL, Blazar BR, Bromberg JS. Treg engage lymphotoxin beta receptor for afferent lymphatic transendothelial migration. *Nat Commun.* 2016 Jun 21;7:12021.

112. Strønen E, Toebes M, Kelderman S2, van Buuren MM2, Yang W1, van Rooij N2, Donia M3, Bösch ML1, Lund-Johansen F4, Olweus J5, Schumacher TN6. Targeting of cancer neoantigens with donor-derived T cell receptor repertoires. *Science.* 2016 Jun 10;352[6291]:1337-41. doi: 10.1126/science.aaf2288. Epub 2016 May 19.

113. S. A. Rosenberg, N. P. Restifo, Adoptive cell transfer as personalized immunotherapy for human cancer. *Science* 348, 62–68 [2015].

114. Vasaturo A, Halilovic A, Bol KF, Verweij DI, Blokx WA, Punt CJ, Groenen PJ, van Krieken HJ, Textor J, de Vries IJ, Figdor CG. T cell landscape in a primary melanoma predicts the survival of patients with metastatic disease after their treatment with dendritic cell vaccines. *Cancer Res.* 2016 Apr 11.

115. Loo K, Daud A. Emerging biomarkers as predictors to anti-PD1/PD-L1 therapies in advanced melanoma. *Immunotherapy.* 2016 Jun;8[7]:775-84.

116. Koguchi Y, Hoen HM, Bambina SA, Rynning MD, Fuerstenberg RK, Curti BD, Urba WJ, Milburn C, Bahjat FR, Korman AJ, Bahjat KS. Serum Immunoregulatory Proteins as Predictors of Overall Survival of Metastatic Melanoma Patients Treated with Ipilimumab. *Cancer Res.* 2015 Dec 1;75[23]:5084-92.

117. Galon J, Pagès F, Marincola FM, Angell HK, Thurin M, Lugli A, Zlobec I, Berger A, Bifulco C, Botti G, Tatangelo F, Britten CM, Kreiter S, Chouchane L, Delrio P, Arndt H, Asslaber M, Maio M, Masucci GV, Mihm M, Vidal-Vanaclocha F, Allison JP, Gnjatic S, Hakansson L, Huber C, Singh-Jasuja H, Ottensmeier C, Zwierzina H, Laghi L, Grizzi F, Ohashi PS, Shaw PA, Clarke BA, Wouters BG, Kawakami Y, Hazama S, Okuno K, Wang E, O'Donnell-Tormey J, Lagorce C, Pawelec G, Nishimura MI, Hawkins R, Lapointe R, Lundqvist A, Khleif SN, Ogino S, Gibbs P, Waring P, Sato N, Torigoe T, Itoh K, Patel PS, Shukla SN, Palmqvist R, Nagtegaal ID, Wang Y, D'Arrigo C, Kopetz S, Sinicrope FA, Trinchieri G, Gajewski TF, Ascierto PA, Fox BA. Cancer classification using the Immunoscore: a worldwide task force. *J Transl Med.* 2012 Oct 3;10:205.

118. Blank CU, Haanen JB, Ribas A, Schumacher TN. CANCER IMMUNOLOGY. The "cancer immunogram". *Science.* 2016 May 6;352[6286]:658-60.

119. Mlecnik B, Bindea G, Kirilovsky A, Angell HK, Obenauf AC, Tosolini M, Church SE, Maby P, Vasaturo A, Angelova M, Fredriksen T, Mauger S, Waldner M, Berger A, Speicher MR, Pagès F, Valge-Archer V, Galon J. The tumor microenvironment and Immunoscore are critical determinants of dissemination to distant metastasis. *Sci Transl Med.* 2016 Feb 24;8[327]:327ra26.
120. Angell H, Galon J. From the immune contexture to the Immunoscore: the role of prognostic and predictive immune markers in cancer. *Curr Opin Immunol* 2013;25:261–7.

A high resolution landscape of the tumor microenvironment in melanoma is nowadays needed for a precise use of immunotherapeutic drugs. In the context of an “in situ” (directly in the tissue of the patient) investigation of the inflammatory response against melanoma, this thesis aims at clarifying the role of poorly investigated or controversial components of the inflammatory infiltrate. In particular we will focus on:

- I. **Plasma cells:** not only the role of B cells is controversial in melanoma, but also the terminally differentiated form of the B cell, the plasma cell, has not been properly investigated in literature. We will quantify plasma cells in melanoma microenvironment and assess their impact on survival. We will explore possible mechanisms through which plasma cells can influence the melanoma microenvironment, such as type of immunoglobulin produced, clonal expansion and recirculation to the lymph nodes. Therefore, we will use immunohistochemistry and Gene Scan Analysis.
- II. **HLA-DR expression in melanoma cells:** MHC II positivity in melanoma cells is still controversial, being associated both with good prognostic factors, such as lymphocytic infiltration and longer survival, but also with the presence of immunosuppressive T cells. Moreover, since HLA-DR expression in melanoma has been identified as one of the possible predictors of response to immunotherapy, we will investigate the associated inflammatory microenvironment, in order to clarify part of the mechanism involved in it. We will do this starting with microdissection and proceeding with next generation sequencing, multiplex ELISA and immunohistochemistry.
- III. **Tumor Infiltrating lymphocytes (TILs):** the morphological classification of the TILs has a known prognostic significance but its predictive value has not been proved yet. Moreover, the activation status of the TILs may add predictive value to the morphological classification of TILs, therefore we will investigate the association of TILs activation/exhaustion with the brisk/non-brisk morphological patterns of TILs infiltration and the presence of regression. Moreover, we will characterize directly on the tissue section the immune microenvironment associated with activation and exhaustion and the relationship of the different cell types involved through neighbours analysis. We will apply a novel high throughput multiplex immunostaining technique, combined with qPCR and shotgun proteomics followed by pathway analysis to confirm the results at multiple levels.

CHAPTER I - PLASMA CELLS IN PRIMARY MELANOMA. PROGNOSTIC SIGNIFICANCE AND POSSIBLE ROLE OF IGA

PUBLISHED

Plasma cells in primary melanoma. Prognostic significance and possible role of IgA

Francesca M Bosisio^{1,2}, James S Wilmott³, Nathalie Volders¹, Marjorie Mercier⁴, Jasper Wouters¹, Marguerite Stas⁵, Willeke AM Blokk⁶, Daniela Massi⁷, John F Thompson³, Richard A Scolyer^{3,8}, Nicolas van Baren⁴ and Joost J van den Oord¹

¹Laboratory of Translational Cell and Tissue Research, University of Leuven, KUL, Leuven, Belgium; ²Università Degli Studi di Milano-Bicocca, Milan, Italy; ³Melanoma Institute Australia, The University of Sydney, Sydney, NSW, Australia; ⁴Ludwig Institute for Cancer Research and de Duve Institute, Université Catholique de Louvain, Brussels, Belgium; ⁵Department of Surgical Oncology, UZ Gasthuisberg and KU Leuven, Leuven, Belgium; ⁶Radboud University Medical Center, Nijmegen, The Netherlands; ⁷Department of Surgery and Translational Medicine, University of Florence, Florence, Italy and ⁸Department of Tissue Pathology and Diagnostic Oncology, Royal Prince Alfred Hospital, Camperdown, NSW, Australia

Abstract

Melanoma is one of the most immunogenic cancers, but also one of the most effective cancers at subverting host immunity. The role of T lymphocytes in tumor immunity has been extensively studied in melanoma, whereas less is known about the importance of B lymphocytes. The effects of plasma cells (PC), in particular, are still obscure.

The aim of this study was to characterize pathological features and clinical outcome of primary cutaneous melanomas associated with PC. Moreover, we investigated the origins of the melanoma-associated PC. Finally, we studied the outcome of patients with primary melanomas with PC.

We reviewed 710 melanomas to correlate the presence of PC with histological prognostic markers. Immunohistochemistry for CD138, and heavy and light chains was performed in primary melanomas (PM) and in loco-regional lymph nodes (LN), both metastatic and not metastatic. In 3 PM and in 9 LN with frozen material, VDJ-rearrangement was analyzed by Gene Scan Analysis. Survival analysis was performed on a group of 85 primary melanomas >2mm in thickness.

Forty-one cases (3.7%) showed clusters/sheets of PC. PC-rich melanomas occurred at an older age and were thicker, more often ulcerated and more mitotically active ($p < 0.05$). PC were polyclonal and often expressed IgA in addition to IgG. In LN, clusters/sheets of IgA+ PC were found both in the sinuses and subcapsular areas. Analysis of VDJ-rearrangements showed the IgA to be oligoclonal. Melanomas with clusters/sheets of PC had a significantly worse survival compared to melanomas without PC while, interestingly, melanomas with sparse PC were associated with a better clinical outcome ($p = 0.002$).

In conclusion, melanomas with sheets/clusters of PC are associated with worse prognosis. IgG and IgA are the isotypes predominantly produced by these PC. IgA oligoclonality suggests an antigen-driven response that facilitates melanoma progression by a hitherto unknown mechanism.

Introduction

Melanoma is one of the most immunogenic cancers, but also one of the cancers that is most adept at circumventing host anti-tumor immunity (1). In fact, the phenomenon of regression in primary melanomas is frequently only partial (23-58%), and complete regression is rare (12.4%), suggesting the presence of mechanisms that allow the tumor to resist immune attack (2). In recent years, the immune response in melanoma has gained much attention due to the efficacy of new therapies that act on its modulation by blocking immune check points (3) (4) (5) (6) (7). The immune response is the result of complex interactions between different types of cells, which can result in an immune stimulatory signal as well as an immune suppressive signal. Moreover, the very same type of cell can be influenced by the microenvironment to polarize into different functional states according to the need for an active immune response or of immune tolerance at a certain moment. This has been demonstrated for macrophages (M1 and M2 polarization) (8) (9) (10) (11), neutrophils (N1 and N2 polarization) (12) (13) and T lymphocytes (Th1, Th2, Th17 responses) (14) (15) (16).

The role of T lymphocytes and macrophages has been extensively studied in melanoma (13) (17) (18) (19) (20) (21) (22), whereas less is known on the role of B lymphocytes and plasma cells (PC). Recently, B lymphocytes have turned out to constitute between 0 and 50% of the tumor infiltrating lymphocytes (23) (24) (25) but controversy exists as to their precise role in melanoma progression (25) (26) (27) (28). Furthermore, the role of PC, the terminally differentiated form of B lymphocytes, has been the subject of two studies, one that links them with an increased risk of lymph node metastasis (29) and one that shows an association with poor survival (30), but the mechanisms underpinning these observations remain obscure.

The aim of the current study was to identify melanomas with a significant PC component in the inflammatory infiltrate, to study their detailed clinico-pathological characteristics and immunoglobulin expression, and to speculate on the origin of the PC response by examining the melanoma-draining loco-regional lymph nodes.

Materials and methods

Evaluation of cases

710 consecutive cases of invasive primary cutaneous melanoma from the Department of Pathology of the University Hospitals Leuven (KU Leuven), Belgium, were reviewed. According to their subtype, there were 544 superficial spreading melanomas (SSM), 83 nodular melanomas (NM), 25 acral lentiginous melanomas (ALM), and 58 "others" category that included special variants, like nevoid or desmoplastic melanomas, or cases with unknown subtype. The age of the patients ranged from 11 to 97 years old (median: 63 years old). 417 were females, and 293 males. 283 melanomas occurred on the limbs, 213 on the trunk, 83 in the head and neck area, and 38 on acral sites; from 93 cases, the site was not known. All lesions were evaluated for histological prognostic factors. In addition, 15 primary melanomas from Radboud University Medical Center (Nijmegen, The Netherlands) and 6 cases from the University of Florence (Florence, Italy), all containing sheets of PC, were available for analysis. Melanoma cases were semi-quantitatively evaluated according to the quantity of PC in the inflammatory infiltrate surrounding the melanoma and subdivided into four groups (Figure 1a). The first group included melanomas without PC (PCneg), while the other three groups included melanomas with increasing numbers of PC (in general, PC+).

All the available slides for each case were screened for the presence of PC. The relative number of PCs was quantified by a scoring system taking both the number and distribution pattern (clusters or single cells) into consideration. Score 1 was assigned when the PC in the infiltrate were sparse and scattered, with no tendency to cluster (PC1). Score 2 was used for melanomas in which PC were more abundant, with a

tendency to group in discrete clusters, containing at least 5 PC in contact with each other (PC2). The score 3 category showed confluent clusters of PC, forming sheets (PC3). To evaluate the impact of PC on the histology and outcome of melanoma, we grouped scores PC2 and PC3 under the heading “plasma cell-rich melanomas” (PC-rich, 34 cases). In 14 cases of PC+ melanoma, loco-regional lymphadenectomy specimens containing, both involved lymph nodes (8 cases) and uninvolved lymph nodes (6 cases), were available for study.

To evaluate the outcome of PC+ melanomas, an additional data set of 85 patients with thick melanomas (>2 mm, range 2.1-47 mm) and clinical follow-up data from a minimum of 3 to a maximum of 12 years (range: 1099 – 4633 days) was collected from the files of the Melanoma Institute Australia, Sydney, and the Departments of Tissue Pathology and Diagnostic Oncology, Royal Prince Alfred Hospital, Camperdown, New South Wales, Australia. We included this series of thick melanomas in order to enrich the samples for PC+ melanomas, and to minimize the impact of Breslow thickness on the outcome. In this melanoma set, the prevalent subtype was NM (31 cases), followed by SSM (24 cases), and ALM (12 cases). 18 cases were from special subtypes, mostly desmoplastic melanomas and malignant blue nevus cases. The most frequent site of occurrence was head and neck (26 cases), followed by trunk (16 cases), acral sites (16 cases) and limbs (15 cases). The outcome of the patients included 36 cases alive without recurrence, 3 alive with melanoma, 20 dead from melanoma, 3 cases dead due to unrelated cause and 11 cases died from unknown cause.

Immunohistochemistry

All biopsies were fixed in 10% buffered formalin and embedded in paraffin. The most representative section for each case was used for immunohistochemistry. Immunohistochemical analyses were performed on routinely fixed paraffin-embedded tissue sections on the Leica Bondmax automatic immunostainer, using ready-to-use antibodies from Dako directed against CD138, IgG, IgA, IgM, IgD, IgE, CD3, CD20 and CD21. The peripheral nodal addressin antibody was from Sigma-Aldrich (PNAd, clone: MECA, dilution 1:3000).

A semi-quantitative score was used to evaluate the number of IgA+ PC relative to the total number of CD138+ PC in the inflammatory infiltrate in sections stained with double IgA(red)/CD138(brown) immunohistochemistry. The quantity of double IgA/CD138 positive PC was scored as “-” if less than 10% of CD138+ PC was IgA+, “+” if IgA+/CD138 PC were between 10 and 50% and “++” if 50% or more of the CD138+ PC was IgA+ (Figure 1b).

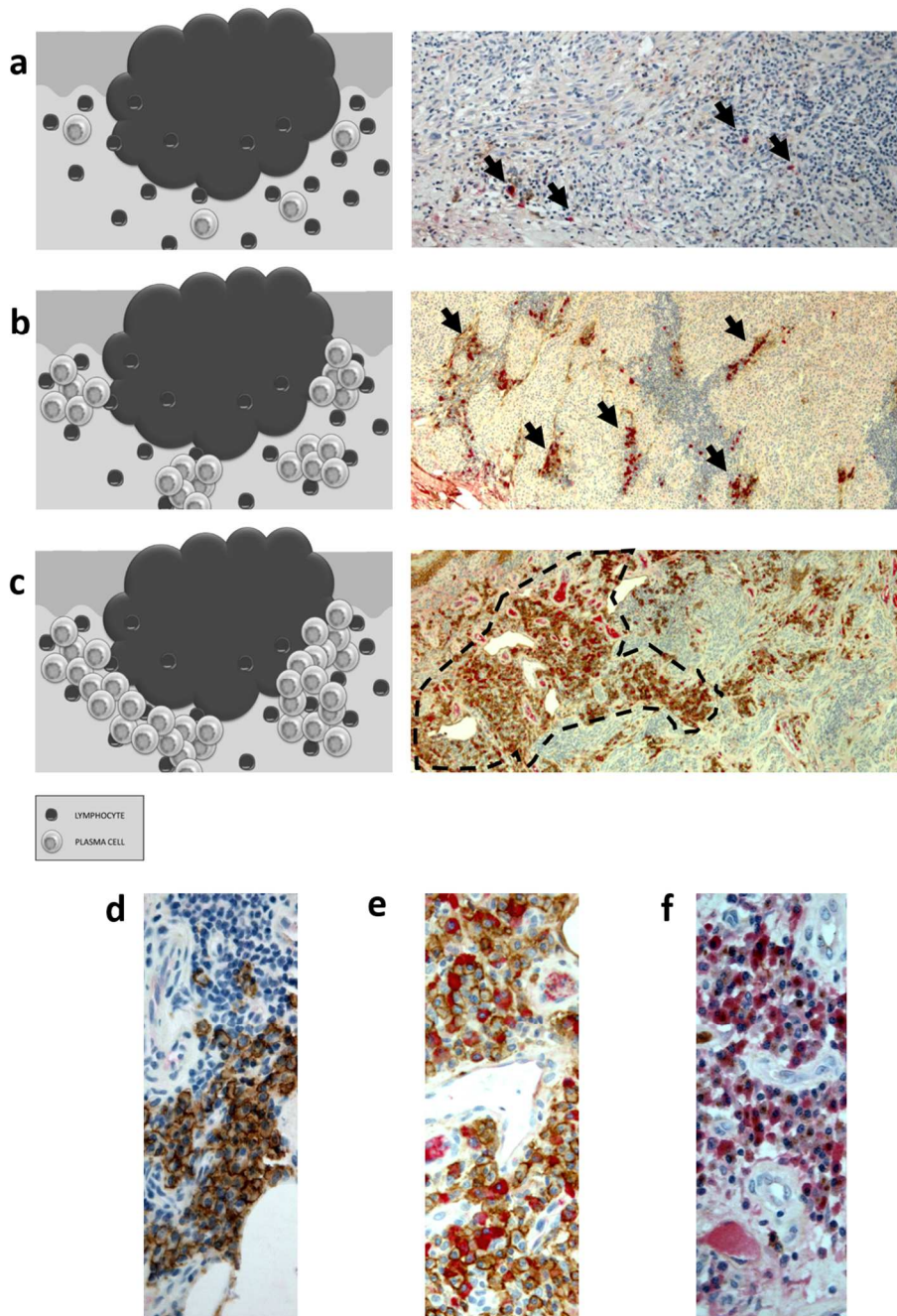


Figure 1 Definition of the plasma cells and IgA scores. (a) PC1 score was assigned when scattered plasma cells were found isolated in the infiltrate (arrows: plasma cells; double immunostaining for CD138 (brown) and IgA (red), 10x). (b) In PC2, plasma cells aggregated in clusters are found in the infiltrate (arrows: clusters of plasma cells; double immunostaining for CD138 (brown) and IgA (red), 10x) (c) Large clusters of PC merge together to form sheets in the tumoral stroma were scored as PC3 (a sheet is contoured by the discontinuous line; double immunostaining for CD138 (brown) and IgA (red), 10x). IgA+CD138+ plasma cells were qualitatively quantified in the infiltrate as less than 10% (20x) (d), between 10 and 50% (20x) (e), and > 50% or more of the total number of plasma cells (20x) (f).

Gene Scan Analysis

Representative material, snap frozen in liquid nitrogen-cooled isopentane, was available from 2 PC+ primary melanomas and 14 lymph nodes draining PC+ melanomas. Total RNA from the tumor samples was isolated with the Total RNA and DNA Purification Kit from Macherey-Nagel, according to the manufacturer's protocol. 500 micrograms of RNA was reversely transcribed into cDNA using Superscript II reverse transcriptase (Invitrogen) and a random hexamer (Fermentas). After treatment with RNaseH (Fermentas), the resulting cDNA was diluted for a final volume of 40 µl. For the Ig heavy chain characterisation of the samples a set of primers specific for the secretory (s) type and the membrane (m) type of all the immunoglobulins isotypes was used to perform the PCRs. Primers for actin and GADPH were used to check the cDNA quality, and a sample with water served as negative control. Amplification was carried out with Taq DNA polymerase (Takara), with 2,5 microl of cDNA in a 25 microl volume, and started with 4 minutes at 94 °C, followed by 36 cycles of 45 seconds at 94°C, 45 seconds at 58°C, 1 minute and 30 seconds at 72°C, and ended by a final step of 5 minutes at 72°C. The amplification products were checked with gel electrophoresis. For the Genescan Analysis the cDNA was amplified by 2 rounds of nested PCR. All the primers used are listed in Supplementary Table 2. For the first PCR, amplification was carried out with 2,5 microl of cDNA in a 25 microl volume, and started with 4 minutes at 94 °C, followed by 30 cycles of 45 seconds at 94°C, 45 seconds at 50°C, 45 seconds +2 sec/cycle at 72°C, for a total of 30 cycles, to end with 10 minutes at 72°C. For the second PCR, amplification was carried out with 2,5 microl of the first PCR product diluted one in a hundred in a 25 microl volume, and started with 4 minutes at 94 °C, followed by 36 cycles of 45 seconds at 94°C, 45 seconds at 57°C, 45 seconds +2 sec/cycle at 72°C, for a total of 30 cycles, to end with 10 minutes at 72°C. The amplification products were checked with gel electrophoresis. Size and quantity of the amplified DNA fragments were analyzed in combination with the Internal Standard Lane 600 (Promega) through the ABI PRISM 310 Genetic Analyzer and the GeneScan® Analysis. A polyclonal control (tonsil) and a monoclonal control (IgA myeloma cell line) were loaded together with the samples.

Statistical analysis

Statistical analysis was performed with Microsoft Office Excel and the GraphPad Prism 6.01 software. The Mann-Whitney test for not normally distributed data was used to calculate the p-values for age and Breslow. The Chi –Square test adjusted for not normally distributed data was used to evaluate the p-Values for the correlation of the other clinical and histological parameters analysed with the presence of PC. Survival rates were calculated according to the Kaplan-Meier method.

Results

Clinico-pathological features of PC+ melanomas

Of 710 primary cutaneous melanomas from the University Hospital Leuven, 41 (3.7%) showed a PC component in the inflammatory infiltrate associated with the melanoma. According to the PC score, 7 (18%) showed scattered PC (score PC1), 24 (58%) had discrete clusters of PC (score PC2) and 10 (24%) contained sheets of PC (score PC3). Since PC1 melanomas represent a condition in which the quantity of PC is low and could be not biologically relevant, we focused in the statistical analysis on PC2 and PC3 cases to better characterize melanomas in which the amount of PC is important, and labelled these 34 cases (82%) as “PC-rich” melanomas. From score PC1 to score PC3, an increase in the number of intra-tumoral PC that were in direct contact with the melanoma cells, was observed. In fact, while in 6 out of 7 PC1 melanomas the PC were only in peritumoral location, PC2 and PC3 melanomas showed the PC to be located within the tumor mass (15/24 (62,5%) and 8/10 (80%) cases with intratumoral PC respectively, p 0,006). Clinical and histological features of PC-rich melanomas are shown in Supplementary Table 1, and the statistical analysis is resumed in Figure 2. The average age at the diagnosis for PC-rich melanomas was 63 years (range 20-86, median 63) and 55 years for melanomas without PC (range 11-97, median 55), suggesting that PC-rich melanomas occur

in patients 10 years older than PCneg melanomas (p 0.005). 19/34 (56%) patients with PC-rich melanomas were males, and 15/34 (44%) were females. PC-rich melanomas affected, in decreasing order, the trunk, limbs, head and neck areas, and acral sites, while PCneg melanomas were mostly on the limbs and less frequently on the trunk, head and neck area, and acral sites. PC-rich melanomas were more often of the nodular subtype than PCneg melanomas (p 0.00046). Three strongly evidence-based markers of bad prognosis in melanoma (high Breslow thickness, >6 mitoses/mm² and the presence of ulceration) were found to be associated with the presence of PC in melanoma (p < 0.0001). The incidence of PC+ melanomas increased to 19.5% if only cases with a Breslow thickness over 2 mm were taken into account. A correlation with the presence of lymphatic/vascular invasion was also found (p 0.015). Histological examination of the 15 cases from Nijmegen, The Netherlands, and 6 cases from Firenze, Italy, revealed similar unfavourable prognostic features in melanomas with sheets of PC.

No significantly different clinical features were found between score PC1, PC2, and PC3. The three PC scores differed significantly only for two histopathological parameters, i.e. the PC distribution in the tumor microenvironment, and the thickness of the melanoma according to Breslow. Regarding the distribution of PC, the number of intratumoral PC increased from score PC1 to score PC3, indicating that with increasing numbers of PC in the inflammatory infiltrate, these PC tended to be more in direct contact with melanoma cells (p 0.006). Moreover, PC3 melanomas were significantly thicker than PC2 and PC1 melanomas (p 0.008). All other histopathological parameters (subtype, mitotic rate, ulceration, regression, lymphatic/vascular invasion, microsatellites) were not significantly correlated with the number of PC in the infiltrate.

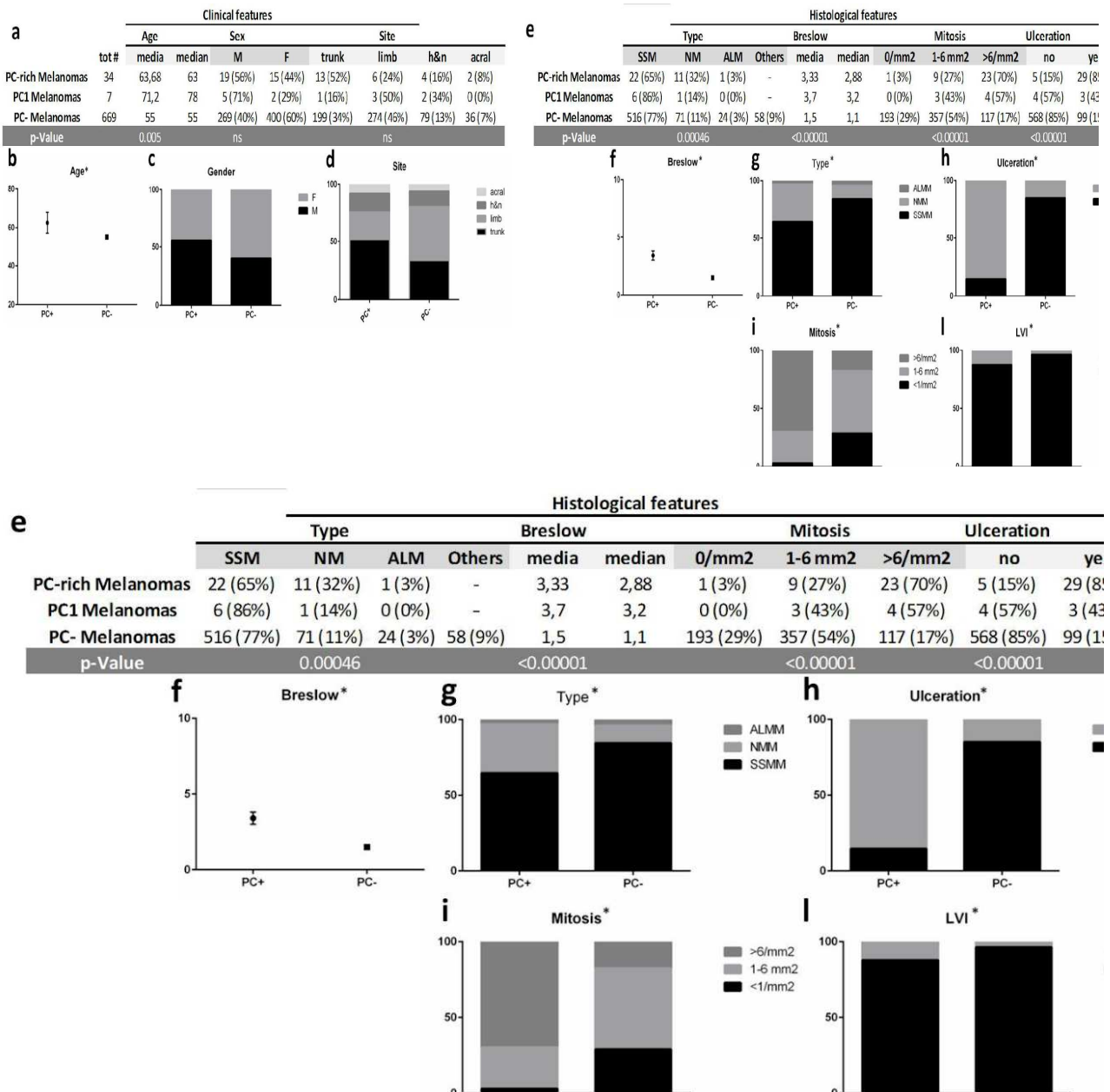


Figure 2 Statistical analysis of the clinical and histopathological features of PC-rich, PC1 and PC- melanomas. Parameters that reach significance are marked by asterisks.

H&N = head and neck

SSM = superficial spreading melanoma

NM = nodular melanoma

ALM = acral lentiginous melanoma

LVI = lymph/vascular invasion

Cases from Leuven (#)	PC SCORE	CLINICAL FEATURES			HISTOLOGICAL FEATURES					
		Sex	Age	Site	Subtype	Breslow thickness (mm)	Ulceration	Regression	Mitoses/mm ²	Lymph/vascular invasion
1	3	F	65	trunk	SSM	2,05	no	no	1-6	no
2	3	F	80	-	NM	2,75	yes	yes	>6	no
3	3	F	72	-	SSM	4,9	yes	no	>6	no
4	3	M	69	trunk	SSM	7,6	yes	no	>6	no
5	3	F	75	limb	SSM	2,5	yes	no	>6	no
6	3	F	86	trunk	SSM	2,4	yes	no	>6	no
7	3	M	51	-	NM	5,3	yes	yes	>6	no
8	3	M	68	h&n	SSM	5,4	yes	no	>6	no
9	3	M	64	trunk	SSM	2,31	yes	no	>6	yes
10	3	M	77	trunk	NM	1,3	yes	no	>6	yes
11	2	M	61	acral	SSM	2,69	yes	no	1-6	no
12	2	M	29	trunk	NM	1,28	yes	no	1-6	no
13	2	M	36	trunk	SSM	3,2	yes	no	>6	yes
14	2	M	29	limb	NM	2,94	yes	no	>6	no
15	2	M	54	acral	ALM	3	no	yes	1-6	no
16	2	F	78	h&n	SSM	4,64	yes	no	>6	no
17	2	M	20	h&n	NM	2,24	yes	yes	1-6	no
18	2	F	62	trunk	SSM	6,29	yes	yes	>6	no
19	2	M	82	h&n	SSM	2,69	yes	no	>6	no
20	2	F	60	trunk	SSM	0,91	no	yes	1-6	no
21	2	M	80	-	NM	5,6	yes	no	>6	no
22	2	M	59	-	SSM	2,13	yes	yes	>6	no
23	2	F	48	limb	NM	2,88	yes	no	1-6	no
24	2	M	26	-	SSM	5,6	yes	yes	>6	no
25	2	F	56	genital	SSM	3,4	yes	no	>6	no
26	2	M	72	limb	SSM	2,16	yes	no	>6	no
27	2	M	73	limb	SSM	2,25	yes	no	>6	no
28	2	M	48	trunk	NM	5,2	yes	no	>6	no
29	2	M	50	trunk	SSM	0,68	yes	yes	1-6	no
30	2	F	69	limb	SSM	2,07	no	yes	>6	no
31	2	F	75	-	NM	3,2	yes	no	>6	no
32	2	F	53	-	NM	4,18	yes	no	1-6	no
33	2	F	85	trunk	SSM	4,3	yes	yes	0	yes
34	2	F	55	trunk	SSM		no	yes	nv	nv
35	1	F	47	limb	SSM	9,2	yes	no	>6	yes
36	1	M	86	trunk	SSM	3,7	no	yes	1-6	no
37	1	M	73	limb	NM	1,86	yes	no	1-6	no
38	1	M	78	-	SSM	2,56	no	yes	>6	no
39	1	M	57	h&n	SSM	3,2	yes	yes	>6	no
40	1	F	80	limb	SSM	3,26	no	no	>6	no
41	1	M	78	h&n	SSM	2,6	no	yes	1-6	no
Cases from Florence (#)										
1	3	F	88	limb	SSM	5	yes	yes	1-6	no
2	3	M	83	trunk	NM	5	yes	no	1-6	no
3	3	M	84	h&n	NM	6	yes	no	>6	no
4	3	M	47	trunk	SSM	6,5	yes	no	1-6	yes
5	3	M	77	h&n	NM	4,1	yes	no	>6	no
6	3	F	67	limb	NM	21,8	yes	no	>6	no
7	3	F	90	limb	SSM	6,5	yes	yes	1-6	yes
8	3	M	78	trunk	NM	4,4	yes	no	1-6	no
9	2	F	78	limb	SSM	6	yes	yes	>6	no
10	2	M	50	h&n	NM	12	yes	no	>6	no
11	2	M	22	trunk	SSM	4,8	yes	yes	1-6	no
12	2	M	81	h&n	NM	13	yes	no	1-6	no
13	1	M	80	trunk	NM	5	yes	no	>6	no
14	1	M	66	trunk	NM	6	no	yes	1-6	yes
15	1	M	88	h&n	NM	5,4	yes	no	>6	no
Cases from Nijmegen (#)										
1	3	F	87	limb	SSM	10	yes	yes	>6	no
2	2	M	88	h&n	SSM	2,8	yes	yes	1-6	yes
3	2	M	62	trunk	NM	5,3	no	no	>6	no
4	2	M	40	-	-	3,9	yes	no	>6	yes
5	2	M	58	trunk	NM	9	yes	no	>6	no
6	1	F	53	genital	SSM	2,3	yes	no	1-6	no

Supplementary Table 1 Clinical and histopathological features of PC-rich, PC1 and PC- melanomas.

Primers for IgH characterization	pan-IgG	NVB097 5'-CAA ^g CCC ^g CAACACCA ^g -3'	NVB044 (s) 5'-gCC ^g TggCACTCATTTACC-3'
	pan-IgA	NVB052 5'-gAA ^g CACTACAC ^g AATCCC ^g -3'	NVB098 (m) 5'-AggAA ^g AgTgTgATgAA ^g ATgg-3'
	pan-IgE	NVB055 5'-ACACTCCATCgTCCAC ^g AC-3'	NVB053(s) 5'-gCCATgACAAC ^g ACACATTgAC-3'
	actin	GCA CCA CAC CTT CTA CAA TG	NVB054(m) 5'-AgAgggTgAggAA ^g TgATg-3'
	GADPH	TGA AGG TCG GAG TCA ACG GAT TTG GT	NVB056(s) 5'-gAggC ^g AggAgTACgTCATTAC-3'
			NVB057(m) 5'-TCACgCTgAgC ^g AggAA ^g AgT-3'
			TGC TTG CTG ATC CAC ATC TG
			CAT GTG GGC CAT GAG GTC CAC CAC
		Sense	Antisense
Primers for Gene Scan Analysis	first PCR: degenerated primers mix*	VHL-1 5'-TCACCATggACTgSACCTgA-3'	NVB047(IgD-s) 5'-TggggCCATggTCTgTTACA-3'
		VHL-2 5'-CCATggACACACTTTgYTCCAC-3'	NVB050(IgM-s) 5'-ATgACCAgggACACgTTgTAC-3'
		VHL-3 5'-TCACCATggAgTTTgggCTgAgC-3'	NVB044 (IgG-s) 5'-gCCgTggCACTCATTTACC-3'
		VHL-4 5'-AgAACATgAAACAYCTgTggTTCTT-3'	NVB053(IgA-s) 5'-gCCATgACAAC ^g ACACATTgAC-3'
		VHL-5 5'-ATggggTCAACCgCCATCCT-3'	
		VHL-6 5'-ACAATgTCTgTCTCCTTCCTCAT-3'	
	second PCR: degenerated primers mix*	VH-1 5'-CAggTSCAgCTggTRCgTC-3'	NVB137(IgD) 5'6FAM-CTgATATgATgggAAC-3'
		VH-2 5'-CAgRTCACCTTgAAggAgTC-3'	NVB1138 (IgM) 5'6FAM-gAAgCCCCgggTACTgCT-3'
		VH-3 5'-SAggTgCAGCTggTggAgTC-3'	NVB1139 (IgG) 5'6FAM-AgTTCCACgACACCgTCAC-3'
		VH-4 5'-CAggTgCAGCTgCaggAgTC-3'	NVB140(IgA) 5'6FAM-gCATgTCACggACTTgCC-3'
		VH-5 5'-gARgTgCAGCTggTgCgTC-3'	
		VH-6 5'-CAggTACAgCTgCAGCgTC-3'	

Supplementary Table 2 Primers

Immunohistochemical features of PC+ melanomas

Sixteen cases of PC+ primary melanomas were available for immunohistochemical analysis. Immunohistochemistry for Ig light chains showed the PC to be polyclonal (data not shown) and staining for different isotypes of immunoglobulins (IgA, IgG, IgM, IgD, IgE) revealed that the major part (usually more than 50%) of the PC in the melanoma-associated inflammatory infiltrate was positive for IgG (data not shown). Interestingly, an equally important PC component of the infiltrate expressed IgA. Using double chromogenic immunohistochemistry for the membranous PC marker CD138 (brown) and cytoplasmic IgA (red) the quantity of IgA+ PC as a fraction on the total of the CD138+ PC was evaluated in PC+ melanomas. In 3/16 (18%) of the cases, more than 50% of PC expressed IgA, in 7/16 (44%), 10-50% of PC expressed IgA, and 6/16 (38%) cases were devoid of a significant IgA+ PC component. In total, 56% of cases showed more than 10% of all PC to express IgA and all these cases had clusters (PC2 score) or sheets (PC3 score) of PC. The distribution of the IgA+CD138+ score from PC1 to PC3 melanomas showed that IgA+ PC increased with increasing numbers of PC in the melanoma (Table 1). In order to rule out that ulceration by itself was the trigger for IgA switch, 20 randomly chosen non-neoplastic ulcers and two (positive control) genital and mucosal ulcers were analyzed histologically and immunohistochemically. Nine had PC in the infiltrate, and these ulcers occurred more frequently in head and neck areas (Supplementary Table 3). On double chromogenic immunohistochemistry, the number of IgA+ plasma cells was generally low in cutaneous non-neoplastic ulcers as compared to those at mucosal sites where equal numbers of IgA+ and IgG+ PC were found.

As they represent a site of plasma cell formation, the occurrence of tertiary lymphoid structures (TLS) in the inflammatory stroma was investigated by immunostainings in consecutive serial sections of 16 cases for CD20 (B-cells), CD3 (T-cells), CD21 (follicular dendritic cells (FDC), and peripheral nodal addressin (PNAd), a high endothelial venule (HEV) marker. The presence of B and T-cells, as well as FDC and HEV together in a lymphoid aggregate was considered to be sufficient to define a TLS (34). According to this criterium, only 2 out of 16 cases of PC+ melanoma presented with TLS (Table 1).

Molecular analysis of Ig genes expressed by PC+ melanomas

We first analyzed the isotype of the immunoglobulin-expressing cells present in 2 PC-rich primary melanomas, for which frozen material was available. We used RT-PCR to detect the IGHD, IGHM, IGHG, IGHA and IGHE transcripts, which encode the constant regions of Ig heavy chains (Figure 3a). The secreted isoforms of IgG and IgA were more expressed than the corresponding membranous isoforms and than the other isotypes, thus confirming that they are the main isotypes expressed by PC in melanoma.

To further characterize the clonality of the infiltrating PC, we analyzed the diversity of the Ig gene repertoire with the immunoscope approach. To this aim, we used two rounds of nested RT-PCR, including fluorochrome-coupled primers for the last PCR round, to amplify all the VDJ sequences present in IgG-s and IgA-s transcripts. The amplified fluorescent fragments were then separated according to their length by high-resolution electrophoresis (Figure 3b). In both tumors, the IgG were found to have a polyclonal pattern whereas the IgA repertoire was more restricted, indicating oligoclonality.

case #	PC Score	IgA+/CD138+	TLS
1	3	>50%	yes
2	3	>50%	no
3	3	10-50%	no
4	3	10-50%	no
5	3	10-50%	no
6	3	<10%	no
7	2	>50%	no
8	2	10-50%	no
9	2	10-50%	no
10	2	10-50%	no
11	2	10-50%	no
12	2	<10%	no
13	1	<10%	yes
14	1	<10%	no
15	1	<10%	no
16	1	<10%	no

Table 1 Immunohistochemical analysis. Double staining for IgA and CD138 showed an increase of the amount of IgA+ plasma cells that goes together with the quantity of plasma cells in the infiltrate. Immunohistochemistry for CD3, CD20, CD21 and pNAD identified the presence of tertiary lymphoid structures in only 2/16 cases.

Non neoplastic Ulcers	Site	PC score	IgA+/CD138+
ulcer nos	trunk	2	n.a.
ulcer nos	trunk	0	
ulcer nos	trunk	0	
ulcer nos	trunk	0	
ulcer nos	trunk	1	<10%
artifactual?	trunk	1	n.a.
Lichen	trunk	0	
ulcer nos	limb	2	10-50%
ulcer nos	limb	0	
ulcer nos	limb	0	
ulcer nos	limb	0	
re-excision melanoma	limb	0	
ulcer nos	h&n	3	<10%
ulcer nos	h&n	2	<10%
ulcer nos	h&n	2	<10%
Nodular condrodermatitis	h&n	0	
ulcer nos	acral	2	<10%
ulcer nos	acral	0	
ulcer nos	genitalia	0	
ulcer nos	mucosal	3	ca 50%

Supplementary Table 3 IgA in non neoplastic Ulcers

Case #	IgG-m	IgG-s	IgD-m	IgD-s	IgM-m	IgM-s	IgA-m	IgA-s	IgE-m	IgE-s
1	+	+++	+/-	+/-	+	++	+	++	-	+/-
2	++	+++	+	++	+	++	++	+++	+/-	+
IgA control	/	/	/	/	/	/	+++	+++	/	/
IgE control	/	/	/	/	/	/	/	/	++	+++

status	Frozen LN		FFPE LN		Gene Scan Analysis Conclusion
	PC score	IgA-s	PC score	IgA+/CD138+	
N+	3	poly	3	-	polyclonal
N+	2	oligo	2	-	IgA restriction
N+	2	oligo	2	+	IgA restriction
N+	1	mono	2	+	IgA restriction
N+	1	oligo	3	+	IgA restriction
N+	1	oligo	1	+	IgA restriction
N+	1	poly	3	+	IgM/IgG restriction
N+	1	oligo	2	+	IgA restriction
N-	2	oligo	2	+	IgA restriction

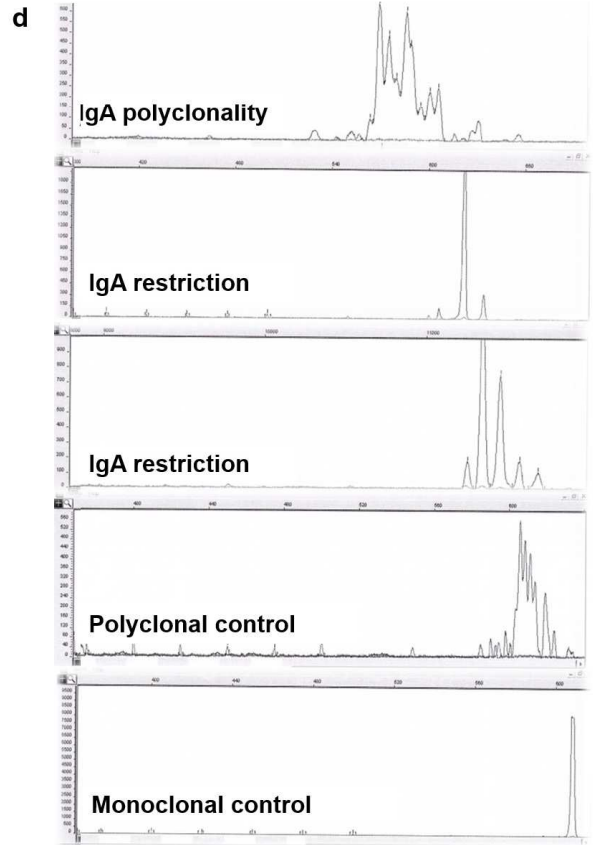
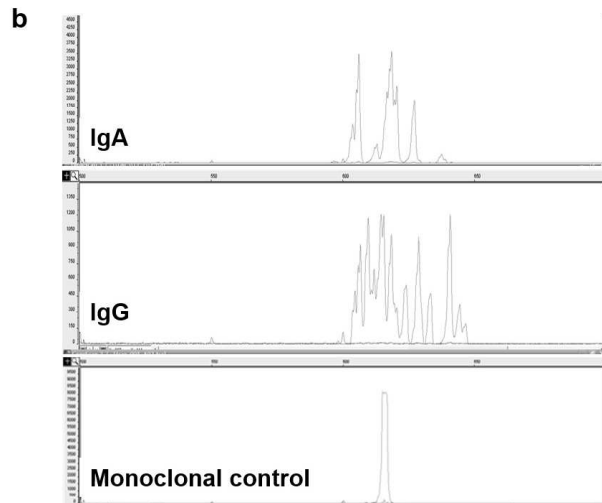


Figure 3 Molecular analysis of Ig genes expressed in PC-rich melanomas. (a) Identification by RT-PCR of the membrane-bound (m) and secreted (s) isoforms of the five Ig isotype families expressed in two primary melanomas with PC infiltration. (b) Immunoscope analysis of IgA-s and IgG-s in one of the two primary melanomas. (c,d) Immunoscope analysis of IgA-s in 9 LN draining PC-rich melanomas.

LN = lymph node, FFPE = formalin fixed paraffin embedded

N- = uninvolved lymph nodes, N+ = lymph nodes involved by the tumor

Analysis of lymph nodes draining PC+ melanomas

In the loco-regional lymph nodes, the same score used for primary melanomas was applied to quantify the amount of PC infiltrates. In lymph nodes with score 1, scattered PC were predominantly localized in the medullary sinuses. In lymph nodes with score 2 and 3, PCneg clusters and sheets were found in the medullary sinuses as well as in the sub-capsular region. In 12/14 lymph nodes draining the site of a PC+ melanoma, the PC score in the lymph node was the same or higher than the score in the corresponding primary melanoma. Therefore, a good correlation existed between the PC score in draining lymph nodes and primary melanoma (Figure 4). Using double IgA/CD138 immunohistochemistry, the percentage of IgA + PC varied between 10 and 50% of the total number of nodal PC in 11 out of 14 cases; moreover, a high percentage of IgA PC was also found in cases with scattered PC (PC1 score).

Gene Scan Analysis, focused on the secretory part of IgA, was performed on frozen material from 9 lymph nodes previously studied by immunohistochemistry. Seven of these cases had 10-50% IgA+ PC in the lymph node, whereas the other 2 had no relevant IgA component in the lymph node. In 7 out of 9 cases, Gene Scan Analysis showed oligoclonality of the secretory IgA component suggesting an antigen-driven IgA-immune response (Figure 3 c, d). In 2 out of 9 cases, a lymph node with sheets of PC (PC3) showed predominance of IgG PC, and a score 1 case with prominent IgA+ PC, had a polyclonal IgA secretory component. These two cases proved that, even in presence of a minority of IgA positive PC in the lymph node, polyclonality could be detected. Moreover, in the latter case (score 1 with prominent IgA+ PC), a restriction of IgM and IgG was detected, suggesting an antigen-driven immune response involving IgG and IgM, but not IgA.

Outcome of patients with PC+ melanomas

Since our data showed that PC are found in a low percentage of primary melanomas and that they are associated with unfavourable prognostic factors, we analyzed their outcome in a series of 85 thick melanomas from Australia. In this series, PC were found in 33 cases (38%), an important increase in comparison to the incidence of 19.5% of PC+melanomas that were found among the thick melanomas subgroup from the KUL data set. This could be due to differences between melanomas arising in the Belgian population compared to the Australian one. PC1 melanomas were 12 (36%), PC2 11 (33%), and PC3 10 (31%). In this series of thick melanomas, the presence of PC correlated again with Breslow thickness (p 0.0002), subtype of melanoma (p 0.0037), and ulceration (p 0.0002). On the other hand, mitotic count and lymphatic/vascular invasion, associated with the presence of PC in the original Leuven data set, lost significance in the series from Australia.

Immunohistochemical staining revealed that 21 out of 33 cases (70%) presented a relevant IgA+ PC component. The distribution of the IgA score was homogeneous among the PC scores: also cases with sparse PC showed predominant expression of IgA. In particular, 9 out of 12 PC1 melanomas presented between 10 and 50% of IgA+ PC in the infiltrate; 6 out of 11 PC2 melanomas had IgA+ PC (which in two cases comprised more than 50% of the PC) and 9 out of 10 PC3 melanomas had in almost all cases more than 50% of IgA+ PC.

Of the 52 cases without PC in the inflammatory infiltrate, 26 patients were alive without disease, 3 alive with melanomas, 11 dead due to melanoma and 12 dead due to a cause unrelated to melanoma or by unknown cause. Of the 21 PC-rich melanomas (PC2 and PC3), 10 patients were alive without disease, 9 dead due to melanoma, 1 dead due to other causes, and none alive with melanoma. Of the 12 PC1 melanoma patients, 8 were alive without disease, 2 were alive with melanomas, 1 dead due to melanoma and 1 dead due to unknown cause. The Kaplan-Meier curves of survival were not significant for the absolute presence or absence of PC in the inflammatory infiltrate, but were significant for the difference in survival of patients with PC-rich melanomas vs those with melanomas lacking PC and and PC1 melanomas (Figure 5). Hence,

patients with PC-rich melanomas showed a worse survival compared to those with PCneg melanomas (p: 0.002). The survival of patients with PC1 melanomas appeared to be better than that of patients with PCneg melanomas, but this finding did not reach statistical significance. The same difference in survival was found when comparing the survival patients with ulcerated melanomas at all sites with that of ulcerated melanomas on the limbs, thereby eliminating the bias of ulceration and site of occurrence (Supplementary figure 1).

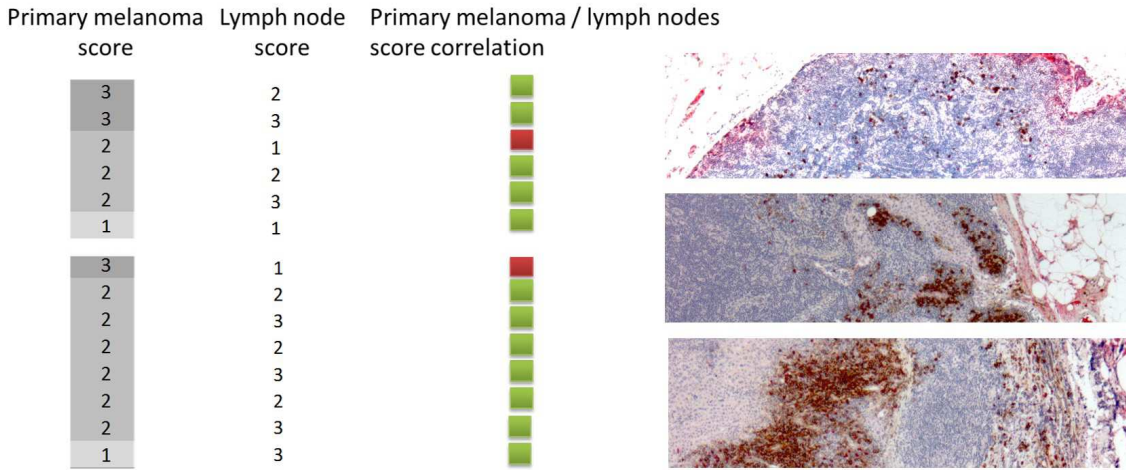


Figure 4 Correlation between the plasma cells score in primary melanomas and in lymph nodes. After application of the same scoring system used in primary melanomas, a good correlation (green = good correlation / red: poor correlation) was found between the amount of plasma cells in the tumoral site and in the draining lymph nodes (pictures on the right, from top to bottom sparse plasma cells, clusters and sheets in the lymph nodes).

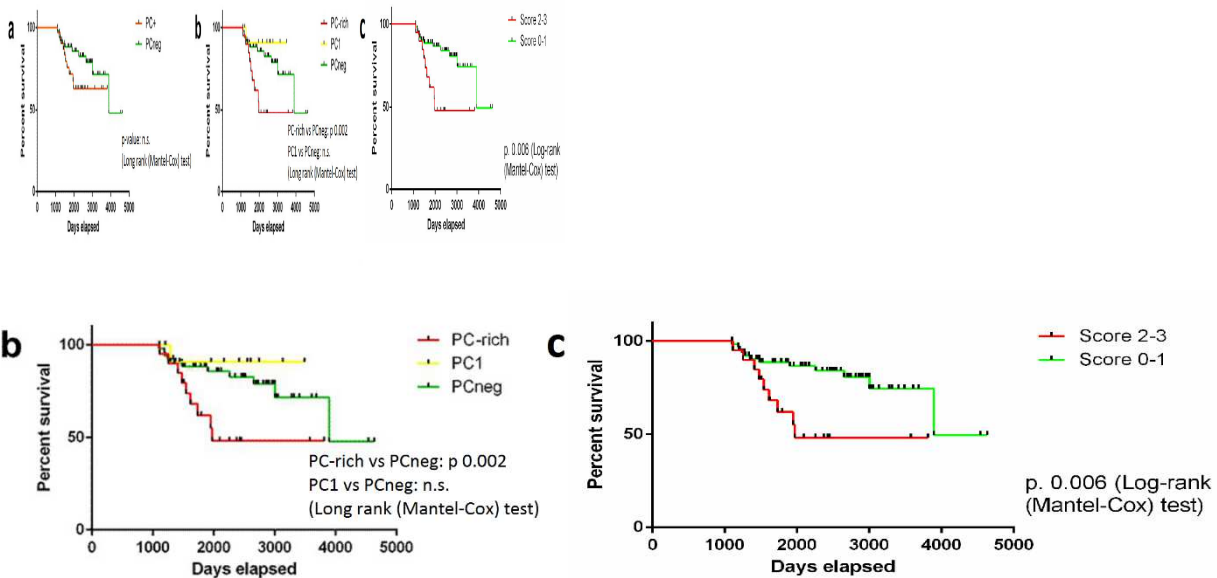
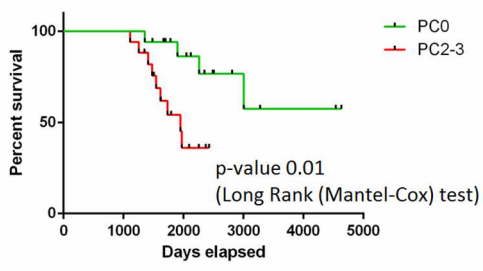
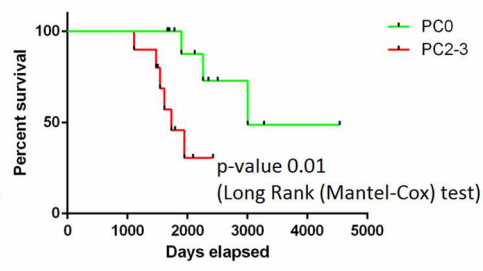


Figure 5 Survival analysis of melanomas with plasma cells. The overall survival does not significantly differ between PC+ and PC- melanomas (a), but among the different PC scores, the score 3 and score 2 melanomas (“PC-rich”), show a worse prognosis than score 0 (“PCneg”) and score 1 melanomas (p 0.002) (b), therefore these two last groups could be prognostically grouped together under the definition of “PClow” melanomas (c).

Survival in Ulcerated Melanomas (all sites)



Ulcerated, Only Limbs



Supplementary Figure 1

Discussion

Our work investigated the significance of PC in melanoma in a wide data set, because in the literature, the role of this B cell subtype in melanoma is almost unexplored. In fact, only two studies (29) (30) have been performed on this topic more than 30 years ago; one study correlates their presence with an increased risk of lymph node metastasis, and the other study shows an association with poor survival. More recently, a third study has quantified PC at around 8% of the total cellularity of the inflammatory infiltrate in melanoma metastases (31).

From our study, it appears that PC+ melanomas are rare, and occur in less than 4% of invasive melanomas. From a clinical point of view, PC+ melanomas occur at an older age, i.e. some 10 years later than the median age of melanomas lacking PC. From a histopathological point of view, we found PC to be associated with features of worse prognosis: high Breslow thickness, high numbers of mitoses, presence of ulceration and of lymphatic/vascular invasion. Moreover, in the PC-rich group, there was a prevalence of NM, the only melanoma subtype known in the literature to have a worse prognosis compared to the other subtypes (32). Ulceration may result in inflammatory infiltrates that contain PC. To verify that the class switching was related to the tumor and not to the ulceration, we examined also a series of non-neoplastic ulcers and found a low percentage of IgA+ PC on the total number of PC in ulcers at non-mucosal sites.

To confirm the poor prognostic significance of PC among the stromal cells in melanomas, we performed a survival analysis in a selected group of thick melanomas (> 2 mm) to minimize the impact of the thickness on the statistical analysis. In this data set, 38% of the melanomas carried PC in the infiltrate. In this "thick melanomas" subgroup, as expected, the most frequent subtype associated with the presence of PC was NM. Moreover, PC+ melanomas occurred more frequently in intermittently sun exposed areas, like trunk and acral sites, while melanomas lacking PC involved head and neck and limbs, that are sites known to be chronically sun-damaged. The mere presence of PC in the infiltrate, irrespective of their number, did not, however, predict a poor outcome. This is in contrast with the previous two papers (29) (30) in which PC were found to correlate with survival, although the relative number of PC in the infiltrate was not specified. In our survival analysis, only PC-rich (PC2-3) melanomas, i.e. those showing clusters and confluent sheets of PC, showed a worse survival compared to PCneg melanomas, while patients with PC1 melanomas (showing scattered PC in the stromal infiltrate) appeared to have a better survival than those lacking PC, although no statistical significance was reached. Therefore, we can divide cases in two groups according to survival, the PC-rich melanomas (PC2-3), and the PC-low melanomas (PC1-0) (Figure 5c). The influence of the quantity of plasma cells on survival could be due to the fact that, at the beginning of the plasma cell response, PC may either have a beneficial effect, or their effect is not yet detectable because it is counterbalanced by other immune mechanisms.

When the isotype of the PC was explored, we found that the two most predominant immunoglobulins produced are IgG and IgA. In general, the presence of tumor-specific antibodies has always been regarded as a good prognostic factor. (33) The presence of tumor-infiltrating B cells and Ig κ chains genes overexpression within the tumor bed have been positively correlated with metastasis-free survival and response to chemotherapy in breast cancer. (34) On the other hand, different immunoglobulin isotypes have been shown to play different roles in human cancers. IgM and IgD identify the naive, pre-switched B cell. The life span of this cell depends on exposure to antigen: according to Burnet's "clonal selection" theory, B cells are rescued from apoptosis by their response to antigens. (35) B cells can respond directly to an antigen, independently from T cell help, or can participate in cognate recognition of the antigen with T cells, through the costimulatory molecules CD80 and CD86. The latter takes place during a germinal center reaction and results in class switching and somatic hypermutations of the immunoglobulin variable domains, thus giving

birth to Ig-variants with various affinities for the antigen, thereby improving its recognition. (35) In this manner, B cells differentiate into PC and switch from expression of the constant region of the IgM ($C\mu$) to expression of the same VHDJH-exon with any of the downstream CH genes ($C\alpha 1,2$, $C\gamma 1,2,3,4$, or $C\epsilon$), thereby becoming an IgA, IgG or IgE molecule. Class switching appears to be dependent on external cytokine signals: IFN- γ favors IgG2 switching, IL-4 favors IgG4 and IgE switching, and transforming growth factor- β (TGF- β) favors IgA switching (35). In our series of PC+ melanomas, we found predominantly IgG and IgA expression in the PC. With regard to IgG, the IgG4 subclass has been linked to a worse outcome, and has turned out to have blocking effects on the binding of tumor-specific IgG1. (36) On the other hand, the ectopic expression of Fc γ RIIB, an inhibitory receptor for IgG, on melanoma cells, was found to promote liver metastasis allowing the tumor to escape humoral immunity. (15)

Unexpectedly, a high proportion of PC expressed IgA. IgA has been found to have blocking properties on cytotoxic T cell reactions against melanoma (37) and has been shown to play a tolerogenic role in the gut (38), and an immunosuppressive role counteracting IgG activities in intestine transplantation. (39) More recently, Shalpour et al. correlated IgA-producing plasmablasts with the failure of immunogenic chemotherapy in mice with prostatic cancer, confirming the role of IgA in counteracting the immune response. (40)

In our data set, the relative number of IgA+ PC tended to increase with the total number of PC (expressed as PC score) as well as with melanoma thickness. Indeed, in the “thick melanomas” data set, IgA+ PC were more frequently found than in the original data set. Moreover, at the Gene Scan Analysis, transcripts of few different lengths were found for IgA indicating oligoclonality, whereas transcripts with high variability in length were found for IgG, indicating polyclonality. This strongly suggests an antigen-driven restriction of the tumor-associated IgA+ PC. The nature of this antigen is as yet unknown, but currently under study.

Finally, we sought to elucidate the origin of the melanoma-associated IgA+ PC. Under normal circumstances, B lymphocytes are not detectable in the skin due to their very low number. (41) The adaptive humoral immune response classically originates in secondary lymphoid organs (SLO), but may be generated in situ within TLS. TLS are inducible and transient structures that occur in non-lymphoid organs, and that share with SLO the same cytokines involved in their genesis, and the same B and T topography. (22) TLS are composed of T-areas containing mature dendritic cells and B-areas containing germinal centers with evidence of isotype switching in B-cells; in addition, TLS possess PNAD + HEV and express a range of cytokines important for the organization of SLO. (42) Not all these features are present at the same time, suggesting evolution over time of TLS. (34) A recent study in lung carcinomas, demonstrated that TLS were able to produce polyclonal IgG and IgA directed against several tumor antigens, (34) and in melanoma metastases, B cells in the follicles of TLS were shown to be involved in IgA responses. (43) However, analysis of our series showed TLS in only 2 of 15 primary melanomas; hence, it is unlikely that the PC were produced «in situ» in the skin.

After contact with the antigen and their phenotype switching in Peyer’s plaques, intestinal plasmablasts migrate to the lymph nodes in order to proliferate and hypermutate; thereafter, they finally reach the lamina propria to mature into IgA-secreting PC. (44). Similarly, B cells continuously recirculate between skin and lymph nodes, (45). Therefore, we investigated the loco-regional lymph nodes draining the PC+ melanoma site. In these lymph nodes, we generally observed a considerable number of IgA+ PC, the number of which correlated with the number in the primary melanoma. This suggests that the IgA response involves a recirculation of IgA+ PC (or plasmablasts) between the skin and the lymph nodes. Finally, the Gene Scan Analysis performed on the DNA extracted from the loco-regional lymph nodes showed oligoclonality of

the secretory IgA component both in the involved and uninvolved tumor draining lymph nodes thereby indicating that the IgA+ PC in the lymph node also showed antigen restriction. This result is in agreement with the finding of oligoclonal patterns in T-cell receptor rearrangements in both primary melanomas and draining lymph nodes. (45)

In conclusion, primary melanomas with clusters and sheets of plasma cells in the inflammatory micro-environment are rare (3.7%), occur in older patients, and are associated with histological markers of poor prognosis and with a poor survival. Melanoma-infiltrating plasma cells are predominantly of the IgG and IgA isotypes. The low incidence of PC positive cases and their already high risk nature limit the utility of these findings in prognostication and, anyway, additional validation would be required before using the findings for clinical decision-making purposes. Nevertheless, we suggest that these IgAs, which are likely antigen-induced, exert a tumor-promoting role, either by interaction with other cells in the micro-environment or by blocking soluble, growth-inhibiting molecules. Characterization of these IgA and determination of their target antigens may help to understand the role of humoral immunity in melanoma.

References

1. Bastian BC. *The molecular pathology of melanoma: an integrated taxonomy of melanocytic neoplasia*. *Annu Rev Pathol*. 2014;9:239-71.
2. Bae JM, Choi YY, Kim DS, et al. *Metastatic melanomas of unknown primary show better prognosis than those of known primary: a systematic review and meta-analysis of observational studies*. *J Am Acad Dermatol*. 2015;72:59-70.
3. Lo JA, Fisher DE. *The melanoma revolution: from UV carcinogenesis to a new era in therapeutics*. *Science*. 2014 Nov 21;346:945-9
4. Powles T, Eder JP, Fine GD, et al. *MPDL3280A (anti-PD-L1) treatment leads to clinical activity in metastatic bladder cancer*. *Nature*. 2014;27;515:558-62.
5. Herbst RS, Soria JC, Kowanzet M, et al. *Predictive correlates of response to the anti-PD-L1 antibody MPDL3280A in cancer patients*. *Nature*. 2014;27;515:563-7.
6. Tumei PC, Harview CL, Yearley JH, et al. *PD-1 blockade induces responses by inhibiting adaptive immune resistance*. *Nature*. 2014;27;515:568-71.
7. Sharma P, Allison JP. *Immune Checkpoint Targeting in Cancer Therapy: Toward Combination Strategies with Curative Potential*. *Cell*. 2015;9;161:205-14.
8. Zhou D, Huang C, Lin Z, et al. *Macrophage polarization and function with emphasis on the evolving roles of coordinated regulation of cellular signaling pathways*. *Cell Signal*. 2014;26:192-7.
9. Martinez FO, Gordon S, Locati M, Mantovani A. *Transcriptional profiling of the human monocyte-to-macrophage differentiation and polarization: new molecules and patterns of gene expression*. *J Immunol*. 2006;177:7303-11.
10. Biswas SK, Mantovani A. *Macrophage plasticity and interaction with lymphocyte subsets: cancer as a paradigm*. *Nat Immunol*. 2010;11:889-96.
11. Zitvogel L, Kroemer G. *CD103+ dendritic cells producing interleukin-12 in anticancer immunosurveillance*. *Cancer Cell*. 2014;26:591-3.
12. Balkwill FR, Capasso M, Hagemann T. *The tumor microenvironment at a glance*. *J Cell Sci*. 2012;125:5591-6.
13. Ladányi A *Prognostic and predictive significance of immune cells infiltrating cutaneous melanoma*. *Pigment Cell Melanoma Res*. 2015 [Epub ahead of print]
14. Kitamura T, Qian BZ, Pollard JW. *Immune cell promotion of metastasis*. *Nat Rev Immunol*. 2015;15:73-86
15. Smith HA, Kang Y. *The metastasis-promoting roles of tumor-associated immune cells*. *J Mol Med (Berl)*. 2013;91:411-29.
16. Bulman A, Neagu M, Constantin C. *Immunomics in Skin Cancer - Improvement in Diagnosis, Prognosis and Therapy Monitoring*. *Curr Proteomics*. 2013;10:202-217.
17. Clemente CG, Mihm MC Jr, Bufalino R, Zurrida S, Collini P, Cascinelli N.. *Prognostic value of tumor infiltrating lymphocytes in the vertical growth phase of primary cutaneous melanoma* *Cancer*, 1996;77:1303–1310
18. Clark WH Jr, Elder DE, Guerry DT, et al *Model predicting survival in stage I melanoma based on tumor progression*. *J Natl Cancer Inst* 1989;81:1893–1904
19. Cipponi A, Wieers G, van Baren N, Coulie PG. *Tumor-infiltrating lymphocytes: apparently good for melanoma patients. But why?* *Cancer Immunol Immunother*. 2011;60:1153-60.

20. Hillen F., Baeten, C.I.M., van de Winkel, A., et al. Leukocyte infiltration and tumor cell plasticity are parameters of aggressiveness in primary cutaneous melanoma. *Cancer Immunol. Immunother.* 2008;57:97–106
21. Hussein, M.R., Elasers, D.A.H., Fadel, S.A., and Omar, A.E.M. Immunohistological characterization of tumour infiltrating lymphocytes in melanocytic skin lesions. *J. Clin. Pathol.* 2006;59:316–324
22. Fridman WH, Remark R, Goc J, et al. The immune microenvironment: a major player in human cancers. *Int Arch Allergy Immunol.* 2014;164:13-26.
23. Linnebacher M, Maletzki C. Tumor-infiltrating B cells: The ignored players in tumor immunology. *Oncoimmunology.* 2012;1:1186-1188.
24. Linnebacher M. Tumor-infiltrating B cells come into vogue. *World J Gastroenterol.* 2013;19:8-11
25. Martinez-Rodriguez M, Thompson AK, Monteagudo C. A significant percentage of CD20-positive TILs correlates with poor prognosis in patients with primary cutaneous malignant melanoma. *Histopathology.* 2014;65:726-8.
26. Fremd C, Schuetz F, Sohn C, Beckhove P, Domschke C. B cell-regulated immune responses in tumor models and cancer patients. *Oncoimmunology.* 2013;1;2:25443.
27. Ladányi A, Kiss J, Mohos A, et al. Prognostic impact of B-cell density in cutaneous melanoma. *Cancer Immunol Immunother.* 2011;60:1729-38.
28. Bruno TC, French JD, Jordan KR, et al. Influence of human immune cells on cancer: studies at the University of Colorado. *Immunol Res.* 2013;55:22-33.
29. Weissmann A, Roses DF, Harris MN, Dubin N. Prediction of lymph node metastases from the histologic features of primary cutaneous malignant melanomas. *Am J Dermatopathol.* 1984;6:35-41.
30. Mascaro JM, Molgo M, Castel T, Castro J. Plasma cells within the infiltrate of primary cutaneous malignant melanoma of the skin. A confirmation of its histoprostic value. *Am J Dermatopathol.* 1987;9:497-9.
31. Erdag G, Schaefer JT, Smolkin ME, et al. Immunotype and immunohistologic characteristics of tumor-infiltrating immune cells are associated with clinical outcome in metastatic melanoma. *Cancer Res.* 2012;72:1070-80.
32. Bolognia JL, Jorizzo JL, Schaffer JV. *Melanoma*, In: Elsevier, *Dermatology 3rd edn.* 2012. pp 922
33. Morton D, Eilber FR, Malmgren RA, Wood WC. Immunological factors which influence response to immunotherapy in malignant melanoma. *Surgery.* 1970;68:158-63
34. Germain C, Gnjjatic S, Dieu-Nosjean MC. Tertiary Lymphoid Structure-Associated B Cells are Key Players in Anti-Tumor Immunity. *Front Immunol.* 2015;23:6-67.
35. Vale AM, Schroeder HW Jr. Clinical consequences of defects in B-cell development. *J Allergy Clin Immunol.* 2010;125:778-87.
36. Karagiannis, P, Gilbert AE, Josephs DH, et al. IgG4 subclass antibodies impair antitumor immunity in melanoma. *J. Clin. Invest.* 2013;123:1457–1474
37. O'Neill PA, Romsdahl MM. IgA as a blocking factor in human malignant melanoma. *Immunological communications* 1974;3:427-438
38. Doi T, Kanai T, Mikami Y, et al. IgA plasma cells express the negative regulatory co-stimulatory molecule programmed cell death 1 ligand and have a potential tolerogenic role in the intestine. *Biochem Biophys Res Commun.* 2012;425:918-23.
39. Ningappa M, Ashokkumar C, Ranganathan S, et al. Mucosal plasma cell barrier disruption during intestine transplant rejection. *Transplantation.* 2012;94:1236-42.

40. Shalpour S, Font-Burgada J, Di Caro G, et al. Immunosuppressive plasma cells impede T-cell-dependent immunogenic chemotherapy. *Nature*. 2015;521:94-8.
41. Egbuniwe IU, Karagiannis SN, Nestle FO, Lacy KE. Revisiting the role of B cells in skin immune surveillance. *Trends Immunol*. 2015;36:102-11.
42. Dieu-Nosjean MC, Goc J, Giraldo NA, Sautès-Fridman C, Fridman WH. Tertiary lymphoid structures in cancer and beyond. *Trends Immunol*. 2014;35:571-80.
43. Cipponi A, Mercier M, Seremet T, et al. Neogenesis of lymphoid structures and antibody responses occur in human melanoma metastases. *Cancer Res*. 2012;72:3997-4007.
44. Hahn A, Thiessen N, Pabst R, Buettner M, Bode U. Mesenteric lymph nodes are not required for an intestinal immunoglobulin A response to oral cholera toxin. *Immunology*. 2010;129:427-36.
45. Thurin M, Marincola FM, *Molecular Diagnostics for Melanoma: Methods and Protocols*, In Springer: *Methods in Molecular Biology*, 2014, pp287-324.

CHAPTER II – ABERRANT HLA-DR EXPRESSION IN MELANOMA TISSUE: HINTS AT A GERMINAL
CENTER-LIKE INFLAMMATORY MICROENVIRONMENT

TO BE SUBMITTED

Aberrant HLA-DR expression in melanoma tissue: hints at a germinal center-like inflammatory microenvironment.

Francesca Maria Bosisio^{1,2}, Zeynep Kalender Atak³, Jasper Wouters³, Asier Antoranz⁴, Vaia Pliaka⁴, Angeliki Minia⁴, Jan Roznac^{4,6}, Leonidas G Alexopoulos^{4,5}, Stein Aerts³, Joost van den Oord¹

1 Laboratory of Translational Cell and Tissue Research, KUL, Herestraat 49, 3000, Leuven, Belgium.

2 Università degli studi di Milano-Bicocca, Milan, Italy.

3 Laboratory of Computational Biology, KUL, Leuven, Belgium;

4 ProtATonce Ltd, Athens, Greece.

5 National Technical University of Athens, Athens, Greece.

6 Life Sciences Research Unit, University of Luxembourg, Belvaux, Luxembourg

To the editor,

Major histocompatibility complex (MHC, also known as Human Leukocyte Antigens, HLA) class II molecules are typically expressed by antigen presenting cells (APCs) to present extracellular proteins to CD4+ T lymphocytes. (1). Three major MHC class II genes are known: HLA-DR, HLA-DQ, and HLA DP. HLA-DR is the most frequently expressed MHC II molecule. In an inflammatory microenvironment, aberrant MHC class II molecule expression can occur on non-hematopoietic cells, including melanoma cells, in particular following interferon- γ (IFN γ) secretion, the most powerful MHC II inducer (2). It may be tempting to assume that MHC II expression by melanoma cells would increase tumour antigen presentation and hence favour the immune response. However, MHC II is also a ligand for checkpoint inhibitor molecules such as Lymphocyte-activation gene 3 (LAG3), expressed by activated T lymphocytes, that can turn these lymphocytes into exhaustion upon contact with MHC II positive melanoma cells (3). Moreover, if MHC II expression in melanoma cells occurs without co-expression of co-stimulatory receptors, there will be no activation of T cells (4) (5). These different mechanisms may explain why some studies link MHC II expression by melanoma cells with an unfavourable clinical outcome, whereas other studies associate it with tumor regression and longer survival (2) (6) (7) (8) (9). Furthermore, analysis of MHC II-positive melanomas and melanoma cell lines usually does not differentiate between constitutive and IFN γ -induced MHC II expression. Constitutive expression is associated with a more rapid progression of the melanoma (4).

Despite all these findings, little is known about the actual immune microenvironment in areas of melanoma cells expressing MHC II. It has been reported that these areas would be characterized by enhanced TILs infiltration and with the expression of lymphocytic activation pathways signatures (10) whereas another study reports the occurrence of tumor-specific CD4+ T lymphocytes in areas of MHC II+ melanoma cells, that prevent the activation of cytotoxic T lymphocytes through production of TNF (11).

We decided therefore to investigate the immune microenvironment in areas of MHC II expression in melanoma using microdissection of HLA-DR+ areas, followed by RNA-seq, qPCR and proteomics.

As only a subset of melanomas expresses MHC II molecules, we analyzed a series of 19 fresh frozen melanoma metastases, collected at the Department of Pathology of the UZ Leuven, Belgium, and stained them for HLA-DR molecules (Abcam, SPM289, 1:1000). To distinguish between IFN γ -induced and constitutive MHC expression, we measured in each case the level of IFN γ expression by qPCR (forward 'TGTTACTGCCAGGACCCA' and reverse 'TTCTGTCACCTCCTCTTTCCA'). We identified 11/19 HLA-DR+ melanomas (Figure 1), and we selected two cases with similar high levels of IFN γ expression for microdissection. In both patients, we microdissected HLA-DR positive and negative areas, with the aim of comparing the gene expression profile through Next Generation Sequencing between MHC II positive and negative areas within the same lesion. Microdissection was restricted to the tumoral nodules and excluded the stromal tissue surrounding the melanoma nodules. We identified two signatures based on GOrilla (Gene Ontology enRICHment analysis and visualizAtion tool) (12) analysis cut-offs, i.e. "HLA-DR-up" (689 genes upregulated in HLA-DR+ areas) and "HLA-DR-down" (2396 genes downregulated in HLA-DR+ areas).

First, we evaluated the enrichment of the HLA-DR-up signature in other databases, i.e. in the Mesenchymal Transition/Mitotic/Lymphocyte-specific signatures (13) and in the Invasive/Proliferative signatures described by Hoek et al. (14) using Gene Set Enrichment Analysis (GSEA) (15) (16). In MHCII+ melanoma areas, we observed an enrichment for genes from the Lymphocyte-specific and the Mesenchymal attractor metagenes (13), as well as from the Invasive signature as reported by Hoek et al. (14). Both these findings were in line with the fact that our samples were taken at the periphery of the melanoma nodules, where IFN γ -induced HLA-DR expression and a lymphocytic infiltrate is often present, and where melanoma cells possibly switch their phenotype towards invasion. However, when we compared our signature with the Invasive/Immune-infiltrated/Proliferative signature identified in the TCGA database (17), HLA-DR-up was enriched only in genes from the "Immune-infiltrated" subgroup, confirming the pivotal importance of the presence of an immune infiltrate for IFN γ -dependent HLA-DR expression in melanoma. This "immune-infiltrated" TCGA subgroup was also the one characterized by the best overall survival (Figure 2). Furthermore, we analyzed the HLA-DR signatures with iRegulon (18), which identifies upstream regulators of these genes. At the HLA-DR-up side, NFKB1 was enriched, together with the NFIC and TCF4 transcription factors. The first two transcription factors are in line with the previously found enrichment in immune-related signatures. In fact, NFKB plays an important role in the immune system by regulating cytokines, growth factors and various enzymes after interaction of T-cell receptors, B-cell receptors (BCRs), TNFR, CD40, BAFFR, LT β R, and Toll/IL-1R with their respective ligands (19); and TCF4 is a regulator of immunoglobulin gene expression (20). At the "HLA-DR-down" side, iRegulon found downregulation of ETS-factors and E2F transcription factors, both involved in cell cycle control (21), as well as MITF, marker of the proliferative phenotype (14), indicating again that MHCII+ melanoma areas, are characterized by a switch towards invasion.

MHCII	INFgamma
HLA-DR+	44,79
HLA-DR+	14,26
HLA-DR+	13,58
HLA-DR+	10,48
HLA-DR+	9,63
HLA-DR+	6,55
HLA-DR+	5,76
HLA-DR+	2,80
HLA-DR+	1,71
HLA-DR+	1,23
HLA-DR+	0,65
HLA-DR-	6,97
HLA-DR-	4,23
HLA-DR-	3,01
HLA-DR-	2,22
HLA-DR-	1,71
HLA-DR-	0,86
HLA-DR-	0,85
HLA-DR-	0,29
media	6,92
median	3,01

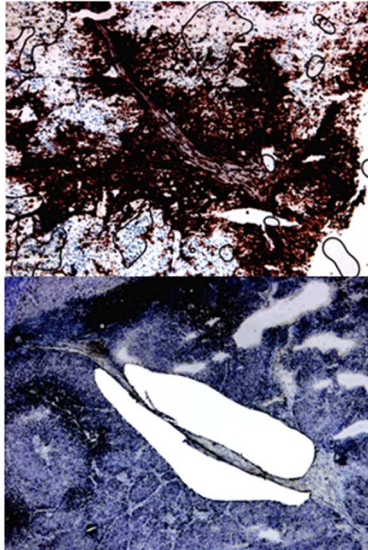


Figure 1. Exploratory data set. In the table, in the left column, we indicate the immunohistochemical expression of HLA-DR in our exploratory data set of melanoma metastasis. This is done as a qualitative evaluation discriminating positive and negative cases. For each case, in the right column, it is indicated the value of mRNA expression of IFN γ measured by qPCR. On the right, the image shows the microdissection of two HLA-DR positive areas. HLA-DR was mostly found expressed at the margins of the tumor nodules.

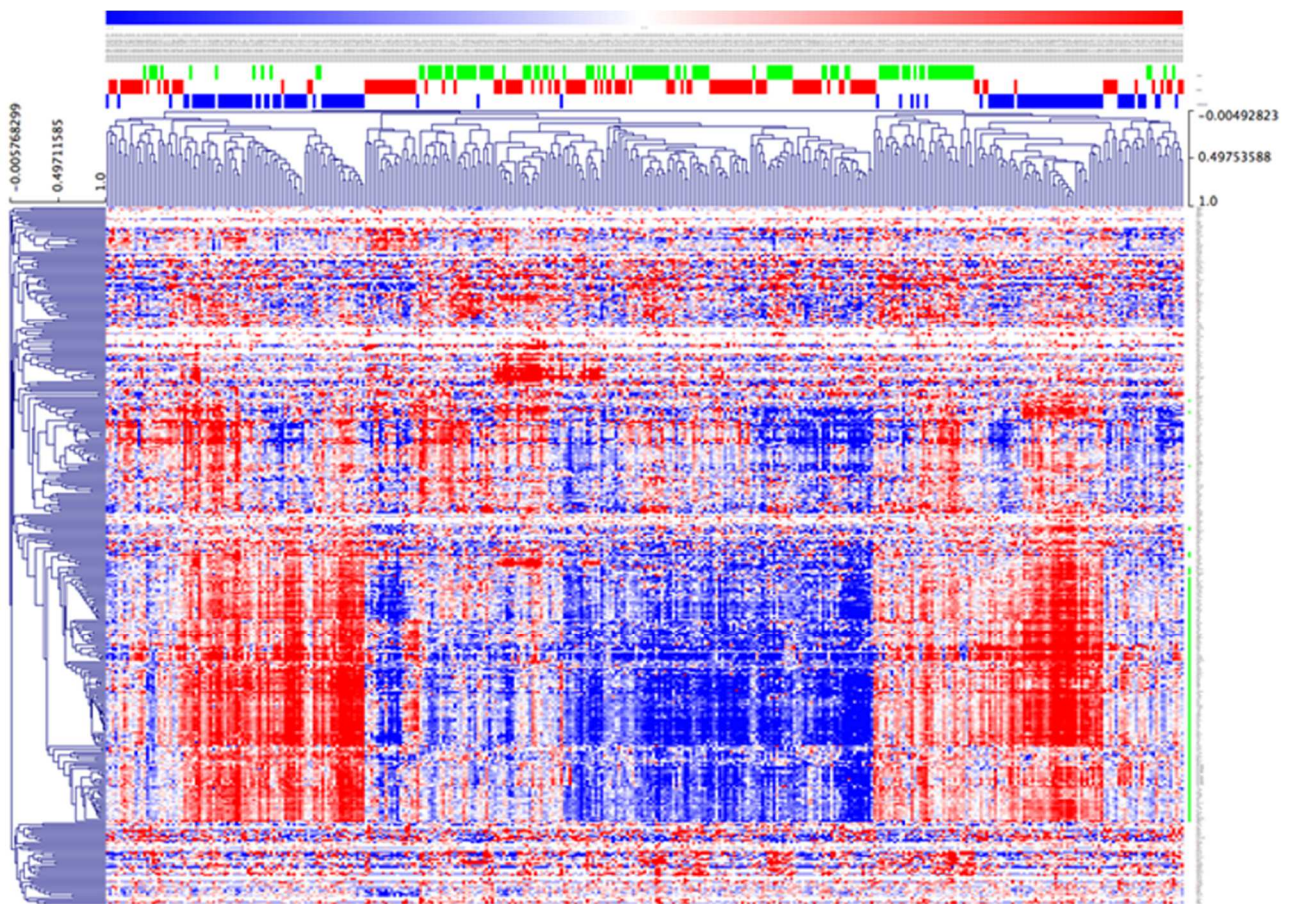


Figure 2. Heatmap of the HLA-DR-up signature in TCGA and survival analysis. We explored the expression of the genes involved in the HLA-DR signature that we found in the TCGA database. We divided the samples in groups according to the Invasive/Immune-infiltrated/Proliferative signature in the upper image (top of the heatmap, green = invasive, blue = immune-infiltrated, red = proliferative). The "leading-edge" genes are marked on the right border of the images in green. These genes that contribute most to the enrichment are clearly upregulated in the immune-infiltrated group, that it is the group characterized also by the better survival (lower image, survival data for the invasive, immune-infiltrated and proliferative samples).

After investigating the significance of the HLA-DR signatures using open access databases, we focused on the top 50 upregulated and downregulated genes of the HLA-DR-up signature (Figure 3) exploring their ontology and involvement in biological pathways through Webgestalt (WEB-based GENE SeT ANALYSIS Toolkit) (22) (23). The top 50 downregulated genes were generally linked to metabolic and cell cycle-related processes, without any specific or particular feature that would further characterized the type of microenvironment in HLA-DR positive melanoma areas. Regarding the top 50 upregulated genes, we could subdivide them into: a) MHC molecules (HLA-DRB1, HLA-DRB5, HLA-H); b) T cell-related genes (CD3E, CD3G, CD52, CORO1A, ITK, PTPRCAP, SH2D1A, TRGC2, ZNF683); c) B cell-related genes (IGHG1, IGHG3, IGHG4, IGHM, IGHV1-24, IGHV4-39, IGHV5-51, IGHV6-1, IGJ, IGKV3-11, IGKV3-20, IGKV3D-20, IGKV4-1, IGLC3, IGLV1-40, IGLV2-14, IGLV3-1, IGLV3-10, ISLR, MZB1); d) cytokines and their receptors (CCR7, CXCL13, DARC, IL10RA, IL2RB, PYHN1, TNFRSF25, CCR5); e) myeloid cells-related genes (LILRB2, MNDA, SELPLG); and f) cell mobility and metabolism-related genes (IGF2, MMP10, MMP7, MYCN, PNPLA1, STRA6, TKTL1, RARRES2, AIPL1, CTD-2147F2.2, DENND1C, FAT3, FBXL21, MAGEA3, OCM2, PCDHA9, RAM3, TUBA4A). Considering the MHC molecules, the expression of HLA-DRB1 and HLA-DRB5 represented an internal control for the correct localization of the microdissection. HLA-H, instead, represented a novel finding. HLA-H is, together with HLA-G, HLA-E, and HLA-F, a non-classical MHC class I molecule (24). It has a role in iron metabolism and in immune suppression, both with repercussions on tumor progression (25). HLA-H is negatively regulated by Tumor Necrosis Factor alpha (TNF α) and IFN γ , which results not only in an increased iron uptake by the tumor, thereby favouring tumor growth, but also an increased MHC I expression, favouring tumor clearance by the immune system (26). Our results show that HLA-H was more expressed in HLA-DR+ melanoma areas, therefore favouring immune escape. Within the upregulated genes, other genes with an immunosuppressive significance were present. The T-cell related CD52 is an inducer of Tregs (27) and Coronin-1A (Coro1A) is a negative regulator of the TCR signalling (28). Within the myeloid cell-related genes, Leukocyte Immunoglobulin-like receptor B2 (LILRB2) is able to bind to MHC class I molecules, thereby inhibiting the immune response (29). Among the cytokines and their receptors, Interleukin 10 Receptor Subunit Alpha (IL10RA) and tumor necrosis factor receptor superfamily member 25 (TNFRSF25) control lymphocyte proliferation and C-C chemokine receptor type 5 (CCR5), expressed on T cells and macrophages, plays an immunosuppressive role via interactions with Tregs (30). On the other hand, immunostimulatory genes such as IL2RB and pyrin and HIN domain family, member 1 (PYHIN1), an IFN-inducible protein, were found. Interestingly, the major part of the top 50 in the HLA-DR-up signature consisted of B- and T-related genes, in particular several immunoglobulins (Ig) genes. Hence, MHC II+ melanoma areas harbour a mixed T and B microenvironment with cross-talk between these cells, e.g. via SH2 domain-containing protein 1A (SH2D1A) (31). Intriguingly, we found CCR7, C-X-C Motif Chemokine Ligand 13 (CXCL13) and Marginal zone B and B1 cell-specific protein (MZB1) co-expressed in the MHC II+ melanoma areas. CCR7 stimulates the migration of memory T cells toward antigen presenting cells (32), CXCL13 is a chemoattractant that stimulates the migration of lymphocytes toward germinal centers in secondary lymphoid organs (SLO) and tertiary lymphoid organs (TLO) (33), and MZB1 is a marginal-zone specific protein involved in Ig production (34). Pathways analysis using String (35) highlighted how HLA-DRB1, HLA-DRB2, CD3E, CD3G, ITK and IL2RB formed a first central core of interconnected proteins participating together in different pathways, in particular the downstream TCR signalling; but additionally, these proteins interact with a second functional core of proteins including CCR7, CXCL13 and CCR5. In conclusion, String analysis supported the existence of a germinal center-like microenvironment in HLA-DR positive areas (Figure 3).

To confirm that HLA-DR expression in melanoma was associated with the presence of an environment rich in germinal center cytokines at the protein level, we extracted proteins from five 10 micrometers-thick cryostat sections from 8 HLA-DR positive and 4 HLA-DR negative melanomas according to Allred et al (36). We built and validated a customized Multiplex ELISA panel for the Luminex Flexmap 3D at Protavio (Athens, Greece), coupling different magnetic beads from Luminex with the capture antibody of the duoset ELISA from R&D Systems against human IFN γ , IL6, IL10, TNF α , IL4, CXCL10, IL17, IL13, CCL18, TGF β , IL23, CXCL13, CXCL12, and CCL19. For data analysis, we applied three unsupervised machine learning clustering methods, i.e. Principal Component Analysis (PCA), t-Distributed Stochastic Neighbour Embedding (tSNE), and Hierarchical Clustering (HC). These three methods separated only partially the HLA-DR positive and negative cases (Figure 4A). This means that we had some informative markers that allowed us to distinguish HLA-DR positive from negative melanomas, and uninformative markers that an unsupervised analysis cannot dismiss. In order to find the informative markers, we performed supervised clustering using Linear Discriminant Analysis (LDA), which identified a minimum number of 5 informative markers (Figure 4B) that would allow perfect separation of the negative from the positive cases; these 5 markers included IFN γ , IL4, and the three germinal center cytokines CCL19, CXCL12 and CXCL13 (Figure 4C), confirming germinal center-like microenvironment in HLA-DR positive areas.

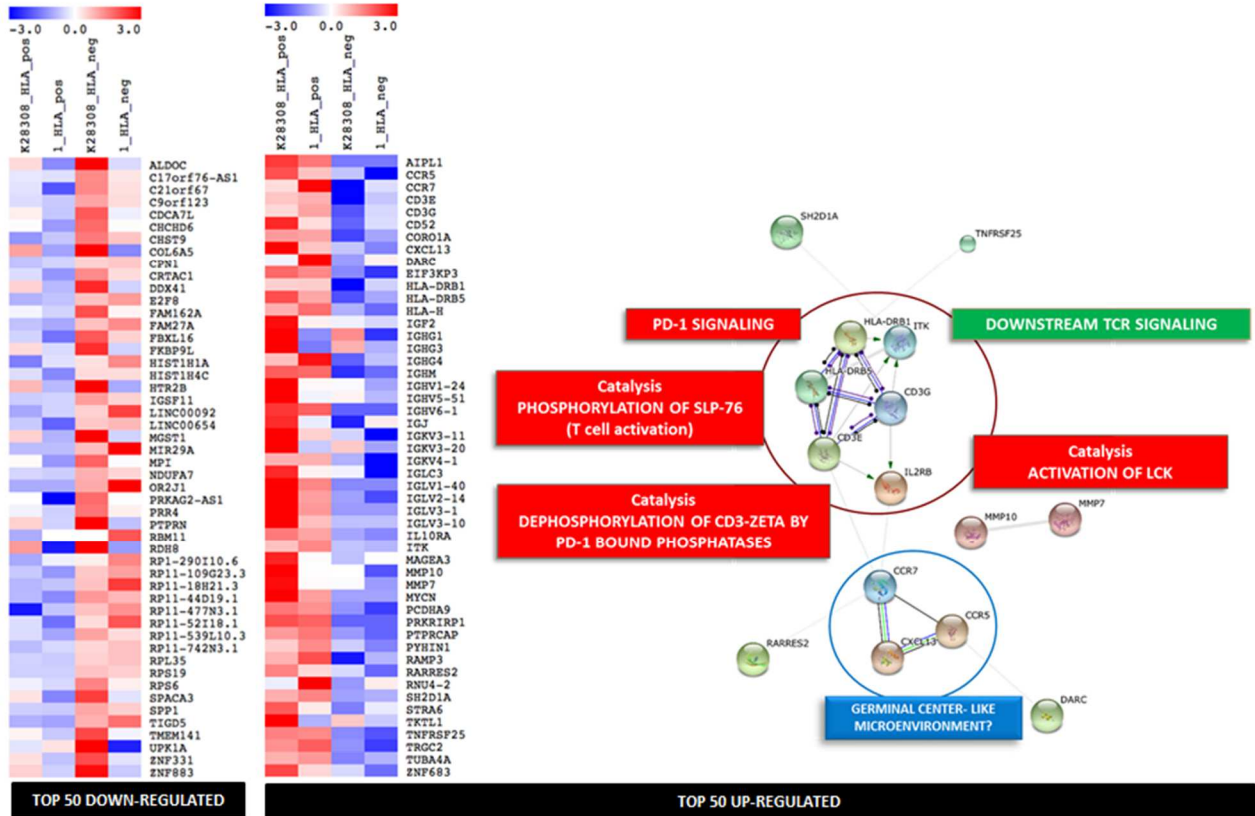


Figure 3. Top 50 upregulated and downregulated genes and pathways analysis. On the left, two heatmaps list the top 50 downregulated genes and the top 50 up-regulated genes. Next to this last group, it is shown the STRING graphic representation of the relationships between the proteins that belongs to the same pathways among the 50 upregulated genes, and the functions of these pathways.

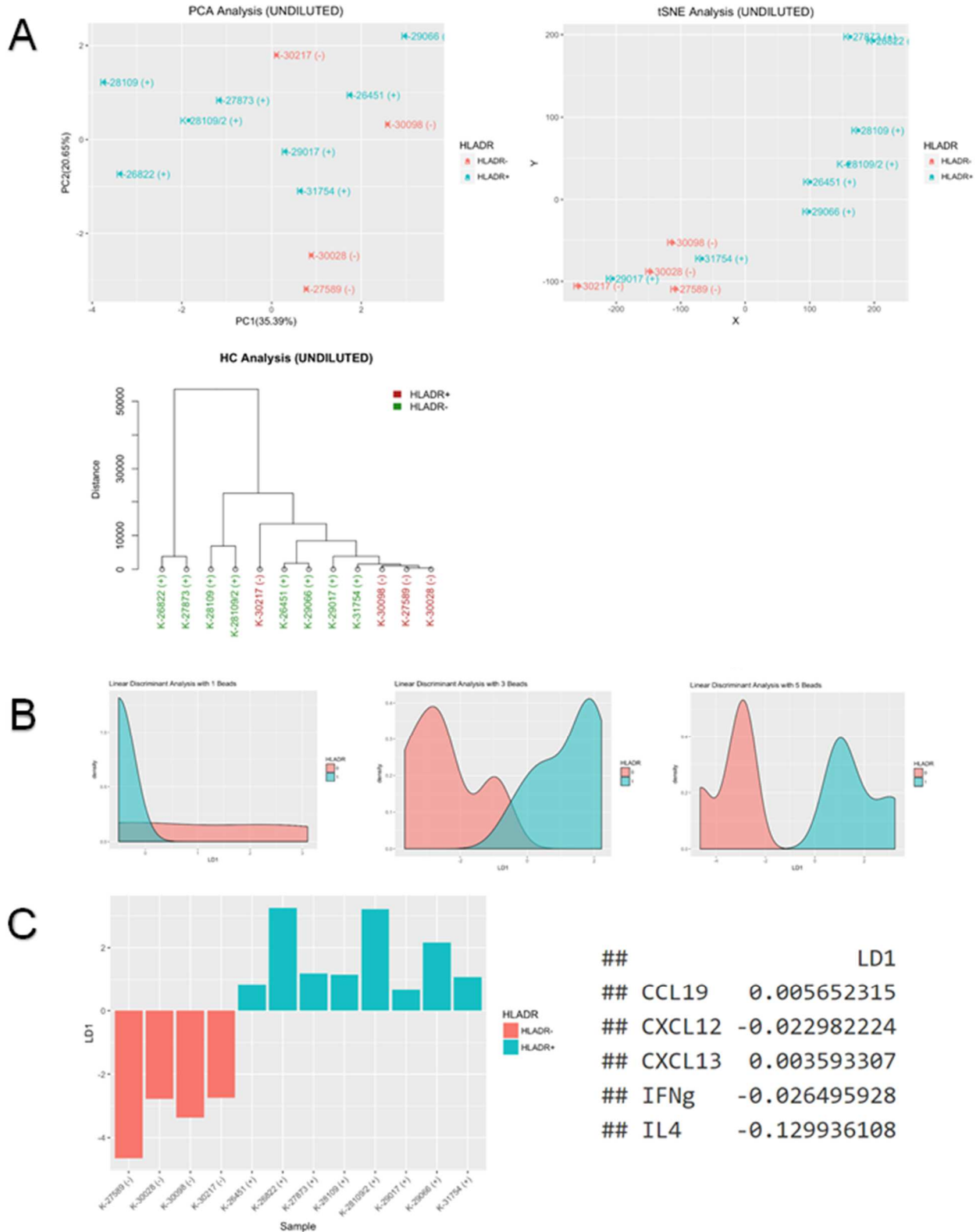


Figure 4. Data analysis of the multiplex ELISA assay. (A) Here we show the unsupervised clustering approach represented with PCA, tSNE and HC (clockwise) done on HLA-DR negative and positive cases; we found a hint of clusterization using all the selected markers between HLA-DR positive and negative cases. We tried successively a supervised clustering approach, defining with linear discriminant analysis the minimal number of markers to distinguish between HLA-DR positive and negative cases (B) and then applying those five markers (CCL19, CXCL12, CXCL13, IFNg and IL4) to our validation data set (C). This allowed a correct classification of the HLA-DR positive and negative cases.

type	Breslow	% HLA-DR+ cells	Cell profiler	%Tfh	Average
s smm	0,42	56,0		0,73	1,66
s smm	1,125	46,2		0,52	
s smm	0,36	42,0		1,16	
s smm	0,71	40,0		2,98	
s smm	0,78	36,0		2,91	
s smm	0,7	0,1		0,08	0,704
s smm	0,22	0,1		0,17	
s smm	0,78	0,3		1,25	
s smm	0,36	0,0		2,02	
s smm	0,28	0,0		0	

Figure 5. Immunohistochemical analysis of 10 primary melanomas. In the table we illustrate the results of the immunohistochemical analysis and image analysis performed on 10 melanomas, 5 classified as HLA-DR positive and 5 as HLA-DR negative by the automatic image analysis with Cell profiler, with the same range of Breslow thickness for the two groups. Although there was a trend indicating that the percentage of Tfh cells in HLA-DR+ cases may be higher, the p-Value was not significant.

Germinal centers are characterized by a specific subset of T-cells, i.e. T follicular helper cells (Tfh) that express the phenotype CD4+CXCL13+PD1+. Tfh cells migrate into the germinal center in response to CXCL13 in order to support proliferation and maturation of B cells by secreting cytokines such as IL-21 and, most importantly, IL-4 (Sage PT et al. Immunol Rev. 2016) To demonstrate enrichment of these cells in the HLA-DR+ melanoma areas, we constructed a Tissue Micro-array of 5 HLA-DR+ and 5 HLA-DR- melanomas, and stained them in immunofluorescence for CD4 (1:140, EPR6855, rabbit, Abcam), MelanA (1:100, PI9-17, mouse IgG1, SCBT), HLA-DR (1:1000, SPM288, IgG2, Abcam), CXCL13 (1:100, 53610, mouse IgG1, R&D) and PD-1 (1:1000, UMAB197, mouse IgG2a, Origene). Images were processed with ImageJ and analyzed with Cell Profiler in order to quantify the number of Tfh. As shown in figure 5, HLA-DR+ cases had generally a higher percentage of Tfh cells as compared to HLA-DR- cases with average Tfh percentages of 1,66% and 0,7% respectively on the total amount of cells in the sample (Figure 5).

In summary, these findings may clarify the significance of aberrant HLA-DR expression in melanoma, and possibly in other cancers and inflammatory conditions as well. T-B cell interactions and antigen presentation usually occurs in the germinal center, allowing B cells to proliferate, differentiate and undergo somatic hypermutation and isotype class switching, most typically from IgM to IgG or IgA. (37) The germinal center cytokines CCL19, CCL21, and CXCL13 are expressed in secondary lymphoid organs (lymph nodes, spleen, tonsils...) in order to attract T and B cells for these purposes. But germinal center cytokines are also fundamental for the formation of tertiary lymphoid organs (TLO). TLO are ectopic, transient lymphoid structures that can develop in non-lymphoid organs during chronic inflammation. They have the same organization of T and B cells that is found in the lymph nodes, and also contain follicular dendritic cells, Tfh cells and high endothelial venules. In tumor biology, they are considered to have a beneficial effect, allowing for a quicker (because developing directly “in loco”) and durable anti-tumor response (33). However, the samples that we microdissected, did not contain TLO, and we limited the microdissection to areas of the melanoma nodules, excluding the surrounding stroma, where TLO are located. The expression of germinal center cytokines directly inside the melanoma tissue at the site where aberrant HLA-DR expression occurs, could represent a shortcut to speed up the process of antigen production, skipping the re-circulation of memory T and B lymphocytes to the lymph node after priming in the tumoral area to return only later as effector T cells in the melanoma (33). An additional argument in favour of a germinal center-like function of HLA-DR+ melanoma areas is the finding of a differentially expressed IgM gene among many IgG genes; IgM is expressed by B cells before completing the isotype switching process to IgA or IgG. Finally, HLA-DR expression by melanoma cells has been suggested to predict the success of immunotherapy (10). In the HLA-DR positive melanoma areas, we detected the expression of several immunosuppressive genes but our data suggest that the microenvironment in these areas resembles a germinal center, with features of antigen presentation, germinal center cytokine production, and Tfh and B cell maturation. It is possible that the prolonged germinal center-like stimulation of the tumor infiltrating lymphocytes in these areas with time results in their exhaustion, and that upon anti-PD-1 therapy, this microenvironment could represent a florid field from which an effective immune response could restart.

References

1. Matsushita H, Vesely MD, Koboldt DC, Rickert CG, Uppaluri R, Magrini VJ, Arthur CD, White JM, Chen YS, Shea LK, Hundal J, Wendl MC, Demeter R, Wylie T, Allison JP, Smyth MJ, Old LJ, Mardis ER, Schreiber RD. Cancer exome analysis reveals a T-cell-dependent mechanism of cancer immunoediting. *Nature*. 2012 Feb 8;482(7385):400
2. Degenhardt Y, Huang J, Greshock J, Horiates G, Nathanson K, Yang X, Herlyn M, Weber B. Distinct MHC gene expression patterns during progression of melanoma. *Genes Chromosomes Cancer*. 2010 Feb;49(2):144-54.
3. Andrews LP, Marciscano AE, Drake CG, Vignali DA. LAG3 (CD223) as a cancer immunotherapy target. *Immunol Rev*. 2017 Mar;276(1):80-96.
4. Deffrennes V, Vedrenne J, Stolzenberg MC, Piskurich J, Barbieri G, Ting JP, Charron D, Alcaïde-Loridan C. Constitutive expression of MHC class II genes in melanoma cell lines results from the transcription of class II transactivator abnormally initiated from its B cell-specific promoter. *J Immunol*. 2001 Jul 1;167(1):98-106. Campoli M, Fitzpatrick JE, High W, Ferrone S. HLA antigen expression in melanocytic lesions: is acquisition of HLA antigen expression a biomarker of atypical (dysplastic) melanocytes? *J Am Acad Dermatol*. 2012 Jun;66(6):911-6, 916.e1-8.
5. Becker JC, Brabletz T, Czerny C, Termeer C, Bröcker EB. Tumor escape mechanisms from immunosurveillance: induction of unresponsiveness in a specific MHC-restricted CD4+ human T cell clone by the autologous MHC class II+ melanoma. *Int Immunol*. 1993 Dec;5(12):1501-8.
6. Martins I, Sylla K, Deshayes F, Lauriol J, Ghislin S, Dieu-Nosjean MC, Viguier M, Verola O, Charron D, Alcaide-Loridan C, Al-Daccak R. Coexpression of major histocompatibility complex class II with chemokines and nuclear NFkappaB p50 in melanoma: a rationale for their association with poor prognosis. *Melanoma Res*. 2009 Aug;19(4):226-37.
7. Barbieri G, Rimini E, Costa MA. Effects of human leukocyte antigen (HLA)-DR engagement on melanoma cells. *Int J Oncol*. 2011 Jun;38(6):1589-95.
8. Carretero R, Wang E, Rodriguez AI, Reinboth J, Ascierto ML, Engle AM, Liu H, Camacho FM, Marincola FM, Garrido F, Cabrera T. Regression of melanoma metastases after immunotherapy is associated with activation of antigen presentation and interferon-mediated rejection genes. *Int J Cancer*. 2012 Jul 15;131(2):387-95.
9. Bernsen MR, L Ha°kansson, B Gustafsson, L Krysanter, B Rettrup, D Ruitter, A Ha°kansson On the biological relevance of MHC class II and B7 expression by tumour cells in melanoma metastases *British Journal of Cancer* (2003) 88, 424 – 431
10. Johnson DB, Estrada MV, Salgado R, Sanchez V, Doxie DB, Opalenik SR, Vilgelm AE, Feld E, Johnson AS, Greenplate AR, Sanders ME, Lovly CM, Frederick DT, Kelley MC, Richmond A, Irish JM, Shyr Y, Sullivan RJ, Puzanov I, Sosman JA, Balko JM. Melanoma-specific MHC-II expression represents a tumour-autonomous phenotype and predicts response to anti-PD-1/PD-L1 therapy. *Nat Commun*. 2016 Jan 29;7:10582.
11. Donia M, Kjeldsen JW, Svane IM. The controversial role of TNF in melanoma. *Oncoimmunology*. 2015 Oct 29;5[4]:e1107699
12. Eran Eden, Roy Navon, Israel Steinfeld, Doron Lipson and Zohar Yakhini. "GORilla: A Tool For Discovery And Visualization of Enriched GO Terms in Ranked Gene Lists", *BMC Bioinformatics* 2009, 10:48.
13. Cheng W-Y, Yang T-HO, Anastassiou D. Biomolecular Events in Cancer Revealed by Attractor Metagenes. Rigoutsos I, ed. *PLoS Computational Biology*. 2013;9(2):e1002920. doi:10.1371/journal.pcbi.1002920.
14. Hoek KS, Eichhoff OM, Schlegel NC, Döbbeling U, Kobert N, Schaerer L, Hemmi S, Dummer R. In vivo switching of human melanoma cells between proliferative and invasive states. *Cancer Res*. 2008 Feb 1;68(3):650-6.
15. Subramanian A, Tamayo P, Mootha VK, Mukherjee S, Ebert BL, Gillette MA, Paulovich A, Pomeroy SL, Golub TR, Lander ES, Mesirov JP. Gene set enrichment analysis: a knowledge-based approach for interpreting genome-wide expression profiles. *Proc Natl Acad Sci U S A*. 2005 Oct 25;102(43):15545-50. Epub 2005 Sep 30.
16. Mootha VK, Lindgren CM, Eriksson KF, Subramanian A, Sihag S, Lehar J, Puigserver P, Carlsson E, Ridderstråle M, Laurila E, Houstis N, Daly MJ, Patterson N, Mesirov JP, Golub TR, Tamayo P, Spiegelman B, Lander ES, Hirschhorn JN, Altshuler D, Groop LC. PGC-1alpha-responsive genes involved in oxidative phosphorylation are coordinately downregulated in human diabetes. *Nat Genet*. 2003 Jul;34(3):267-73.

17. Verfaillie A, Imrichova H, Atak ZK, Dewaele M, Rambow F, Hulselmans G, Christiaens V, Svetlichnyy D, Luciani F, Van den Mooter L, Claerhout S, Fiers M, Journe F, Ghanem GE, Herrmann C, Halder G, Marine JC, Aerts S. Decoding the regulatory landscape of melanoma reveals TEADS as regulators of the invasive cell state. *Nat Commun.* 2015 Apr 9;6:6683.
18. Janky R, Verfaillie A, Imrichová H, Van de Sande B, Standaert L, Christiaens V, Hulselmans G, Herten K, Naval Sanchez M, Potier D, Svetlichnyy D, Kalender Atak Z, Fiers M, Marine JC, Aerts S. iRegulon: from a gene list to a gene regulatory network using largemotif and track collections. *PLoS Comput Biol.* 2014 Jul 24;10(7):e1003731
19. Hayden MS, Ghosh S. Signaling to NF-kappaB. *Genes Dev.* 2004;18:2195–2224.
20. Gloury R, Zotos D, Zuidschewoude M, Masson F, Liao Y, Hasbold J, Corcoran LM, Hodgkin PD, Belz GT, Shi W, Nutt SL, Tarlinton DM, Kallies A. Dynamic changes in Id3 and E-protein activity orchestrate germinal center and plasma cell development. *J Exp Med.* 2016 May 30;213(6):1095-111.
21. Dimova DK, Dyson NJ. The E2F transcriptional network: old acquaintances with new faces. *Oncogene.* 2005 Apr 18;24(17):2810-26.
22. Zhang, B., Kirov, S.A., Snoddy, J.R. (2005). WebGestalt: an integrated system for exploring gene sets in various biological contexts. *Nucleic Acids Res*, 33(Web Server issue), W741-748.
23. Wang, J., Duncan, D., Shi, Z., Zhang, B. (2013). WEB-based GENE SeT Analysis Toolkit (WebGestalt): update 2013. *Nucleic Acids Res*, 41 (Web Server issue), W77-83.
24. Kochan G, Escors D, Breckpot K, Guerrero-Setas D. Role of non-classical MHC class I molecules in cancer immunosuppression. *Oncoimmunology.* 2013 Nov 1;2(11):e26491.
25. Pascolo S, Ginhoux F, Laham N, Walter S, Schoor O, Probst J, Rohrlisch P, Obermayr F, Fisch P, Danos O, Ehrlich R, Lemonnier FA, Rammensee HG. The non-classical HLA class I molecule HFE does not influence the NK-like activity contained in fresh human PBMCs and does not interact with NK cells. *Int Immunol.* 2005 Feb;17(2):117-22.
26. Reuben A, Godin-Ethier J, Santos MM, Lapointe R. T lymphocyte-derived TNF and IFN- γ repress HFE expression in cancer cells. *Mol Immunol.* 2015 Jun;65(2):259-66.
27. Watanabe T, Masuyama J, Sohma Y, Inazawa H, Horie K, Kojima K, Uemura Y, Aoki Y, Kaga S, Minota S, Tanaka T, Yamaguchi Y, Kobayashi T, Serizawa I. CD52 is a novel costimulatory molecule for induction of CD4+ regulatory T cells. *Clin Immunol.* 2006 Sep;120(3):247-59.
28. Siegmund K, Thuille N, Posch N, Fresser F, Baier G. Novel protein kinase C ϑ : coronin 1A complex in T lymphocytes. *Cell Commun Signal.* 2015 Mar 31;13:22.
29. Hirayasu K, Arase H. Functional and genetic diversity of leukocyte immunoglobulin-like receptor and implication for disease associations. *J Hum Genet.* 2015 Nov;60(11):703-8.
30. Patterson SJ, Pesenacker AM, Wang AY, Gillies J, Mojibian M, Morishita K, Tan R, Kieffer TJ, Verchere CB, Panagiotopoulos C, Levings MK. T regulatory cell chemokine production mediates pathogenic T cell attraction and suppression. *J Clin Invest.* 2016 Mar 1;126(3):1039-51.
31. <https://www.ncbi.nlm.nih.gov/gene/4068>
32. Quigley MF, Gonzalez VD, Granath A, Andersson J, Sandberg JK. CXCR5+ CCR7- CD8 T cells are early effector memory cells that infiltrate tonsil B cell follicles. *Eur J Immunol.* 2007 Dec;37(12):3352-62.
33. Dieu-Nosjean MC, Giraldo NA, Kaplon H, Germain C, Fridman WH, Sautès-Fridman C. Tertiary lymphoid structures, drivers of the anti-tumor responses in human cancers. *Immunol Rev.* 2016 May;271(1):260-75.
34. Rosenbaum M, Andreani V, Kapoor T, Herp S, Flach H, Duchniewicz M, Grosschedl R. MZB1 is a GRP94 cochaperone that enables proper immunoglobulin heavy chain biosynthesis upon ER stress. *Genes Dev.* 2014 Jun 1;28(11):1165-78.
35. Szklarczyk D, Franceschini A, Wyder S, Forslund K, Heller D, Huerta-Cepas J, Simonovic M, Roth A, Santos A, Tsafou KP, Kuhn M, Bork P, Jensen LJ, von Mering C. STRING v10: protein-protein interaction networks, integrated over the tree of life. *Nucleic Acids Res.* 2015 Jan; 43:D447-52. PubMed
36. Allred CC, Krennmayr T, Koutsari C, Zhou L, Ali AH, Jensen MD. A novel ELISA for measuring CD36 protein in human adipose tissue. *Journal of Lipid Research.* 2011;52(2):408-415. doi:10.1194/jlr.M008995.

37. Quan H, Fang L, Pan H, Deng Z, Gao S, Liu O, Wang Y, Hu Y, Fang X, Yao Z, Guo F, Lu R, Xia K, Tang Z. An adaptive immune response driven by mature, antigen-experienced T and B cells within the microenvironment of oral squamous cell carcinoma. *Int J Cancer*. 2016 Jun 15;138(12):2952-62.

CHAPTER III – TILS HIGH-DIMENSIONAL “IN SITU” SINGLE CELL-ANALYSIS OF TUMOUR INFILTRATING LYMPHOCYTES IN PRIMARY MELANOMA USING MULTIPLEX IMMUNOSTAINING ON TISSUE SECTIONS.

SUBMITTED

High-dimensional “in situ” single cell-analysis of Tumour Infiltrating Lymphocytes in primary melanoma using Multiplex Immunostaining on tissue sections.

Francesca Maria Bosisio* (1)(2), Asier Antoranz* (3)(4), Maddalena Maria Bolognesi (2), Clizia Chinello (2), Jasper Wouters (1), Fulvio Magni (2), Leonidas Alexopoulos (3)(4), Giorgio Cattoretti (2), Joost van den Oord (1)

(1) *Laboratory of Translational Cell and Tissue Research, KUL, Leuven, Belgium*

(2) *Pathology, Department of Medicine & Surgery, Università degli studi di Milano-Bicocca, Milan, Italy*

(3) *ProtATonce Ltd, Athens, Greece*

(4) *National Technical University of Athens, Greece*

*These two authors equally contributed

Mailing address: Francesca Maria Bosisio, f.bosisio1@gmail.com, +393420342028

Introduction

A thorough investigation of the tumor microenvironment has been urged in recent years by the introduction of immunotherapy in clinical practice. Immune-based therapies have achieved a previously impossible, long term survival in metastatic melanoma, but Ipilimumab, Pembrolizumab and Nivolumab as monotherapy yield response rates of only 15%, 33% and 40% respectively (1) (2) (3). These low response rates, as well as the possible severe adverse effects and the high cost of these drugs have prompted the search for predictive biomarkers of response, in order to identify the subgroup of patients that could benefit from these therapies. Several studies have appeared, and some of them have found molecular signatures associated with durable response (4) (5) that share an enrichment in immune-related genes. Moreover, heavy CD8+ T cell infiltration of the tumor at the baseline is another characteristic shared by patients with durable response (4) (5) (6) (7) (8) (9) (10) (11).

The lymphocytic infiltrate in melanoma has been known for a long time to be a prognostic parameter and is described in the pathology report according to the pattern of tumor-infiltrating lymphocytes (TILs). A “brisk” pattern (diffuse TILs all over the invasive tumor area or all around its periphery and making contact with melanoma cells) has a better prognosis compared to the “non-brisk” pattern (in which peripheral tumor areas with TILs alternate with peripheral areas without TILs) or to the “absent” pattern (TILs absent or presence of TILs but without contact with melanoma cells) both in primary melanoma and in metastasis (12) (13) (14). There are multiple pitfalls in the purely morphological evaluation of the lymphocytic infiltrate in melanoma (reviewed in 15). One of these pitfalls is that morphology alone cannot determine the activation status of the TILs. Indeed, the contact between cytotoxic lymphocytes (Tcy) and melanoma cells does not always lead to

lysis of the tumor cell but, due to immune modulation, can also result in the inactivation of the Tcy, e.g. in the case of longstanding antigen (Ag) exposure. These “exhausted” and functionally inert Tcy would still be present in the tumor microenvironment, but morphologically indistinguishable from active lymphocytes. A recent study using CyTOF hypothesized on the composition of the tumor microenvironment by analyzing inflammatory populations in the peripheral blood of both responders and non-responders to immunotherapy (16). Interestingly, this study also investigated the functional status of the lymphocytes, highlighting that anti-PD-1 immunotherapy supports functionally activated T cells. Hence, the morphological (17) and functional side of the tumor microenvironment (16) have been investigated, but integration of both types of data is still lacking. Another recent study evaluating the morphological patterns of the TILs across different cancer types from the TCGA histological image repository, found a group of tumors with brisk pattern associated with relatively poor outcome, hypothesizing that brisk infiltrates unable to control tumor growth do exist (17). Moreover, no studies have been published that report a predictive value for immunotherapy according to the morphological TILs pattern. These data strongly suggest that functional information should be added to the morphological data.

A vast portion of the studies looking for predictive biomarkers for immunotherapy finds predictive parameters in peripheral blood (reviewed in 18). Peripheral blood markers give an idea of the systemic immune response, which should reflect the immune response against the tumor at the tumor site. However, there is also evidences for substantial differences between circulating inflammatory cells and their tissue-based counterparts (19). It is intuitive that it is the behavior of the inflammatory cells and not that of circulating inflammatory cells near the tumor that will determine the response to immunotherapy. In the latest years, several methods for single cell-analysis have been implemented in order to obtain a high resolution landscape of the tumor microenvironment, as highlighted in one dedicated issue of Nature in 2017 (20). Nevertheless, most of these methods rely on dissociation of the cells from fresh material. This approach makes a study of the microenvironment in primary melanomas impossible, as these lesions are diagnosed and removed nowadays at earlier stage, with very limited material that must be fully dedicated to the pathological diagnosis. Moreover, according to a recent review by Binnewies et al (21), high resolution means also to be able to characterize not only the heterogeneity of the immune infiltrate but also to define the spatial distribution of each component within it. Spatial distribution adds information that allows to make inferences about the interactions of the cells in the tissue, a feature that is completely lost with tissue dissociation. Until recently, an effective method to stain tissue sections with multiple markers at the single cell resolution was lacking.

Here, we took advantage of the emergence of new technologies in image analysis with single cell resolution in order to study the primary melanoma microenvironment “in situ” (i.e. on tissue sections) integrating its morphological and functional features. We characterized the immune landscape at the single cell-level in 29 primary melanomas based on a panel of 40 immune markers applied on one single tissue section. In particular, we have studied the differences in the immune microenvironment between melanomas with brisk and non-brisk infiltrates, not only in terms of quantification of the inflammatory populations but also in terms of their social organization, using neighborhood analysis. To this end, we applied on a data set of primary melanomas with brisk and non-brisk infiltrates, a high-density immunophenotypic characterization (22), and validated the data by RT-PCR expression and shotgun proteomic analysis. This approach allowed us a) to further categorize the brisk and non-brisk morphological patterns of TILs into three functional categories, i.e. predominantly active, transitional and predominantly exhausted; b) to define the correlation between T-cell activation and spontaneous melanoma regression; and c) to investigate the most important inflammatory subpopulations involved in the process of TILs exhaustion. Finally, we obtained a “dynamic” picture of the

“in situ” inflammatory microenvironment in melanoma that may be helpful in the search for predictive markers in patients undergoing immune checkpoint therapy.

Material and methods

Patients

Twenty-nine invasive primary cutaneous melanomas from the Department of Pathology of the University Hospitals Leuven (KU Leuven), Belgium, were classified based on the H&E staining according to the pattern of the inflammatory infiltrate into brisk (6 cases) and non-brisk (23 cases). According to their subtype, 24 superficial spreading melanomas, 3 nodular melanomas, and 2 lentigo maligna melanoma were included.

TMA construction

Tissue Micro Arrays (TMAs) were constructed with the GALILEO CK4500 (Isenet Srl, Milan, Italy). For each patient, one to five representative regions of interest were sampled according to the size of the specimen and the morphological heterogeneity both of the melanoma and of the distribution of the infiltrate. According to the morphological TILs pattern, we sampled brisk areas (i.e. 6 brisk areas in melanomas with brisk TILs pattern, termed “brisk in brisk” and 10 brisk areas in melanomas with non-brisk TILs pattern, termed “brisk in non-brisk”) and non-brisk areas (i.e. 15 non-brisk areas in non-brisk melanomas, termed “non-brisk in non-brisk”); in addition, areas showing “early regression” (7), “late regression” (5) and “no regression” (17) according to current morphological criteria (23) were sampled. After processing, cutting and staining of the TMA blocks, a total of 60 cores was available for analysis.

Multiplex-Stripping Immunofluorescence

The multiplex-stripping method was performed as published in Bolognesi MM, et al (22). The antibodies used for the multiplex staining are listed in Table 1. Slides were scanned and images acquired with the Hamamatsu Nanozoomer S60 scanner (Nikon, Italia) equipped with an Nikon 20X/0.75 lambda objective. Complete removal of previous layers was monitored a) by checking for unexpected staining consistent with the subcellular and tissue distribution of a previously detected marker, b) by spurious co-clustering of unrelated molecules in the hierarchical clustering images (see below).

Image Pre-processing

Fiji/ImageJ (version 1.51u) were used to pre-process the images (File format: from. ndpi to.tif 8/16 bit, grayscale). Registration was done through the Turboreg and MultiStackReg plugins, by aligning the DAPI channels of different rounds of staining, saving the coordinates of the registration as Landmarks and applying the landmarks of the transformation to the other channels. Registration was followed by autofluorescence subtraction (Image process → subtract), previously acquired in a dedicated channel, for FITC, TRITc and Pacific Orange. A macro was written in Fiji/Image J and used for the TMA segmentation into single images. Cell segmentation, mask creation, and single cell measurements were done with a custom pipeline using CellProfiler (version 2014-07-23T17:45:00 6c2d896). Quality Control (QC) over the Mean Fluorescence Intensity (MFI) values was performed using feature and sample selection. In short, those cells that did not have expression in at least three markers, and those markers that were not expressed in at least 1% of the samples were removed. MFIs were further normalized to Z-scores as recommended in (24). Z-scores were trimmed between -5 and +5 to avoid a strong influence of any possible outliers in the downstream analysis. The correlation between the different markers was calculated using Pearson’s correlation coefficient.

Protein	Concentration	Species	Clone	Company	RRID_AB:
CD4	1 µg/ml	rabbit Mab	EPR6855	Abcam	N/A
HLA-DR	1 µg/ml	mouse IgG2b	SPM288	Abcam	1125217
TAP2	1 µg/ml	mouse IgG1	TAP2.17	Abcam	N/A
CD141	1 µg/ml	rabbit Mab	EPR4051	Abcam	2201805
MYC	1 µg/ml	rabbit Mab	EP121	Sigma Aldrich	N/A
FOXP3	1 µg/ml	mouse IgG1	236A/E7	Abcam	445284
MX1	1 µg/ml	Rabbit		Abcam	10678925
LAG3	1 µg/ml	mouse IgG1	11E3	Abcam	776102
PD-L1	1 µg/ml	rabbit Mab	28-8	Abcam/Epitomics	2687878
CD1a	1 µg/ml	Rb mAb	EP3622	Abcam/Epitomics	626957
CD123	1 µg/ml	mouse IgG2b	NCL-L-CD123	Leica-Microsystem/ Novocastra	10555271
Phospho-Stat1	1 µg/ml	rabbit Mab	58D6	Cell Signaling	561284
CD20	1 µg/ml	mouse IgG2a	L26	Dako	782024
CD1a	1 µg/ml	mouse IgG1	O10	Dako	N/A
CD1c	1 µg/ml	mouse IgG1	2D4	Dako	2623049
PRDM1	1 µg/ml	rat	6D3	Dako	628168
S100AB	1 µg/ml	rabbit		Dako	N/A
CD56	1 µg/ml	mouse IgG1	123C3.D5	Neomarkers	627127
Ki-67	2 µg/ml	mouse IgG2a	UMAB107	Origene	2629145
Lysozyme	1 µg/ml	rabbit		Origene	1004766
PD-1	1 µg/ml	mouse IgG2a	UMAB197	Origene	2629198
TIM3	1 µg/ml	goat		R&D	355235
CXCL13	1 µg/ml	mouse IgG1	53610	R&D	2086049
OX40	1 µg/ml	mouse IgG1	Ber-ACT35	Santa Cruz	626897
IRF4	1 µg/ml	goat	M-17	Santa Cruz	2127145
cMAF	1 µg/ml	rabbit	M-153	Santa Cruz	638562
BCL6	1 µg/ml	rabbit	N3	SCBT	1158074
CD16	1 µg/ml	mouse IgG2a	2H7	SCBT	563508
CD68	1 µg/ml	mouse IgG3	PGM1	Thermo Fisher	10979558
p16	1 µg/ml	mouse IgG2a	JC8	SCBT	785018
MelanA	1 µg/ml	rabbit Mab	A19-P	NovusBio	1987285
podoplanin	1 µg/ml	rat IgG2a	NZ-1.2	Sigma Aldrich	10920577
CD69	1 µg/ml	rabbit		Sigma Aldrich	2681157
CD3	1 µg/ml	rabbit		Sigma Aldrich	2335677
GBP1	1 µg/ml	rat	4D10	Sigma Aldrich	828964
Langerin	1 µg/ml	rabbit		Sigma Aldrich	1078453
IRF8	1 µg/ml	rabbit		Sigma Aldrich	1851904
CD8	1 µg/ml	rabbit Mab	SP16	Thermo Fisher	627211
CD138	1 µg/ml	mouse IgG1	MI-15	Thermo Fisher	10987019

Table 1 List of antibodies.

Image Analysis

We selected two activation (CD69, OX40) and two exhaustion (TIM3, LAG3) markers after literature review and preliminary testing of the antibody performance on control FFPE under the conditions of the multiplex protocol. The expression levels of these markers were measured selectively on CD8+ lymphocytes using a first mask focused only on CD8+ cells. Principal Component Analysis (PCA) was applied over the expression values to evaluate the functional structure of the data and to assign an activation value in the [-1, 1] range to each cell (Supplementary Figure 1). Briefly, principal components (PCs) 2 and 3 were used as the rotation matrix revealed that PC1 contained all the markers in the same direction (same sign). The point of maximum activation (Activation = 1), was defined where the projected value of CD69 (marker of activation) over PCs 2 and 3 was at the maximum while the point of maximum exhaustion (Activation = -1) where the projected value of TIM3 (marker of exhaustion) over PCs 2 and 3 was at the maximum (Figure 1.A). The gradient of transition was defined between the previously defined points and the centroid of the projected dataset. Pairwise t-tests with pooled standard deviation (sd) were used to find significant differences in the level of activation of the images regarding multiple histopathologic parameters (brisk/non-brisk infiltrate, regression, number of lymphocytes, ulceration, Breslow thickness, mitoses, subtype of melanoma). For this purpose, the activation level of each image was represented by the mean of its cells while the intrinsic degree of heterogeneity was captured by the sd (Figures 2.A and C). Continuous values of the histopathological parameters were fitted using linear models instead. P-values were adjusted for multiple comparisons using the holm method. A cut-off of 0.05 was used as significance threshold for the adjusted p-values. Images were further classified into: 'Active', 'Transition', and 'Exhausted' (from now on, core status) using one-tailed t-tests comparing the distribution of the activation values in a specific image versus the background distribution (combination of all images) (Figure 2.B). P-values were adjusted using the False Discovery Rate (fdr) method. A cut-off value of 0.001 over the adjusted p-values was used as classification threshold.

To evaluate the cell subpopulations, a second mask based on the DAPI staining expanded by 5 pixels was created. A two-tier approach was followed for the identification of cell subpopulations: phenotypic and functional. The phenotypic identification was conducted by applying three different clustering methods: PhenoGraph, ClusterX, and K-means, over the phenotypic markers: CD3, CD20, CD4, HLA-DR, Bcl6, CD16, CD68, CD56, CD141, CD1a, CD1c, Blimp1, Langerin, Lysozyme, Podoplanin, FOXP3, S100A, S100AB, IRF4, IRF8, CD1a, CXCL13, CD8, CD138, CD123, PD-1, and MelanA. PhenoGraph and ClusterX were implemented using the cytofkit package from R (25). Clusters were represented by a vector containing the mean of each marker and were used to further associate them to a cell subpopulation using prior knowledge. Cluster stability was evaluated by comparing the weighted Pearson correlation coefficient of clusters belonging to the same cell subpopulation with the background distribution (all pairwise comparisons). The geometric average of the absolute value of the mean expression was chosen as weight. A confidence value was assigned to each cell population using one-tailed t-tests. For a phenotype to be assigned to a cell, at least two clustering methods should agree on their predicted phenotype (Supplementary Figure 2 and Supplementary Figure 3). Prior to functional identification, PCA was repeated over the Tcy cells (CD8+) using CD69, OX40, LAG3, and TIM3 markers in order to confirm that with the new mask, the same dataset with the same structure as with the CD8+ mask could be retrieved (Supplementary Figure 4). The functional identification was conducted by applying PhenoGraph over the functional markers: CD69, Ki-67, TAP2, GBP1, MYC, p16, MX1, OX40, c-Maf, PD-L1, LAG3, TIM3, and Phospho-Stat1 (with the exception of Tcy cells for which we used a personalized panel consisting of: CD8, CD69, OX40, LAG3, TIM3, PD-1, and Ki-67). Clusters were represented, associated to cell subpopulations, and evaluated for stability as described for the phenotypic identification. One-way Analysis of Variance (ANOVA) models were fitted to identify if the percentage of cells in any subpopulation

was linked to the core status. The same approach was repeated for the brisk infiltrate histopathologic parameter.

An unbiased quantitative analysis of cell-cell interactions was performed using an adaptation of the algorithm described in (26) for neighborhood analysis to systematically identify social networks of cells and to better understand the tissue microenvironment. Our adaptation also uses a kernel based approach (radius = 30 px) to define the neighborhood of a cell and a permutation test (N = 1000) to compare the number of neighboring cells of each phenotype in a given image to the randomized case. This allows the assignment of a significance value to a cell-cell interaction representative of the spatial organization of the cells. Significance values were further classified into: avoidance (-1), non-significant (0), and proximity (1) using a significance threshold of 0.001 (more significant than all the random cases). Interactions across images were integrated according to equation 1:

$$P_{i,j} = \frac{\sum_{k=1}^M (c_{i,j,k} \cdot \sqrt{N_{i,j,k}})}{\sum_{k=1}^M (\sqrt{N_{i,j,k}})}$$

where $C_{i,j,k}$ is the significance value (-1, 0, or 1) of the interaction between cell types i and j for image k , and $N_{i,j,k}$ is the geometric average of the number of cells of type i and j for image k . Cell-cell interactions were considered strong if they were significant in at least 75% of the N-adjusted cases ($\text{abs}(P) > 0.75$), moderate if 50%, ($0.5 < \text{abs}(P) \leq 0.75$), weak if 25% ($0.25 < \text{abs}(P) \leq 0.5$), and non-significant otherwise ($\text{abs}(P) \leq 0.25$). A comparative analysis of the above described method was performed for the different core statuses as well as for the different brisk infiltrate cases.

Even though neighbour analysis allows evaluation of cell-cell interactions, the mathematical model applied is limited in cases where there are dominant cell types that grow in nests, with cells packed next to each other. Therefore, for melanoma cells, we evaluated the closest neighbours by counting the number of cells of each subpopulation (apart from melanoma cells) that were in their neighborhood and divided the amount by the geometric average of the number of melanoma cells and the number of cells of the specific population across all the cores in which the specific population appears. This analysis was repeated for the different brisk and activation cases.

Laser Microdissection

18 fresh frozen melanoma metastasis with different types of TILs patterns (9 brisk, 7 non brisk, 1 absent and 1 tumoral melanosis) were collected in the Department of Pathology of the University Hospitals Leuven (KU Leuven), Belgium. 10 micrometer-thick sections were cut from each fresh frozen block and put on a film slide (Zeiss, Oberkochen, Germany). Sections were stained with crystal violet. Areas with dense TILs infiltrate were microdissected with the Leica DM6000 B laser microdissection device (Leica, Wetzlar, Germany). A calculation was made in order to microdissect the same surface in all the samples in order to minimize differences between the samples (around 10.000 lymphocytes/sample).

qPCR of laser microdissected samples

RNA extraction was done with RNeasy® Plus Micro Kit (Qiagen) according to the protocol. cDNA retrotranscription followed by an amplification step was done with Ovation® Pico SL WTA System V2 (Nugen) according to protocol. Primers for Interferon gamma (IFNg, forward 'TGTTACTGCCAGGACCCA' and reverse 'TTCTGCTACTCTCTCTTTCCA'), TIM3 (forward 'CTACTACTTACAAGGTCCTCAGAA' and reverse 'TCCTGAGCACCGTTG'), LAG3 (forward 'CACCTCTGCTGTTTCTCA' and reverse 'TTGGTCGCCACTGTCTTC'), CD40-L (forward 'GAAGTTGGACAAGATAGAAGATG' and reverse 'GGATAAGGATCTTTCTCTGTGT'), CD45

(forward 'GCTACTGGAAACCTGAAGTGA' and reverse 'CACAGATTTCTGGTCTCCAT'), Beta2microglobulin (forward 'ACAGCCCAAGATAGTTAAGTG' and reverse 'ATCTTCAAACCTCCATGATGC'), HPRT (forward 'ATAAGCCAGACTTTGTTGGA' and reverse 'CTCAACTGAACTTCATCTTAGG') were designed with Perl Primer® and tested in our laboratory. 96-wells plates were loaded with Fast SYBR® Green Master Mix, the primers and the samples in the recommended proportions, and analyzed with the 7900 HT Fast Real-Time PCR system (Applied Biosystems). The log fold change (logFC) of the expression values towards the expression value of CD45 were calculated. If the log(IFNg/CD45) was positive, the sample was classified as positive.

Shotgun Proteomics of laser microdissected samples

The materials used for the shotgun proteomics analysis were Trifluoroacetic acid, porcine trypsin, DTT (dithiothreitol), IAA (Iodoacetamide), ABC (Ammonium Bicarbonate), HPLC grade water, acetonitrile, were from Sigma-Aldrich (Sigma-Aldrich Chemie GmbH, Buchs, Switzerland). All solutions for Mass Spectrometry (MS) analysis were prepared using HPLC-grade. LCM collected material corresponding to about 10^4 cells for each sample group was re-suspended in 90 μ l of bidistilled water and immediately stored at -80°C. For the bottom-up MS analysis, all the samples were processed and trypsinized. Briefly, thawed cells were submitted to a second lysis adding 60 μ l of 0.25% w/v RapiGest surfactant (RG, Waters Corporation) in 125mM ammonium bicarbonate (ABC) and sonicated in the Elmasonic P (Elma Schmidbauer GmbH, Singen, Germany) sonication bath for 10 min. Samples were then centrifuged at 14 000 \times g for 10 min. About 140 μ l of supernatants were collected, transferred in a new tube and quantified using bicinchoninic acid assay (Pierce -Thermo Fisher Scientific). After 5min denaturation (95°C), proteins were reduced with 50mM DTT in 50mM ABC at room temperature and alkylated with 100mM IAA in 50mM ABC (30 min incubation in dark). Digestion of samples was performed overnight at 37°C using 2 μ g of MS grade trypsin (Sigma-Aldrich Chemie GmbH). RG surfactant were removed using an acid precipitation with TFA at a final concentration of 0.5% v/v. Samples were then spun down for 10 min at 14000 \times g and supernatants collected for MS analysis. Peptide mixtures were desalted and concentrated using Ziptip™ μ -C8 pipette tips (Millipore Corp, Bedford, MA). An equal volume of eluted digests were injected at least three times for each sample into Ultimate™ 3000 RSLCnano (ThermoScientific, Sunnyvale, CA) coupled online with Impact HDTM UHR-QqToF (Bruker Daltonics, Germany). In details, samples were concentrated onto a pre-column (Dionex, Acclaim PepMap 100 C18, cartridge, 300 μ m) and then separated at 40°C with a flow rate of 300 nL/min through a 50 cm nano-column (Dionex, ID 0.075mm, Acclaim PepMap100, C18). Phase A was constituted of 0.1% formic acid in water and solvent B was 0.1% formic acid in 80% acetonitrile. A multi-step gradient of 4 hours ranging from 4 to 66% of phase B in 200min was applied (27). NanoBoosterCaptiveSpray™ ESI source (Bruker Daltonics) was directly connected to column out. Mass spectrometer was operated in data-dependent acquisition mode, using CID fragmentation assisted by N₂ as collision gas setting acquisition parameters as already reported (28). Briefly, Fragmentation spectra were acquired using IDAS (Intensity Dependent Acquisition Speed) and RT2 (RealTime Re-Think) functionalities. Mass accuracy was assessed using a specific lock mass (1221.9906 m/z) and a calibration segment (10 mM sodium formate cluster solution) for each single run. Precursor selection was applied in a fixed cycle time of 5 sec over 300-2200 m/z window (excluding 1221.5–1224 m/z), using a ramp for spectra rate from 4Hz for low intensity ions (2500cts per 1000sum). The active exclusion of precursors was executed for one minute after two spectra. Raw data from nLC ESI-MS/MS were elaborated through DataAnalysis™ v.4.1 Sp4 (Bruker Daltonics, Germany) and converted into peaklists. Resulting files were interrogated for protein identification through in house Mascot search engine (version: 2.4.1), using Mascot Daemon tool. The search was restricted to human swissprot database (accessed Feb 2017, 553,655 sequences; 198,177,566 residues) setting the following parameters: Trypsin as enzyme; carbamidomethyl as fixed modifications; a tolerance of 20 ppm for precursor mass tolerances and 0.05 Da for the product ions. Data were filtered searching into automatic decoy database for estimating related False

Discovery Rates. A built-in Percolator algorithm for rescoring peptide-spectrum matches was used. Identity was accepted for proteins recognized by at least one unique and significant (p -value < 0.05) peptide.

Pathways Analysis

Gene-set enrichment analysis was performed with DAVID 6.8 (29). Pathways were visualized and partially analyzed with STRING v10 (30).

Results

Functional analysis of TILs at tissue-based single cell level

We classified each CD8+ cell in the TMA cores as part of a spectrum (“cell status”) (Figure 1) ranging from active cells (CD69^{high} and/or OX40^{high}) to exhausted cells (TIM3^{high}CD69^{low}OX40^{low}) with bioinformatics and image analysis algorithms. Two intermediate states between activation and exhaustion were identified, one passing through a gradual decrease of CD69 with parallel increase of TIM3 expression, and the other in which OX40 was co-expressed with LAG3. Correlation analysis of the markers of activation and inhibition showed that these latter two markers actually had the highest Pearson correlation coefficient among all the activation and exhaustion markers ($R = 0.35$). As shown in Supplementary Materials 3, the same 4 markers emerged in the classification of CD8+ Tcy when the mask was not focused only on CD8+ T cells but on cells with nuclei in general; moreover, this approach confirmed that we could recover the structure of the data as well as the same trend for activation/exhaustion markers in Tcy (Supplementary Materials 3).

The definition of the cell status allowed us to assign a label to every core: active (17/60 cores), in transition (23/60 cores), or exhausted (20/60 cores) (Figure 2a, b, c). This approach allowed us not only to study the differences in TILs activation between the patients, but also the heterogeneity in activation status of the TILs in different areas of the same tissue section, as we sampled multiple areas in most melanomas. In 8 patients, the size of the melanoma allowed to sample only a single core and therefore we could not assess intra-patient heterogeneity. In the remaining 21 patients, 10 showed homogeneous activation statuses among their cores (4 active, 5 in transition, and 1 exhausted) and 11 showed heterogeneity in activation status (Figure 2c). In most of the latter melanomas, areas of exhaustion or activation were associated with transition areas (3 activation + transition, 6 exhaustion + transition) rather than with areas of full activation or exhaustion, respectively (2 patients). In summary, we observed a spatially homogeneous TILs infiltrate in 6 active cases (20.8%) and in 5 exhausted ones (17.2%), while in 18 cases (62%) there were areas of transition suggesting an ongoing dynamic process of exhaustion.

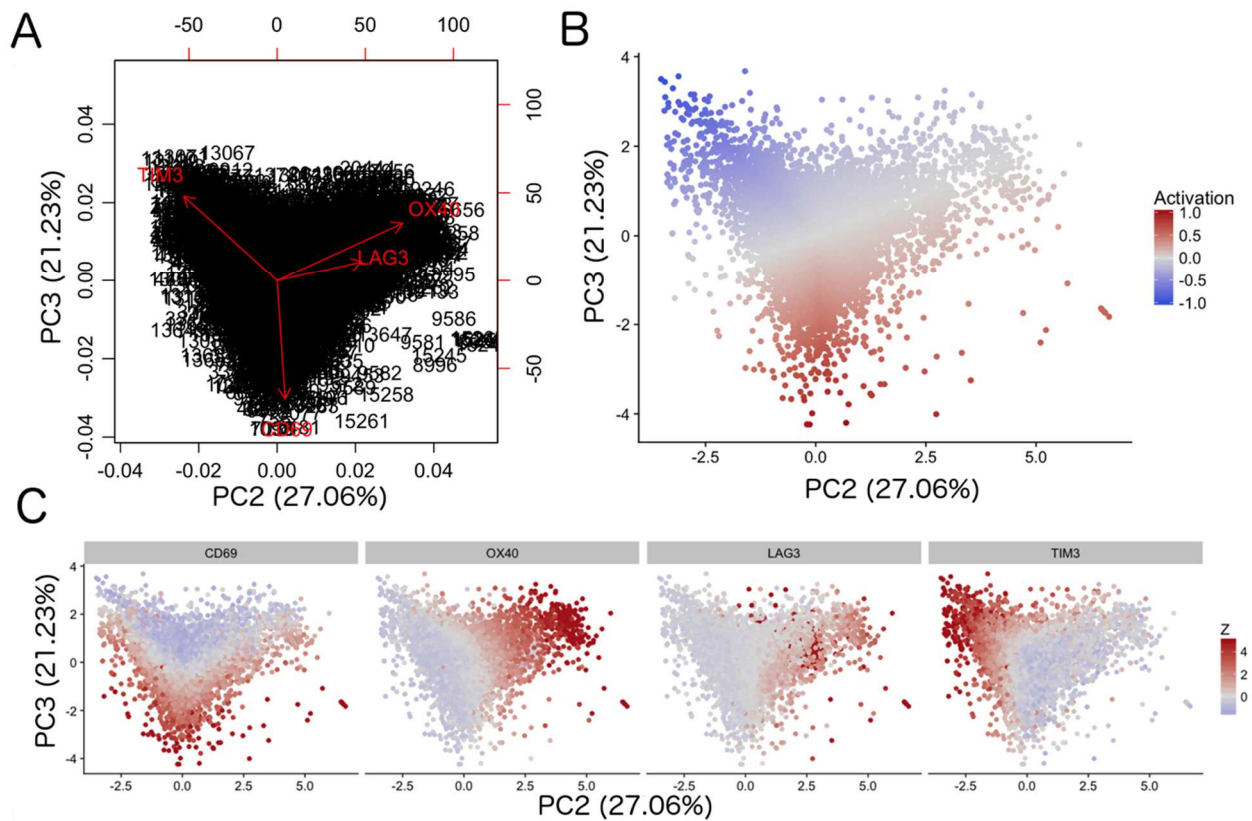


Figure 1. Definition of activation. (A) Here we show a biplot with the projection of all CD8+ cells in the cores as well as the rotation vectors of the markers over PC2 and PC3. (B) This was our approach to define a gradient of activation in the CD8+ mask, going from the maximum projected value of CD69 (maximum activation) to the maximum projected value of TIM3 (maximum exhaustion). (C) Here we show the coexpression of the markers in the different areas of the biplot by indicating in a colorimetric scale the Z-scores of the original markers over PC2 and PC3. LAG3 is most often coexpressed with OX-40, while CD69 and TIM3 occupy two opposite ends of a spectrum of activation/exhaustion.

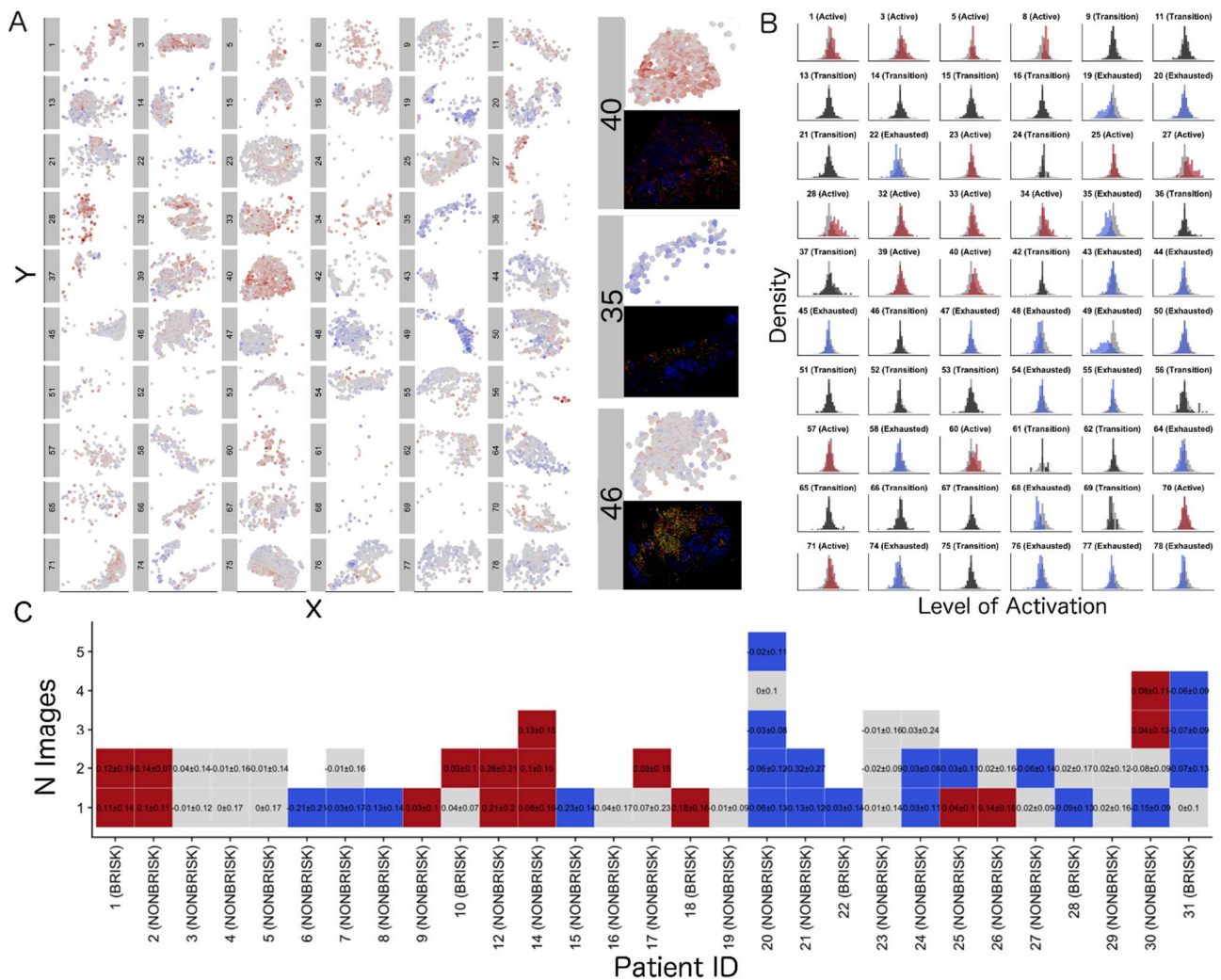


Figure 2. A) Definition of the activation status of each single CD8+ cell. A) Here we show the *in silico* reconstruction of the 60 cores showing on the left the single cell activation level of every CD8+ cells present in each of them (blue = exhausted cell, grey = transition cell, red = active cell). After defining the activation status for each cell in the core as explained in Figure 1, we added to it the spatial location (x, y coordinates). On the right, core 40, 35 and 46 are shown as examples of how our graphical representation of the CD8+ infiltrate corresponds to the respective immunofluorescence images (S100 = blue, CD3 = green, CD8 = red). **B) Definition of the activation status of each core.** Here we show the global activation status for all 60 cores using a one-tailed t-tests to compare the distribution of the activation values in a specific image versus the background distribution of all the images, in order to further classify each core into the ‘Active’, ‘Transition’, or ‘Exhausted’ category (gray= background values, blue, left shift = exhausted core, black, no shift = transition core, red, right shift = active core). **C) Visual representation of the inter- and intra-patient heterogeneity.** The cores are grouped for each patient, giving at-a-glance representation of the heterogeneity of the activation status in different areas of the melanoma in the same patient and between the 29 patients (blue = exhausted core, grey = transition core, red = active core).

Association of the TILs activation status with brisk/non-brisk status, regression and other histopathological prognostic parameters

We first investigated the association between functional status of the TILs and their morphological classification into brisk and non-brisk categories. Statistical analysis revealed that the morphological patterns of the TILs were not significantly associated with the mean level of activation of the TILs since brisk and non-brisk cases were distributed across the active, exhausted and transition statuses (Table 2). Moreover, analyzing only the lymphocytes inside the tumor in both brisk and non-brisk cases (the so-called “brisk in brisk” and “brisk in non-brisk” areas), we similarly found no significant association between activation status of the TILs and their contact with melanoma cells.

Spontaneous regression of melanoma is regarded as the result of a successful aggression from the patient’s own lymphocytes, resulting in variously sized areas of the melanoma that are removed and replaced by scar tissue. Therefore, we checked whether the mean level of activation of the cores was significantly associated with spontaneous regression of the tumor. Late regression areas indeed showed significant differences in the mean level of activation of the cores as compared to early regression and no regression. No significant differences were instead found between early regression and no regression (Figure 3, Table 2).

The mean level of activation of the TILs in the cores was further investigated for their association with other histopathological parameters (histological subtype, ulceration, Breslow thickness, mitoses). Table 2 summarizes the significance values for each histopathological prognostic parameter. The mean level of activation of Lentigo Maligna Melanoma (LMM) cores was significantly different from the Superficial Spreading Malignant Melanoma (SSMM) cores and the Nodular Malignant Melanoma (NMM) ones. However, since only three LMM cores from two patients were included in our data set, no definite conclusions can be drawn from this data. The other histopathological prognostic parameters did not show significant associations with the mean level of activation of the TILs.

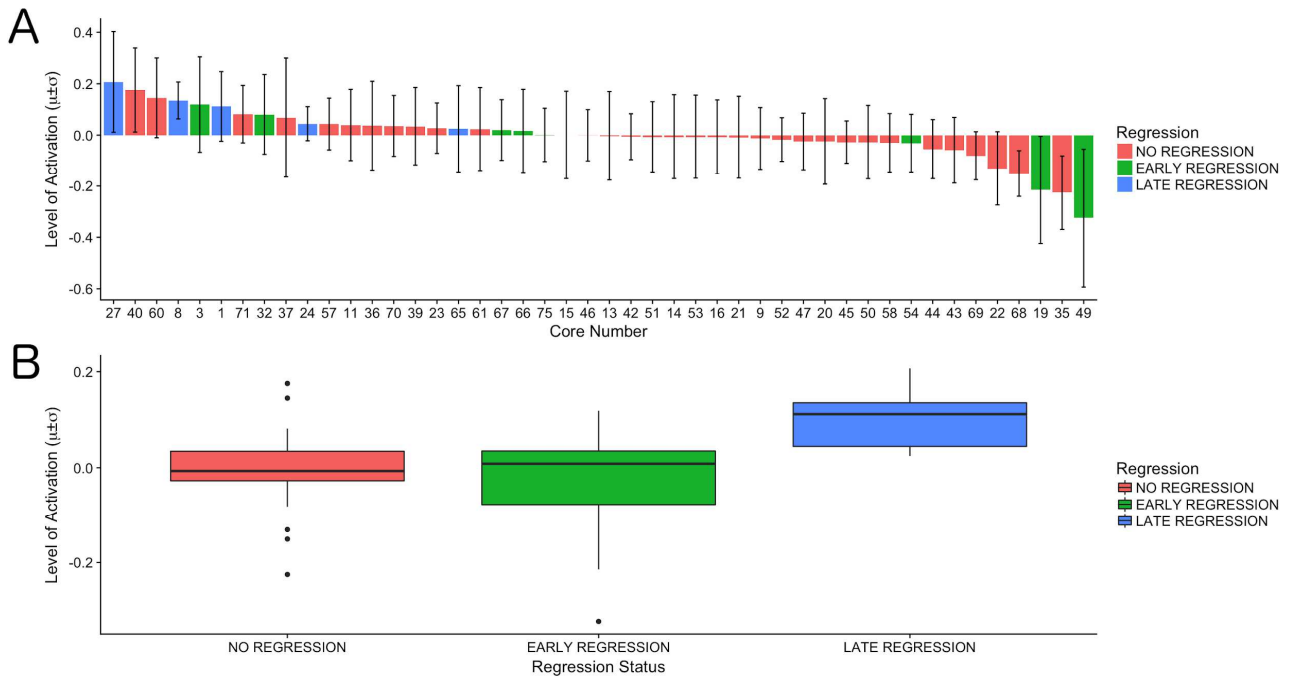


Figure 3. Association between the activation status and regression status of the cores. A) Bar plots showing the level of activation (y-axis: mean \pm sd) of the cores (x-axis) in decreasing order. All late regression cases are at the left side of the graph. B) Box plots showing the mean level of activation of the cores (y-axis) for the different regression statuses (x-axis). Lymphocytes in late regression have a significantly higher activation value than in the two other regression statuses.

Parameter	Comparison	Adj.p-value
Brisk Infiltration	Brisk vs Non Brisk	0.89
Brisk Infiltration	Brisk vs Brisk In Non Brisk	1
Brisk Infiltration	Brisk vs Non Brisk In Non Brisk	1
Brisk Infiltration	Brisk In Non Brisk vs Non Brisk In Non Brisk	1
Regression	Regression vs No Regression	0.52
Regression	Early Regression vs No Regression	0.329
Regression	Late Regression vs No Regression	0.031*
Regression	Late Regression vs Early Regression	0.022*
Count Lymphocytes	Number of Lymphocytes vs Level of Activation	0.539
Histotype	LMM vs NMM	0.029*
Histotype	LMM vs SSMM	0.02*
Histotype	NMM vs SSMM	0.86
Breslow Thickness	Breslow vs Level of Activation	0.996
Ulceration	Positive vs Negative	0.73
Number of Mitoses	More than 6 vs 1 to 6	1
Number of Mitoses	More than 6 vs 0	1
Number of Mitoses	1 to 6 vs 0	1

Table 2. Association between the activation status of the cores and different histopathologic parameters. Reported *p*-values come from linear models in the continuous case (Breslow, Count Lymphocytes) and pairwise *t*-test otherwise. Significant associations ($p < 0.05$) are marked by asterisks.

Study of the inflammatory microenvironment associated with activation and exhaustion: cluster analysis

Three different unsupervised clustering methods (KMeans, PhenoGraph, and ClusterX) were compared to identify the clusters corresponding to each inflammatory subpopulation present in our tissue cores according to their phenotype by high-dimensional immunostaining. The type of cell identified by each cluster was manually annotated by the pathologist, and the clusters were validated assessing their solidity across the clustering methods (Figure 4 and Supplementary Results 1). We were able to classify solidly 198302 cells out of 242224 cells across all cores (81.87%). This resulted in 19 clusters, 17 of which could be recognized as phenotypically well-defined groups of cells, while the profile of two clusters (“IDK” and “BLANK”) could not be associated to a determined cell lineage, and were therefore discarded from further analysis, leaving a total of 179304 out of 242224 cells (74.02%). The cell populations were further classified based on their functional markers using PhenoGraph in order to explore specific functional phenotypes for each cell population. This functional classification further divided the original 17 cell populations into 55 functional groups. The molecular profile of each of the 55 functional groups is represented in Figure 4.B.

The most abundant cell population consisted of melanoma cells (35,64% of all cells examined), functionally subdivided in 3 phenotypic subpopulation and 6 functional subclusters (described in Figure 5). There were no significant differences in the percentages of the melanoma subpopulations between active/transition/exhausted cases; only a LAG3+PD-L1+ S100+MelanA+ population of melanoma cells was present exclusively in brisk cases (Supplementary Figure 5B).

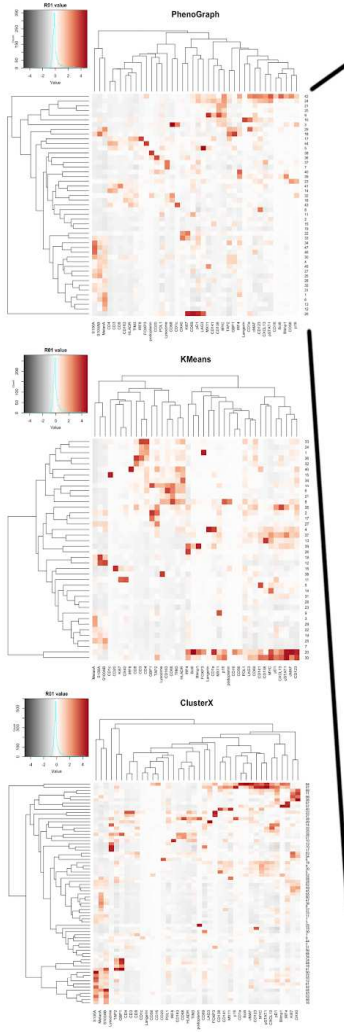
The second most abundant cell type, and the most frequent among the inflammatory subpopulations, were the macrophages (“macroph”, CD68+CD163+Lysozyme+HLA-DR+, 15,24%), one quarter of them expressing at least one of the immunosuppressive markers TIM3, LAG3 or PD-L1 (Figure 5). Regarding the putative M1/M2 markers, we found a small population of cMAF-positive macrophages (3,34%), but we did not observe pSTAT1 expression in macrophages; instead, pSTAT1 was expressed by cDC1 and Langerhans cells, in the latter cells in co-expression with cMAF. Macrophage distribution between active/transition/exhausted cases and between brisk/non-brisk cases was significantly different for some subclusters: proliferating macrophages and TIM3+ macrophages were more abundant in exhausted cases, and macrophages in general as well as proliferating and LAG3+ macrophages were more abundant in brisk cases (Supplementary Figure 5).

The lymphoid compartment accounted for multiple subpopulations. Tcy (CD3+CD8+) and T helpers (“Th”, CD3+CD4+FOXP3-) were the most abundant subtypes, accounting respectively for 9,48% and 8,37% of all the cells, while regulatory T cells (“Treg”, CD3+CD4+FOXP3+) represented 2,35% of all lymphocytes. We interpreted the last T cell cluster as T follicular helpers (“Tfh”, CXCL13+PD1+, 2,16%) even though this cluster did not express the full Tfh phenotype, (i.e. no CD3 and no CD4 expression). Within the Tcy cluster, we could identify the active (predominantly CD69+, 16,1%), transition (balanced expression of both exhaustion and expression markers, 29,6%) and exhausted (high expression of LAG3 and/or TIM3, low/absent CD69, 12,8%) functional subgroups, plus a clonally expanding subgroup (6%), and one with low or absent expression of all functional markers, that we defined as “anergic” (34,9%) (Figure 5). Th could also be subdivided according to their expression of activation and exhaustion markers (28,5% active Th, 18,46% Th with active/exhaustion “balanced” expression, 13,08% TIM3+ or LAG3+ Th). As expected, active Th were much more numerous in active cases while TIM3+ Th were increased in exhausted cases. Exhausted cases had also more Treg in general and more TIM3+ Treg. Interestingly, all the Tcy functional groups were significantly higher in brisk cases compared to non-brisk cases. A brisk infiltrate was also associated with more “balanced” Th and LAG3+ Th, higher T reg proliferation rates and more LAG3+ Treg and LAG3+ Tfh (Supplementary Figure 5). NK cells, as expected in melanoma, were extremely infrequent (0,44%) and significantly more abundant in brisk cases,

but evenly distributed among active/transition/exhausted cases (Supplementary Figure 5). B cells ("BC", CD20+) represented 5,03% of the total number of cells in the cores. Another cluster, CD20 negative, characterized by high expression of IRF4 and Blimp1 ("IRF4_Blimp1", 1,05%), was interpreted as most probably a subgroup of post-germinal center BC, due to their low but still detectable expression of Bcl6 suggesting that these cells underwent a process of terminal differentiation into plasma cells (31). Interestingly, PD-L1 was expressed on all BC with the exception of the BC expressing IFN γ -related proteins. These IFN γ BC were also the only subgroup being increased in the brisk group, while BC in general did not show differences among the morphological and functional groups (Supplementary Figure 5).

Finally, we could identify among the dendritic cell group the classical dendritic cells type 1 ("cDC1", CD141+CD4+IRF8+, 3,51%), classical dendritic cells type 2 ("cDC2", CD1c+CD4+HLA-DR+, 1,99%), Langerhans cells ("Lang", CD1a+Langerin+, 1,92%), and plasmacytoid dendritic cells ("pDC", CD123+, 0,28%). There were no significant differences for DC subtypes among the functional categories; however, LAG3+ cDC1, LAG3+ cDC2 and LAG3+ Lang were virtually only present in the brisk cases, which also had more TIM3+ cDC1 (Supplementary Figure 5B).

A



Top 15 Expressed Markers per Cluster (PhenoGraph)

Cluster	Marker 1	Marker 2	Marker 3	Marker 4	Marker 5	Marker 6	Marker 7	Marker 8	Marker 9	Marker 10	Marker 11	Marker 12	Marker 13	Marker 14	Marker 15	Percentage
42	pSTAT1	Bcl6	cMAF	CD123	CD56	CD1a	MYC	CXCL13	IRF4	Blimp1	CD16	p16	FOXP3	p16	CD141	0.67
24	pSTAT1	MYC	CXCL13	CD141	CD123	pD1	MX11	cMAF	CD138	TAP2	LAG3	IRF4	CD69	Bcl6	3.88	
21	MYC	CD138	cMAF	CD141	PDL1	MX11	LAG3	pSTAT1	OX40	CXCL13	CD123	pD1	CD1a	Langerin	podoplanin	4
20	CD138	MYC	pSTAT1	CXCL13	MX11	pD1	TAP2	cMAF	CD1a	CD141	LAG3	CD69	MelanA	CD123	p16	2.77
9	MX11	CD138	MYC	CD141	cMAF	PDL1	LAG3	Langerin	CD1a	CD16	CD123	CXCL13	CD56	podoplanin	OX40	0.26
10	Langerin	CD1a	CD138	cMAF	MYC	CD123	pSTAT1	CD141	S100AB	HLADR	TAP2	MX11	TIM3	pD1	CXCL13	2.77
3	CD56	CD1c	p16	MYC	CD138	Blimp1	CD163	PDL1	podoplanin	Lysozyme	CD56	CD69	CD16	Langerin	LAG3	0.08
29	CD1a	MelanA	TAP2	GBP1	S100AB	IRF4	cMAF	CD123	pD1	Bcl6	PDL1	TIM3	MYC	CD69	pSTAT1	0.05
18	GBP1	S100AB	TAP2	MelanA	S100A	IRF4	TIM3	MX11	HLADR	CD56	CD123	CD16	CD8	Langerin	pSTAT1	0.18
17	IRF8	TIM3	HLADR	TAP2	CD141	CD123	CD4	CD68	Lysozyme	CD8	PDL1	CD163	CD3	MX11	CD69	2.22
44	FOXP3	CD4	CD3	HLADR	CD69	TIM3	cMAF	CD163	TAP2	CD68	PDL1	CD123	CD8	GBP1	OX40	1.76
5	LAG3	pD1	CD3	PDL1	HLADR	MX11	GBP1	cMAF	CD4	CD123	CD8	CD141	Lysozyme	MYC	OX40	0.67
38	podoplanin	CD141	GBP1	CD56	CD16	Lysozyme	IRF8	Bcl6	HLADR	p16	LAG3	CD8	Langerin	FOXP3	CD4	0.71
36	CD20	Ki67	podoplanin	PDL1	IRF8	OX40	pD1	CD123	CD1c	CD69	LAG3	CD141	Blimp1	CD16	Bcl6	3.86
37	Lysozyme	CXCL13	pD1	CD20	cMAF	Bcl6	p16	CD123	PDL1	CD69	LAG3	IRF8	CD16	pSTAT1	CD1c	1.55
7	Lysozyme	CD69	p16	PDL1	Ki67	CD56	CD16	Bcl6	FOXP3	CD20	Langerin	podoplanin	LAG3	Blimp1	CD1c	1.4
40	IRF4	CD20	pD1	PDL1	Blimp1	podoplanin	OX40	CXCL13	TAP2	CD123	CD69	Ki67	LAG3	IRF8	CD8	0.24
39	Blimp1	IRF4	CXCL13	pSTAT1	CD1a	Bcl6	MYC	cMAF	Langerin	pD1	LAG3	p16	CD56	CD16	CD123	1.24
23	CD56	p16	CD123	LAG3	PDL1	CD69	cMAF	CD20	HLADR	CD8	CD163	Blimp1	CD4	CD68	FOXP3	0.9
41	CD8	CD3	CXCL13	CD69	TAP2	CD4	CD163	HLADR	TIM3	CD68	PDL1	cMAF	CD123	CD56	7.17	
14	CD4	CD3	HLADR	CD69	TIM3	CD163	CD8	PDL1	cMAF	TAP2	CD68	CD123	CD1c	GBP1	CD16	6.91
32	CD68	podoplanin	p16	TIM3	Lysozyme	CD163	HLADR	pD1	S100A	CD1a	Bcl6	PDL1	cMAF	pSTAT1	MelanA	1.19
16	CD68	CD163	HLADR	CD56	TIM3	GBP1	CD4	IRF8	CD123	cMAF	CD16	CD69	TAP2	CD56	podoplanin	9.12
8	CD1c	HLADR	CD4	TIM3	CD1a	CD123	Lysozyme	CD8	CD68	CD3	IRF4	PDL1	TAP2	CD163	GBP1	2.55
43	CD123	cMAF	MYC	CD1c	CD69	CD1a	Lysozyme	CD16	TIM3	p16	Langerin	FOXP3	CD56	podoplanin	FOXP3	0.33
11	CD69	PDL1	Ki67	LAG3	CD123	CD16	CD56	CD20	pSTAT1	p16	Bcl6	CD1a	FOXP3	Langerin	Blimp1	1.08
2	pSTAT1	CD1a	MYC	CXCL13	pD1	MX11	CD16	Langerin	CD56	Bcl6	TAP2	CD163	podoplanin	Blimp1	p16	1.75
15	CD141	GBP1	CD123	TAP2	PDL1	CD16	Bcl6	CD56	Langerin	MX11	FOXP3	podoplanin	Blimp1	LAG3	TIM3	2.33
19	CD16	CD56	Bcl6	Langerin	FOXP3	podoplanin	p16	Blimp1	CD1c	CD20	IRF8	CD1a	MX11	Ki67	CD138	4.96
22	Ki67	OX40	pD1	MYC	LAG3	MX11	MelanA	CD138	cMAF	PDL1	TAP2	CD123	CXCL13	GBP1	IRF4	2.72
33	OX40	Ki67	pD1	S100A	IRF4	S100AB	MelanA	LAG3	TIM3	CD16	CXCL13	CD56	Langerin	Bcl6	podoplanin	1.88
34	S100A	TAP2	IRF4	pD1	S100AB	pSTAT1	MelanA	CXCL13	CD69	LAG3	TIM3	OX40	GBP1	CD16	MYC	0.67
47	S100A	S100AB	MelanA	PDL1	CD69	pD1	Blimp1	IRF4	OX40	cMAF	TIM3	LAG3	Ki67	CXCL13	TAP2	1.63
46	S100A	cMAF	MelanA	CD69	PDL1	IRF4	OX40	pD1	LAG3	CD16	TIM3	CD56	Langerin	Bcl6	IRF8	0.16
30	S100A	S100AB	TAP2	GBP1	MelanA	CD68	CD163	Lysozyme	CD8	TIM3	MX11	HLADR	CD56	CD16	pD1	2.02
4	GBP1	MelanA	TAP2	S100AB	PDL1	OX40	CD123	S100A	LAG3	pD1	MX11	CD69	CD56	CD16	Ki67	1.88
45	MX11	S100AB	MelanA	TAP2	S100A	IRF4	MYC	CD16	CD56	Langerin	CD1a	TIM3	Bcl6	pSTAT1	podoplanin	2.25
27	S100AB	CD69	S100A	GBP1	MelanA	TAP2	MX11	CD56	IRF4	p16	CD16	pSTAT1	LAG3	Langerin	Bcl6	0.53
25	S100AB	S100A	MelanA	CD16	IRF4	CD56	Langerin	Blimp1	p16	Bcl6	FOXP3	podoplanin	CD1c	Lysozyme	IRF8	3.6
28	MelanA	pD1	CD141	IRF4	CXCL13	LAG3	S100AB	MYC	pSTAT1	OX40	S100A	Blimp1	CD16	PDL1	CD56	1.94
35	S100A	MelanA	pD1	IRF4	S100AB	LAG3	CD69	pSTAT1	CXCL13	CD16	OX40	CD56	Langerin	Bcl6	FOXP3	3.17
31	S100A	pD1	MelanA	S100AB	IRF4	TIM3	CXCL13	CD16	CD56	Langerin	Bcl6	FOXP3	pSTAT1	podoplanin	CD1a	5.02
1	MelanA	IRF4	S100AB	TIM3	p16	podoplanin	MYC	PDL1	CD16	CD56	Bcl6	MX11	cMAF	Langerin	S100A	2.8
6	MelanA	S100AB	S100A	TIM3	PDL1	IRF4	p16	CD16	CD56	Bcl6	Blimp1	OX40	Langerin	podoplanin	CD141	1.11
13	MelanA	MX11	PDL1	OX40	IRF4	Blimp1	LAG3	Ki67	Lysozyme	pD1	CD163	CD123	CD56	CXCL13	Langerin	1.86
12	MelanA	IRF4	Blimp1	CD16	S100AB	Lysozyme	CD56	Langerin	Bcl6	FOXP3	p16	podoplanin	CD1c	IRF8	OX40	2.44
26	CD69	Ki67	pD1	LAG3	CD1a	PDL1	TIM3	OX40	CD20	CXCL13	CD56	FOXP3	CD8	IRF4	CD16	0.04

M 4 3 2 1 0

B

Analyses	Final Clusters															N	Cells																										
	1	2	3	4	5	6	7	8	9	10	11	12	13	14	15																												
BCProlif	0.02	0.12	0.21	-0.27	0	-0.04	-0.4	-0.3	0.01	3.83	-0.18	-0.37	-0.09	-0.21	0.1	-0.37	-0.23	-0.18	-0.13	-0.34	-0.09	0.01	0.78	2.23	0.13	-0.12	-0.2	-0.69	-0.29	-0.21	1.01	-0.12	0.47	0.72	0.77	-0.52	-0.48	-0.62	-0.48	-0.43	3638	2.03	
BCLAG3+	-0.02	0.12	0.44	-0.28	-0.01	-0.04	-0.29	-0.23	0.14	4.1	0.62	0.34	-0.02	0.57	-0.17	-0.02	-0.02	-0.02	-0.23	0.22	0.25	0.64	0.7	2.71	-0.11	-0.27	-0.7	-0.24	-0.32	0.52	-0.08	0.96	0.7	0.64	-0.45	-0.48	-0.63	-0.37	-0.09	31	0.02		
BCIFNg	-0.11	-0.12	0.28	-0.24	-0.1	-0.04	-0.19	-0.12	-0.25	-2.42	-0.01	0.11	-0.05	0.68	0.14	-0.01	-0.01	-0.01	-0.13	0.68	0.56	0.56	-0.1	0.14	0.12	-0.08	-0.17	-0.38	0.01	0.12	0.60	-0.17	-0.44	-0.53	0.68	0.16	0.05	0.05	0.05	0.05	321	0.05	
BCD69+	-0.01	0.13	0.29	-0.27	-0.35	-0.04	-0.38	-0.26	-0.13	3.72	-0.03	-0.07	-0.08	0.88	-0.3	0.12	-0.21	-0.13	-0.33	0.09	0.03	0.35	0.4	0.2	-0.1	-0.17	-0.65	-0.33	-0.4	0.44	-0.15	0.33	1.03	-0.45	-0.55	-0.34	-0.64	0.34	0.21	0.18	0.05	321	0.18
BC	-0.1	-0.01	0.08	-0.27	-0.05	-0.04	-0.39	-0.29	0.19	3.36	-0.28	-0.36	-0.08	-0.16	0.05	-0.38	-0.25	-0.23	-0.13	-0.03	-0.13	0.41	0.05	0	-0.12	-0.1	-0.66	-0.3	-0.17	0.09	-0.1	0.14	0.63	0.62	-0.47	-0.48	-0.59	-0.44	-0.38	5917	3.3		
cDC1TIM3+	0.2	-0.08	1.28	-0.26	2	-0.02	0.25	-0.06	-0.17	0.22	0.8	-0.02	-0.03	0.17	0.26	0.07	-0.11	-0.06	0.7	1.91	-0.1	0.38	-0.14	-0.1	-0.09	0.64	-0.61	0.09	-0.34	-0.05	-0.11	0.04	0.46	-0.12	-0.03	-0.21	0.28	2.14	2.12	216	1.18		
cDC1Prof	0.77	0.05	0.81	-0.04	2.53	-0.02	-0.06	-0.07	-0.11	-0.19	0.05	0.11	-0.04	-0.09	-0.01	0.29	0.18	-0.07	-0.01	0.78	0.3	2.67	2.33	0.33	-0.08	-0.43	-0.56	0.23	0.4	1.83	-0.13	0.75	0.4	-0.11	0.09	-0.33	-0.15	0.85	1.06	551	3.03		
cDC1LAG3+	0.1	-0.06	1.88	-0.26	0.1	0.07	0.26	0.68	0.77	-0.13	0.45	1.39	-0.06	0.17	0.23	0.11	0.92	-0.19	-0.05	7.7	2.78	-0.01	0.2	-0.11	0.04	0.53	-0.66	0.68	-0.33	0.08	-0.14	1.05	1.27	-0.15	-0.27	-0.43	0.42	0.8	54	0.03			
cDC2	-0.04	-0.11	0.36	-0.27	-0.19	-0.04	0.05	0.46	0.76	-0.19	-0.02	0.74	-0.06	0.14	-0.1	0.05	-0.36	-0.1	0.22	1.25	-0.11	0.03	-0.23	-0.21	0.06	0.38	-0.59	-0.4	-0.43	-0.25	-0.15	0.51	0.03	-0.12	-0.23	-0.4	-0.35	0.08	0.48	2513	1.4		
Epith	-0.11	-0.07	0.29	0.72	0.02	-0.04	-0.36	0.11	-0.18	-0.22	-0.35	-0.45	-0.08	-0.41	0.05	-0.37	0.61	0.4	-0.14	-0.18	-0.48	-0.17	-0.24	-0.03	0.36	-0.01	-0.33	-0.16	0.66	1.67	0.27	-0.03	0.4	0.26	-0.1	0.73	-0.52	-0.42	-0.04	-0.43	1445	18.06	
IRFBLIMP1	0.61	0.65	0.02	-0.11	-0.33	-0.03	-0.35	0.68	-0.18	-0.19	-0.27	-0.44	-0.03	-0.37	-0.07	-0.34	0.31	0.75	-0.12	-0.22	-0.44	0.33	-0.22	-0.21	0.07	0.32	-0.3	-0.63	-0.07	0.4	-0.26	-0.01	0.37	-0.13	-0.14	-0.75	-0.44	-0.59	-0.17	-0.46	2089	1.17	
LangProlif	0.09	-0.09	0.82	-1.1	0.46	-0.04	-0.35	3.05	-0.1	-0.21	-0.09	-0.07	-0.34	-0.03	-0.24	1.24	0.4	-0.13																									

Figure 4. Phenotype Identification. Here we show how we identified the phenotypic groups, corresponding to the different inflammatory cell types that we had in the cores, using the DAPI-mask that took into account all the cells in the cores and the set of phenotypic markers that we selected (CD3, CD20, CD4, HLA-DR, Bcl6, CD16, CD68, CD56, CD141, CD1a, CD1c, Blimp1, Langerin, Lysozyme, Podoplanin, FOXP3, S100AB, IRF4, IRF8, CD1a, CXCL13, CD8, CD138, CD123, PD-1, and MelanA). A two-tier approach was implemented for the identification of cell subpopulations. A) Initially, KMeans, PhenoGraph, and ClusterX (heatmaps on the left) were used to identify the main inflammatory subpopulations, resulting in clusters named after manual annotation by the pathologist based on the level of expression of the phenotypic markers (heatmap on the right, example of expression of the markers in the clusters from PhenoGraph analysis). The final phenotypes were defined after evaluating their stability (See supplementary material for cluster solidity evaluation). B) The final clusters represented here were obtained by further sub-clusterization into functional subgroups using the set of functional markers (CD69, Ki-67, TAP2, GBP1, MYC, p16, MX1, OX40, c-Maf, PD-L1, LAG3, TIM3, and Phospho-Stat1) and PhenoGraph as clustering method.

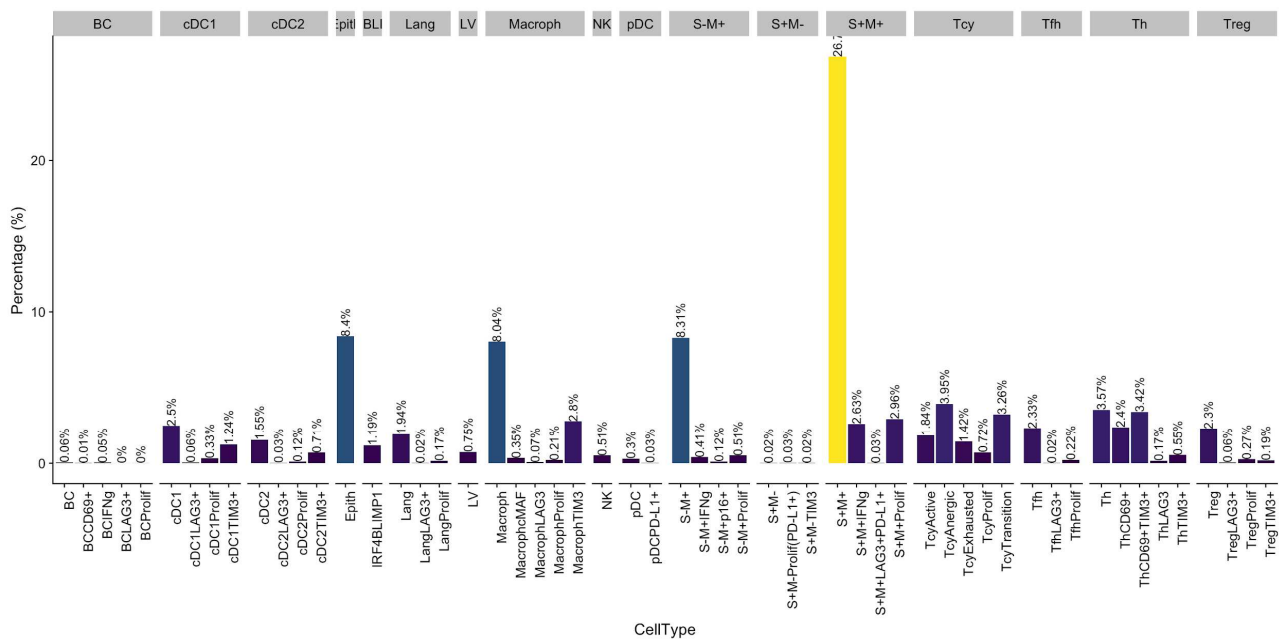


Figure 5. Composition of the cells clusters and respective subclusters. Melanoma cells could be divided into 3 different phenotypic clusters, i.e. double positive for melanocytic markers S100 and MelanA (“S+M+” 77,46%), positive for MelanA only (“S-M+”, 22,44%), and positive for S100 only (“S+M-”, 0,1%). Regarding the immunosuppressive molecules, TIM3 was expressed by 29,27% of S+M-, and PD-L1 was expressed only by a small part of the melanoma cells (0,07%); within this population, the S+M+ melanoma cells co-expressed PD-L1 with LAG3 and the S-M+ melanoma cells co-expressed PD-L1 with IFNg-related proteins. Two small clusters expressed IFNg-related proteins in S+M+ (8,26%) and S-M+ (4,38%). S-M+ melanoma cells also expressed p16 in a small percentage of cells (1,3%). Proliferating subclusters were found in all three melanoma clusters, ranging from 5.39% (in S-M+ cluster) over 8,87% (in S+M+ cluster) to 43,9% (in S+M- cluster). Among macrophages, a dominant immunosuppressive subcluster expressed TIM3 (24,59%) and a smaller subcluster expressed LAG3 and PD-L1 (0,59%). Another subcluster consisted of cMAF-positive macrophages (3,34%) in which we did not observe pSTAT1 expression; instead, pSTAT was expressed by cDC1 and Langerhans cells, in the latter cells in co-expression with cMAF. Proliferating macrophages were found at a frequency of 1,89%. Within Tcy (CD3+CD8+) we could identify active (16,1%), transition (29,6%) and exhausted (12,8%) subclusters, plus two additional categories, i.e. one with high Ki-67 and OX-40 expression, representing the clonally expanding Tcy (6%), and one with low or absent expression of all functional markers (“anergic”, 34,9%). PD-1 was mainly co-expressed with OX-40. Among Th, cells with high expression of CD69 alone or with an additional low expression of TIM3 represented 28,5% of the total Th; balanced expression of the two markers was found in 18,46% of the cells and 13,08 had high TIM3 or, less frequently, LAG3 expression. PD-L1 was expressed in 31,64% of the cells, but stronger expression was found in cases with higher LAG3 and TIM3. The proliferative fraction of Th accounted for 3,39% of the cells. A minor part (6,82%) of the Tregs expressed TIM3 and LAG3 (2,2%), and PD-L1 was detected in this last subgroup. In total, 5,64% Treg were in the proliferative phase. In the Tfh subgroup, only a very small fraction (0,65%) expressed LAG3. 8,52% of the cells were proliferating. A minority of the Th expressed CD69 (3,1%), LAG3 (0,31%), or IFNg-related proteins (0,87%), but their proliferation rate was higher than in the other subgroups (36,4%). Among dendritic cells, in both cDC1 and cDC2 immunosuppressive subgroups could be discerned based on the expression of TIM3 alone (30,47% and 29,86%) or co-expression with LAG3 (1,4% and 1,37%); the latter group also strongly expressed PD-L1. On the other hand, PD-L1 was expressed only weakly on most of the cDC1 (75,56%) and cDC2 (59,07%) subtypes, and in a subcluster of pDC (10,38%). In the Langerhans cell population, a LAG3 positive population (1,08%) was found without co-expression of PD-L1. Proliferation rate for all DC subtypes was similar, ranging between 4,77 and 8%. Finally, we identified lymph vessels (“LV”, podoplanin+, 0,64%) and keratinocytes (“Epith”, CD138+, 7,29%). Visual inspection of the cores showed a lack of CD138+ plasma cells.

Study of the inflammatory microenvironment associated with activation and exhaustion: neighborhood analysis

Neighborhood analysis systematically identifies social networks of cells by giving a picture of the tumor microenvironment and allowing to draw conclusions on actual cell-cell interactions. To understand what is the immune context that determines activation and exhaustion, we compared the results of the neighborhood analysis between the three functional subgroups (Figure 6).

Most of the interactions were shared by the active, transition and exhausted groups. Some of these confirmed expected findings, such as the moderate to strong interaction of Langerhans cells with the epithelium, and some revealed new information on transition from active to exhausted status, such as Tcy in transition interacting with TIM3+cDC1 and TIM3+macrophages, TIM3+CD69+Th interacting with TIM3+cDC1, or Tcy in general without interactions with cDC2. Nevertheless, there were some peculiar differences in the interactions between active, exhausted and transition cases. First of all, the strength of the interactions between Th and Tcy subtypes varied from active to exhausted cases. In active cases, active Th interacted with active Tcy, and active Th were also the main subtype interacting with all the other Tcy subtypes. In transition cases instead, Tcy interacted mostly with the less active Th and CD69+TIM3+Th subgroups. CD69+TIM3+Th also interacted with IFNg BC and with TIM3+cDC2 in exhausted and in transition cases but not in active cases; only in the transition group, CD69+TIM3+Th interacted with proliferating and TIM3+Treg, justifying the lower level of activation of these Th cells. In the exhausted subgroup, we observed interactions between Tcy and TIM3+Th, that were not seen in the other functional groups. Moreover, Treg interacted with transition Tcy and anergic Tcy, and with all the Th subgroups in transition and exhausted cases respectively, but Treg showed no interaction with Tcy in general and very limited interactions with CD69+Th in the active microenvironment. A low-strength interaction between IFNg-BC and anergic Tcy was observed in the exhausted group. BC had very limited other interactions; in active cases, proliferating BC were most often in contact with both anergic and proliferating Tcy, and in transition cases, BC were in contact with anergic Tcy. Macrophages, showed contact with PD-L1+pDC in active cases while avoiding the other pDC, and in transition and exhausted cases they avoided Tfh and cDC1. TIM3+ macrophages also interacted with TIM3+ Treg in exhausted cases. NK cells did not show much interactions, but in active cases they tended to avoid active Tcy and to co-localize with Tfh. Tfh contacted exhausted Tcy in active cases while they tended to avoid anergic/in transition T cells in transition and exhausted cases. In exhausted cases, they interacted instead with cDC1. Finally, the active subgroup was enriched in LAG3+ cells that were very infrequent in the other two subgroups. The peculiar features of these cells were that most of them (cDC1, cDC2, Treg, macrophages, Th but not BC, Tfh, Lang and melanoma cells) were neighbors of each other and, hence, formed cohesive clusters; in addition, they clearly avoided all other cells clusters with the exception of exhausted T cells, with which they showed a strong interaction.

For melanoma cells, neighborhood analysis turned out not to be the best way to investigate their interactions with surrounding cells since melanoma cells showed only avoidance with all the cells of the inflammatory infiltrate. As this is an incoherent result considering that melanoma cells can be seen under the microscope to interact with Tcy in brisk cases we applied an alternative analysis. , and. Actually, even though neighborhood analysis is good to evaluate interactions of inflammatory cells in an infiltrate, the mathematical model is biased by the cohesive type of growth of melanoma cells; indeed, they grow in closely packed nests resulting in very low chances that stronger interactions than those between melanoma cells are picked up. To determine which inflammatory subpopulations appear more often in the neighborhood of melanoma cells, we counted the number of cells of each subpopulation that were in the neighborhood of the melanoma cells and divided their number by the geometric average of the number of melanoma cells and the number of cells of the specific population across all cores in which the specific population appeared. This revealed

that macrophages and epithelial cells were in general the subtypes most often located in close proximity to the melanoma cells, without differences among their functional and morphological categories; this represented a good positive control for the method. Tcy were the third category of cells most often in contact with melanoma cells and brisk cases had more Tcy in close proximity with melanoma cells than non-brisk cases (Figure 7). In particular, brisk cases showed a higher prevalence of transition and active Tcy in contact with melanoma cells compared with non-brisk cases (Active/Exhausted ratio: Brisk = 2.108762, Non-Brisk = 1.331195); the latter instead had relatively more exhausted and anergic cells in contact with melanoma cells (Active/Anergic ratio: Brisk = 1.743081, NonBrisk = 0.7704947) (Figure 7).

Finally, we used the neighborhood analysis to compare the morphological categories brisk and non-brisk (Figure 6). At first sight, there appears to be a strict similarity between the social networks of the active cases and the one of the brisk cases. This is due to the fact that active cases and brisk cases account for almost the total number of LAG3+ cells, which are virtually missing in the non-brisk heatmap. However, at a closer look it is clear that both the brisk and non-brisk categories contain a mixture of the interactions that are hallmarks of exhaustion (i.e. anergic Tcy-IFN γ BC, CD69+TIM3+ Th-IFN γ BC, exhausted Tcy-TIM3+Treg, ...), transition (Treg-TIM3+ macroph, TIM3+ Treg-CD69+TIM3+ Th, ...) and activation (proliferative BC-TIM3+CDC1, Tfh-NK, proliferative BC-anergic Tcy/prolif Tcy, ...), confirming once more that the functional and morphological categories, yielding different types of information, complement each other and result in a multidimensional view on the immune microenvironment in primary melanoma.

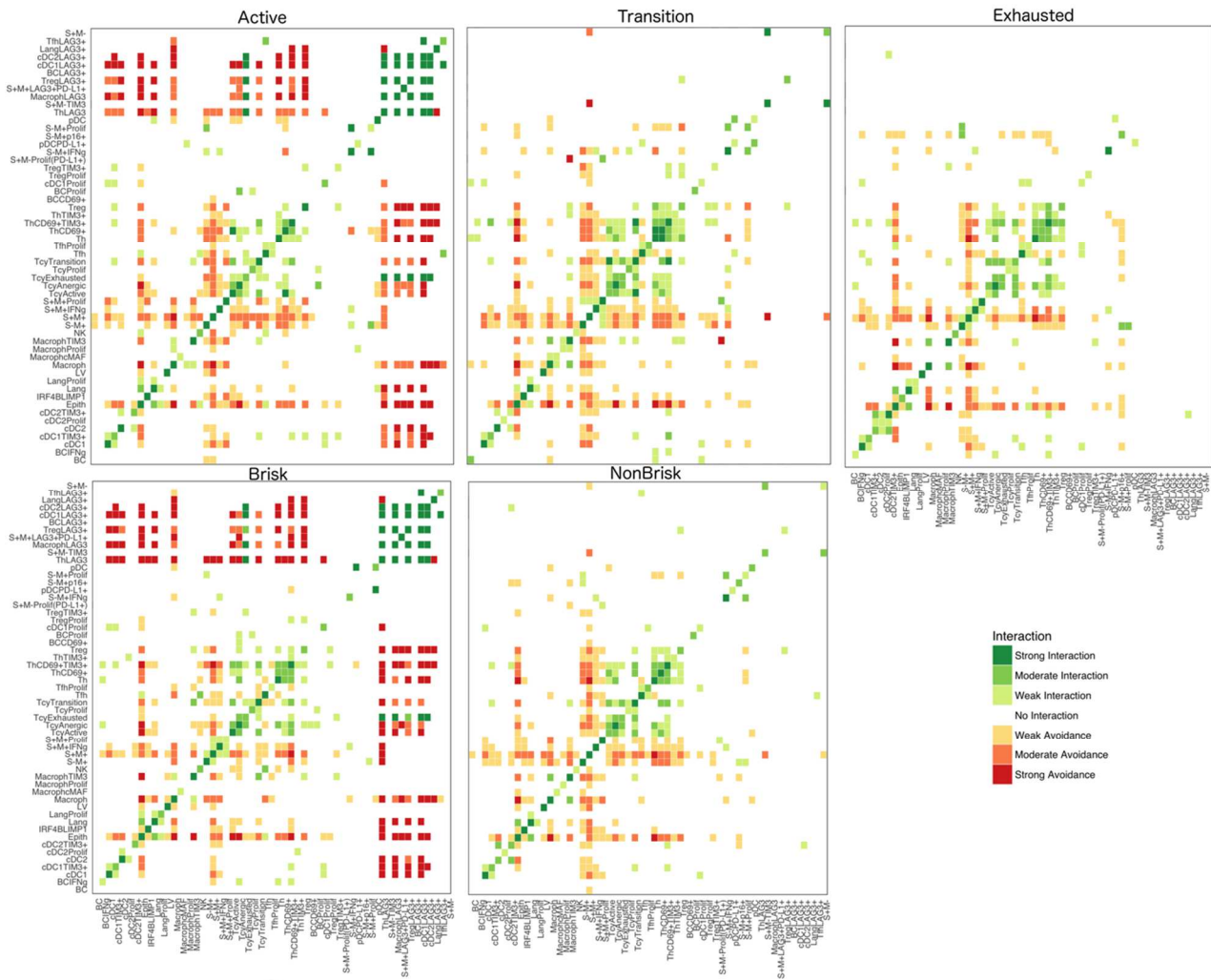


Figure 6. Neighborhood analysis of the active, transition and exhausted microenvironment. The figure shows all the interactions detected with neighbourhood analysis according to the functional (top) and morphological (bottom) categories. The interactions between different cell types are represented in a colorimetric scale (green closeness, red avoidance). In active cases the strongest interaction was observed between CD69+ Th and active Tcy; CD69+ Th were also the main subtype interacting with all the other Tcy subtypes; Treg showed no interaction with Tcy in general and very limited interactions with CD69+Th; proliferating BC were most often in contact with anergic and proliferating Tcy; macrophages showed contact with PD-L1+pDC while avoiding the other pDC; NK cells tended to avoid active Tcy and to co-localize with Tfh; Tfh contacted exhausted Tcy; enriched in LAG3+ cells that were very infrequent in the other two subgroups. In transition cases, Th and CD69+TIM3+Th were the main interactors with the Tcy; CD69+TIM3+Th interacted with proliferating and TIM3+Treg; BC were in contact with anergic Tcy. In both exhausted and in transition cases, CD69+TIM3+Th also interacted with IFN γ BC and with TIM3+cDC2; Treg interacted with all the Th subgroups; macrophages avoided Tfh and cDC1; Tfh tended to avoid anergic/in transition T cells. In the exhausted subgroup, we had interactions between Tcy and TIM3+Th; Treg interacted with transition Tcy and anergic Tcy; there was a low-strength interaction between IFN γ -BC and anergic Tcy; TIM3+ macrophages interacted with TIM3+ Treg; Tfh interacted with cDC1. The morphological subgroups “brisk” and “non-brisk” showed a mixture of interactions that could be found in active, transition and exhausted case respectively.

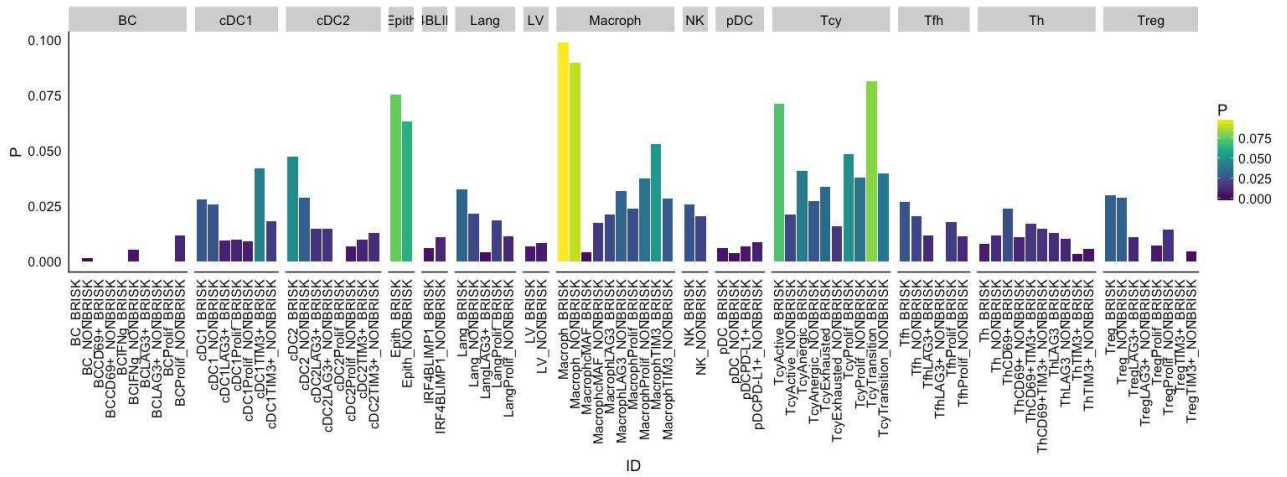


Figure 7. Analysis of the interactions between melanoma cells and the inflammatory subpopulations. Here we show the alternative approach that we used to investigate the neighborhood of melanoma cells. The main inflammatory cells in contact with melanoma cells in our data set are macrophages and epithelial cells in both brisk and non-brisk cases, followed by Tcy with active and in transition Tcy in brisk cases and proliferating and anergic Tcy in non-brisk cases. Another small difference between brisk and non-brisk cases is an increased number of TIM3+ cDC1, cDC2 and TIM3+ macrophages in contact with melanoma cells in brisk cases.

Validation of the functional subclassification of the brisk/non-brisk categories using qPCR and proteomics on microdissected TILs from melanoma metastases

To confirm the existence of the same functional subcategories by qPCR and proteomics, we measured 2 activation and 2 exhaustion markers after microdissection of TILs-rich areas in 8 brisk and 7 non-brisk samples. This analysis was done on metastatic melanoma samples, from which fresh frozen material was available; this allowed us to perform qPCR followed by proteomics and to measure directly the levels of expression of IFN γ , the best indicator of CD8 $^+$ activation, for which no suitable antibody exists that works on FFPE material. Groups of lymphocytes in brisk and non-brisk areas were microdissected; in addition, we studied groups of lymphocytes present in the surrounding stroma in an “Absent” frozen sample as well as lymphocytes associated with melanophages in a case of tumoral melanosis (i.e. complete melanoma regression with persistence of melanin-loaded macrophages). For the measurement of activation, qPCR for IFN γ and CD40L was done, whereas LAG3 and TIM3 were chosen as markers of exhaustion. A case with positive log(IFN γ /CD45) ratio was considered active. Using this approach, 4/8 melanomas with a brisk TILs pattern, and 3/7 with non-brisk TILs pattern proved active, confirming that we could subclassify from a functional point of view also metastatic lesions (Figure 8a). On the other hand, as expected, LAG3 and TIM3 expression was very variable, as these markers are normally expressed upon activation, and as exhaustion was defined by expression of LAG3 and/or TIM3 with lack of IFN γ and CD40L expression.

To correlate the gene expression measured by qPCR with the actual protein expression we performed a proteomic analysis on the microdissected material in 3 representative cases, i.e. one with high IFN γ expression (“IFN γ -high”), one with high LAG3 and no IFN γ expression (“LAG3-high”), and one with none of the four markers strongly expressed (“none”). The results showed a higher number of proteins identified in the “IFN γ -high” sample (324) compared to “LAG3-high” (93) and “none” (134). As we minimized the difference in the number of microdissected cells in each sample, the observed vast difference can only be explained by a higher production of proteins in the TILs of the active case compared to the anergic and the exhausted one. This was furthermore confirmed by the fact that almost two thirds of the proteins (210/324) identified in the “IFN γ -high” sample were specific for that sample and not shared with the other two samples. Analyzing the protein ontology, the 59 proteins shared by the 3 samples were enriched in proteins participating in general metabolic pathways and leukocyte migration; the specific proteins for the (exhausted) “LAG3-high” (17) and (anergic) “none” (29) samples were implicated in general cellular functions. In contrast, those specific for the “IFN γ -high sample” were enriched for proteins involved in different inflammatory pathways (innate immunity, TNFR1 signalling pathway, FAS signalling pathway, T cell receptor and Fc-epsilon receptor signalling pathway), including the interferon gamma-mediated signalling pathway (Figure 8b).

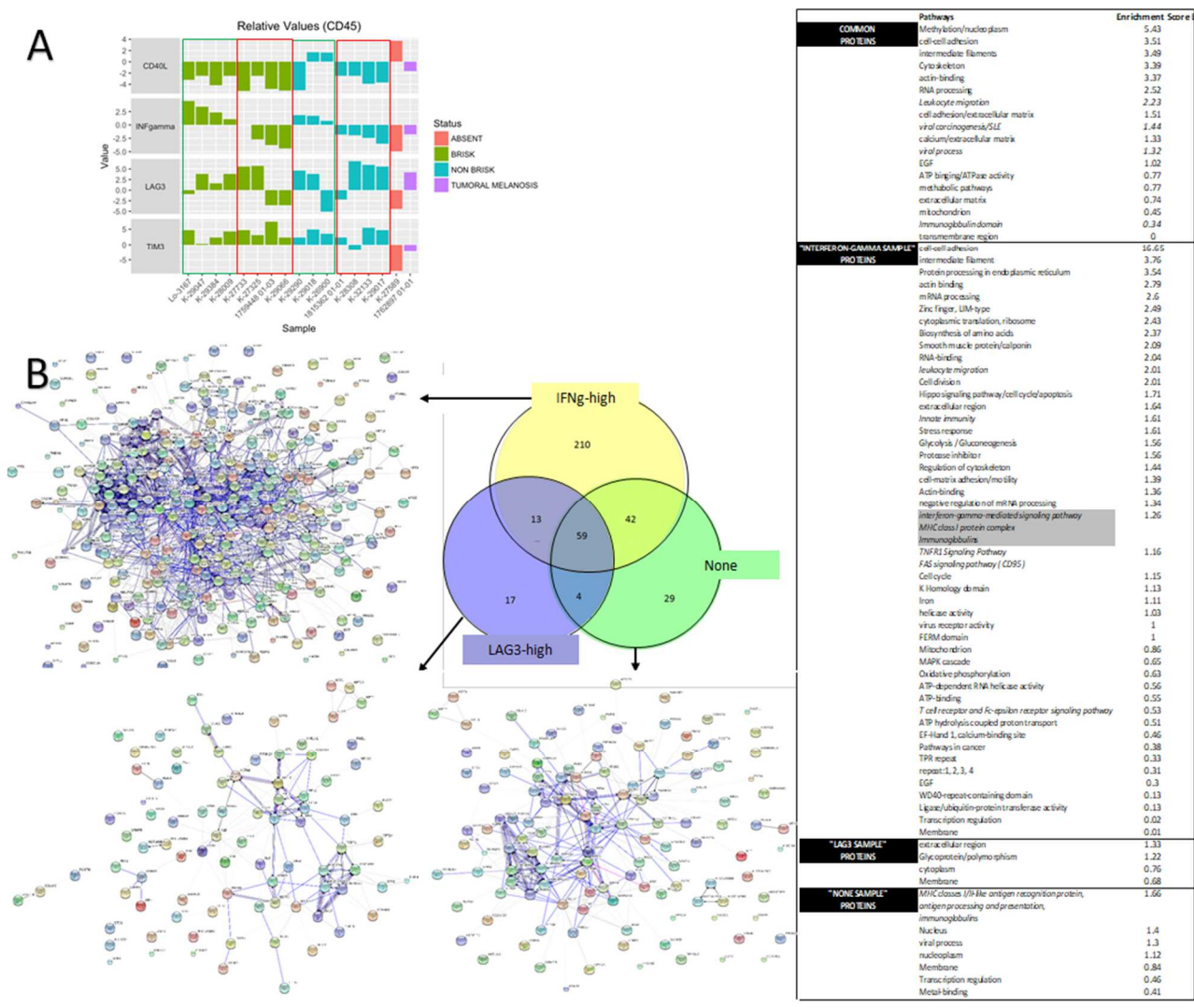


Figure 8. Confirmation of the functional subgroups by qPCR and shotgun proteomics plus pathway analysis. (A) Here we show the expression levels of activation and exhaustion markers in metastatic cases. With qPCR we were able to identify in both brisk and non brisk cases active (green rectangles) and exhausted (red rectangles) statuses. Tumoral melanosis showed an exhausted environment, while non infiltrating lymphocytes in a case in the absent category showed only CD40L expression. (B) The amount of interactions involving the proteins found in the representative cases selected for proteomics are schematically shown as STRING pathways. In table, the main pathways involved in each representative case are listed. We confirmed that the “IFNg-high” case compared to the “LAG3-high” and the “none” case had more proteins involved in inflammatory pathways among which the IFNg-related pathway (in grey).

Discussion

Using a high dimensional multiplex immunostaining technique on TMAs of a series of primary melanomas with various morphological patterns of TILs infiltrates and with various stages of spontaneous regression, we wanted to investigate (1) whether the morphological patterns of TILs have a functional correlate; (2) whether an active T cell infiltrate is associated with melanoma regression; and (3) which inflammatory microenvironment is associated with the morphological and functional TILs categories.

As the activation and exhaustion status of lymphocytes is characterized by the simultaneous expression of several molecules, and as the measurement of the interactions between cells requires preservation of the tissue architecture, we performed this study with the use of a recently developed sensitive multiplex staining technique that is based on sequential staining, scanning and stripping (22). Previous studies on TILs were limited to 6 markers based on the Opal™ System (32) or used a multispectral approach based on the Vectra Intelligent Slide Analysis System but used serial tissue sections. Our study is the first to assess the activation status of TILs directly on tissue sections at the single cell resolution without losing their spatial distribution. Associating the TMA technique with the multiplex staining method, we were able to focus on multiple pre-determined areas for each patient, and to assess both inter-patient heterogeneity as well as intra-patient heterogeneity. Furthermore, the possibility to assess more than 40 markers on the same section allowed us to identify inflammatory subpopulations and to study their spatial relationships, thereby obtaining a screenshot of the dynamic landscape of the local antitumor inflammatory response.

From the analysis of the activation status of the cores we can conclude that both brisk and non-brisk cases can harbor predominantly exhausted TILs or predominantly active TILs; therefore, within the morphological classification (brisk – non-brisk – absent), a complementary functional classification (active – transitional - exhausted) exists. The importance of going beyond the morphologic classification of TILs was previously raised by others, who claimed that a functional analysis could help not only in understanding brisk and non-brisk patterns but also in the application of an immunoscore for therapeutic prediction (33). Adding the functional level to the morphological classification could therefore, first of all, explain the finding by Saltz et al (17) of a group of tumors with brisk pattern but associated with poor outcome. Indeed, one would expect that a brisk infiltrate matches with the concept of activation of the TILs, while a non-brisk infiltrate should represent a more heterogeneous microenvironment, with areas of “brisk” infiltrate representing “active” areas and areas devoid of lymphocytes representing areas of immune ignorance and exhaustion. In our study however, there was a lack of association between activation status of TILs and areas with evidence of direct contact with melanoma cells (“brisk in brisk” and “brisk in non-brisk”), confirming that the contact with melanoma cells in a brisk infiltrate does not necessarily activate the CD8+ lymphocyte.

In melanoma, indeed, a brisk lymphocytic infiltrate is associated most frequently with excellent prognosis (13) (14). Nevertheless, the fact that not all brisk infiltrates have a good prognosis (17) (34), that TILs populations can be very heterogeneous (35) (36) and that anti-PD-1 immunotherapy was found to support functionally activated T cells (16) is urging a thoughtful investigation of the TILs not only concerning their morphological patterns of infiltration but also their functional status.

The functional status of lymphocytes is identified by the expression of distinctive molecules. There are multiple activation markers, such as CD69, CD28, CD40, OX40, GITR, 4-1BB, ICOS, and multiple exhaustion markers, such as PD1, TIGIT, TIM3, LAG3, CTLA4, PD-1, 2B4, CD160, BTLA, VISTA (37) (38) (39). However, none of these markers by itself can effectively determine the activation status of the cell, and therefore have to be evaluated as a panel (38). Moreover, exhaustion markers are expressed upon activation in order to prevent

hyperimmunity and autoimmune reactions (39), exhaustion markers can be transiently expressed by functional T cells, and it is only after a strong and sustained expression that they bring the cell to exhaustion (39). Therefore, real exhaustion can be defined as the expression of exhaustion markers without co-expressed activation markers, while all intermediate states of co-expression of activation and exhaustion markers can be defined as “transitional” statuses.

With regard to the activation status of the TILs, we observed co-expression of activation and inhibition markers. Among activation markers, OX40 is a powerful co-stimulatory molecule expressed only in activated T cells. We found a strong correlation between Ki-67, PD-1 and OX40, confirming the role of OX40 in preventing T cells to die and in sustaining their clonal expansion (40). From the qPCR results, it appeared that CD40L expression was higher in the “absent” samples, in which lymphocytes did not make contact with the melanoma cells, while it had a very low expression during IFN γ production. This suggests that CD40L represents a very early marker of activation, or of priming of the cell before contact with dendritic cells or melanoma cells. Interestingly, the stroma in the case of tumoral melanosis, characterized by a complete disappearance of the melanoma cells due to a successful immune response, showed lymphocytes expressing only LAG3, suggesting a shut-down of the inflammatory process after destruction of the target. With respect to the immunosuppressive molecules, LAG3 was expressed on very small subclusters of different cell types, such as DC, BC, T cells, and macrophages and in all of these subgroups, LAG3 was associated with PD-L1, known to be its co-inhibitory molecule (41). An exception to this co-expression was found on Langerhans cells, that expressed LAG3 but not PD-L1, suggesting a different mechanism of immunosuppression in these cells.

The immunosuppressive role of BC has been addressed by several authors; recently, a role for BC in resistance to BRAF/MEK inhibitors (42) and an anti-tumor effect of B cell depletion was reported (43). Interestingly, we observed PD-L1 expression on all subtypes of BC, except those expressing IFN γ -related proteins; the latter cells probably exert a less immunosuppressive function.

To assess M1/M2 polarization in macrophages, we used pSTAT1 and cMAF as suggested by Barros et al. (44). However, the macrophages in our samples did not express pSTAT1, and only 3,34% of them expressed cMAF, whereas co-expression of these markers did occur in other cell subtypes (mainly DCs). Therefore, we cannot draw grounded conclusions on macrophage polarization based on our data. Finally, we noticed that expression of MelanA in melanoma cells was associated with a more differentiated, less aggressive cell type, showing lower proliferation rates and occasional expression of p16. Moreover, these melanoma cells retained the ability to respond to IFN γ , as highlighted by the expression of IFN γ -related proteins and expressed less frequently immunosuppressive molecules such as PD-L1, LAG3, TIM3.

From the analysis of the spatial heterogeneity of the immune response in the same melanoma sample, we observed that a minority (15%) of patients presented with only active cores and that 30% of patients presented with at least one active core, whereas the great majority of the patients presented with only exhausted or transition areas at the moment in which the melanoma was removed. Since the percentage of patients that obtains a durable response with single agent checkpoint therapy (1) (2) (3) lies between 15 and 30%, and since Krieg et al (16) reported that anti-PD-1 immunotherapy supports functionally activated T cells, it is tempting to speculate that the 15% “mostly active” TILs cases could correspond to the durable responders to immunotherapy, while the “mostly exhausted” cases could benefit instead from combination approaches with immunotherapy and other type of therapies in order to rescue the exhausted T cells. Therefore, adding the functional evaluation could definitely improve the predictive value of the

morphological TILs patterns in melanoma. This aspect is currently under study by analyzing samples from responders and non-responders with a similar multiplex approach.

We also studied the association of activation of TILs with spontaneous melanoma regression, as regression is considered to be the end-results of the melanoma-eliminating capacities of active TILs. Spontaneous partial regression is present in 10-35% of the melanomas and, interestingly, is particularly found in thin melanomas of the superficial-spreading or lentigo maligna type. The most important histopathological criterium to define an area of partial regression is a disappearance of the tumor next to a (junctional or dermal) area with remaining melanoma cells. To distinguish between early and late regression, other criteria are taken into account, the most important of which are a dense inflammatory infiltrate for the early and largely extended fibrosis for the late regression stages (23). Our data showed a clear-cut association of activation of TILs with late regression areas, indirectly proving the functional meaning of an active infiltrate. No association was found with early regression, but this could be due to the fact that early regression is a controversial entity that is more difficult to unequivocally identify by the pathologist. Moreover, a dense infiltrate in early regression mimics the dense infiltrate of a brisk pattern and the definition of “small foci of fibrosis”, present in early fibrosis is very subjective. Other histopathological prognostic parameters did not show any association with activation or exhaustion of TILs.

Finally, we tried to obtain a functional picture of the inflammatory landscape in brisk versus non-brisk cases and in active/transition/exhausted TILs microenvironments. To this end, we not only quantified the different cell subpopulations, but also investigated their spatial relationships by neighborhood analysis. Comparing brisk and non-brisk cases, we observed that brisk infiltrates harbored increased T_{cy} clusters, irrespective of their phenotypic subtypes and irrespective of their activation status. This is in line with observations by Saltz et al. (17), who found CD8⁺ cells to be more abundant in brisk tumors. However, they also observed a group of tumors with brisk infiltrates that showed poor outcome; this can be explained by our finding that both active and exhausted cells were significantly increased. A previous study on T cell clonality already casted some doubts on the significance of the brisk pattern, as they found no evidence of clonally expanded TILs in some cases with a brisk infiltrate (36). They hypothesized that clonally expanded T cells might represent not only cytotoxic cells but also regulatory cells. We indeed found other T cell phenotypes increased in brisk cases, in particular NK cells, CD69⁺TIM3⁺ Th, LAG3⁺ Th, LAG3⁺ Tfh⁺, LAG3⁺ Treg, and proliferating Treg. Moreover, we observed also a higher number of immunosuppressive/immunosuppressed cells in brisk cases, such as macrophages, PD-L1⁺S⁺M⁺ melanoma cells, TIM3⁺ cDC1, and almost all LAG3⁺ cells except BC (i.e. melanoma cells, macrophages, Th cells, Tregs, Tfh). The only BC subtype that was significantly increased in brisk cases corresponded to the BC expressing IFN γ -related proteins; as these cells did not express PD-L1, we assume that this BC subset has no immunosuppressive role. In summary, even although a brisk infiltrate is generally associated with good prognosis, it is enriched not only with immune stimulating cells, but also with cells with an immunosuppressive role.

Active and exhausted cases were functionally rather coherent categories. An active microenvironment was enriched for active T_{cy} and contained increased numbers of (activated) CD69⁺ Th and LAG3⁺Treg. On the other hand, an exhausted microenvironment was enriched for proliferating and TIM3⁺ macrophages, TIM3⁺ Th, and various subsets of Tregs, i.e. a wide range of immunosuppressive cells. The functional coherence of the functional classification was highlighted also by the neighborhood analysis. While brisk and non-brisk cases both showed a mixture of activating, transitional and exhausting interactions, active, transitional and exhausted groups showed instead interesting and peculiar differences, that revealed the main actors in the process that turns activation into exhaustion. In active cases, the interactions between

the most active T-cell subtypes i.e., CD69+ Th and activated Tcy, were stronger than in transition and exhausted cases, where interactions between Th and Tcy were characterized by additional expression of inhibitory marker TIM3 (CD69+TIM3+ Th and TIM3+ Th). Moreover, from the neighborhood analysis we could detect in exhausted and transition cases but not in active cases the specific cell types that contributed to Tcy exhaustion: BC, TIM3+cDC2, and Treg.

Different subgroups of various type of cells were found to express LAG3, i.e. LAG3+ cDC1, cDC2, Treg, macrophages, and Th. LAG3 is a MHC class II ligand, broadly expressed on different cell types, and expressed very early and only transiently during T cell activation; persistent T cell activation with sustained expression of LAG3 together with expression of other exhaustion markers (e.g. PD-L1) results in T cell dysfunction. Moreover, LAG3-expressing Tregs have been shown to suppress DC maturation (45). These LAG3+ cDC1, cDC2, Treg, macrophages and Th, were arranged in small clusters, that were peculiar both to active and brisk cases. In particular, these LAG3+ cells strongly interacted with exhausted T cells in active and brisk cases whereas they avoided interactions with most of the other cells in the microenvironment. These LAG3+ clusters may therefore be an important factor involved in the early onset of the exhaustion program, and these cells may therefore represent one of the most interesting targets to prevent the formation of an exhausted microenvironment.

In conclusion, we untangled some aspects of the immune microenvironment in situ, using clinical tissue samples of primary melanomas and analyzing not only the composition of the immune infiltrate, but also the functional status of TILs and the spatial relationships between the inflammatory cells. We hypothesize that the good prognosis of melanomas with a brisk pattern of TILs could be based on the fact that the melanoma is excised and analyzed at a moment in which it is still in control by the inflammatory cells that are still abundant in the immune microenvironment. Therefore, quantity, in addition to quality, may be an important determinant in the prognosis of this morphological category; this is in accordance with the data of Azimi et al (46) who added a quantitative dimension to the morphological categories. Nonetheless, in this paper we have shown that the activation status of the TILs does not necessarily parallel the morphological categories, and that within a single melanoma, the inflammatory response may vary considerably. This should be taken in consideration when assessing the response to immunotherapy. We are currently investigating this in a data set of immunotherapy-treated patients, to find out whether inflammatory subpopulations that we identified as associated with activation and exhaustion are determinants for response to immunotherapy. This will ultimately lead to the identification of functional inflammatory microenvironments that may benefit from personalized combined therapy protocols.

References

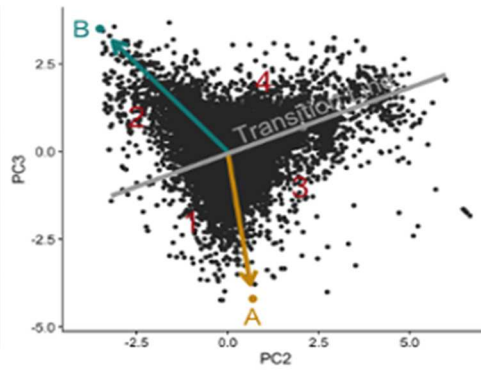
1. Ribas A, Flaherty KT. Gauging the Long-Term Benefits of Ipilimumab in Melanoma. *J Clin Oncol*. 2015 Jun 10;33[17]:1865-6.
2. Ribas A, Hamid O, Daud A, Hodi FS, Wolchok JD, Kefford R, Joshua AM, Patnaik A, Hwu WJ, Weber JS, Gangadhar TC, Hersey P, Dronca R, Joseph RW, Zarour H, Chmielowski B, Lawrence DP, Algazi A, Rizvi NA, Hoffner B, Mateus C7, Gergich K, Lindia JA, Giannotti M, Li XN, Ebbinghaus S, Kang SP, Robert C. Association of Pembrolizumab With Tumor Response and Survival Among Patients With Advanced Melanoma. *JAMA*. 2016 Apr 19;315[15]:1600-9.
3. Robert C, Long GV, Brady B, Dutriaux C, Maio M, Mortier L, Hassel JC, Rutkowski P, McNeil C, Kalinka-Warzocha E, Savage KJ, Hernberg MM, Lebbé C, Charles J, Mihalcioiu C, Chiarion-Sileni V, Mauch C, Cognetti F, Arance A, Schmidt H, Schadendorf D, Gogas H, Lundgren-Eriksson L, Horak C, Sharkey B, Waxman IM, Atkinson V, Ascierto PA. Nivolumab in previously untreated melanoma without BRAF mutation. *N Engl J Med*. 2015 Jan 22;372[4]:320-30.
4. Seremet T, Koch A, Jansen Y, Schreuer M, Wilgenhof S, Del Marmol V, Liènard D, Thielemans K, Schats K, Kockx M, Van Criekinge W, Coulie PG, De Meyer T, van Baren N, Neyns B. Molecular and epigenetic features of melanomas and tumor immune microenvironment linked to durable remission to ipilimumab-based immunotherapy in metastatic patients. *J Transl Med*. 2016 Aug 2;14(1):232.
5. Hugo W, Zaretsky JM, Sun L et al. Genomic and Transcriptomic Features of Response to Anti-PD-1 Therapy in Metastatic Melanoma. *Cell* 2016; 165: 35-44. [2016].
6. Gibney GT, Weiner LM, Atkins MB. Predictive biomarkers for checkpoint inhibitor-based immunotherapy *Lancet Oncol*. 2016 Dec;17(12):e542-e551.
7. Teixido C, Gonzalez-Cao M, Karachaliou N, Rosell R: Predictive factors for immunotherapy in melanoma. *Ann Transl Med* 2015; 3 [15]: 208-218
8. Vasaturo A, Halilovic A, Bol KF, Verweij DI, Blokx WA, Punt CJ, Groenen PJ, van Krieken HJ, Textor J, de Vries IJ, Figdor CG. T cell landscape in a primary melanoma predicts the survival of patients with metastatic disease after their treatment with dendritic cell vaccines. *Cancer Res*. 2016 Apr 11.
9. Loo K, Daud A. Emerging biomarkers as predictors to anti-PD1/PD-L1 therapies in advanced melanoma. *Immunotherapy*. 2016 Jun;8[7]:775-84.
10. Koguchi Y, Hoen HM, Bambina SA, Rynning MD, Fuerstenberg RK, Curti BD, Urba WJ, Milburn C, Bahjat FR, Korman AJ, Bahjat KS. Serum Immunoregulatory Proteins as Predictors of Overall Survival of Metastatic Melanoma Patients Treated with Ipilimumab. *Cancer Res*. 2015 Dec 1;75[23]:5084-92.
11. Teng MW, Ngiew SF, Ribas A, Smyth MJ. Classifying Cancers Based on T-cell Infiltration and PD-L1. *Cancer Res*. 2015 Jun 1;75[11]:2139-45.
12. Lee N, Zakka LR, Mihm MC Jr, Schatton T. Tumour-infiltrating lymphocytes in melanoma prognosis and cancer immunotherapy. *Pathology*. 2016 Feb;48[2]:177-87.
13. Clemente CG, Mihm MC Jr, Bufalino R, Zurrada S, Collini P, Cascinelli N. Prognostic value of tumor infiltrating lymphocytes in the vertical growth phase of primary cutaneous melanoma. *Cancer*. 1996 Apr 1;77[7]:1303-10.
14. Mihm MC Jr, Clemente CG, Cascinelli N. Tumor infiltrating lymphocytes in lymph node melanoma metastases: a histopathologic prognostic indicator and an expression of local immune response. *Lab Invest*. 1996 Jan;74[1]:43-7.
15. Bosisio FM, van den Oord JJ. Immunoplasticity in cutaneous melanoma: beyond pure morphology. *Virchows Arch*. 2017 Apr;470(4):357-369.
16. Krieg C, Nowicka M, Guglietta S, Schindler S, Hartmann FJ, Weber LM, Dummer R, Robinson MD, Levesque MP, Becher B. High-dimensional single-cell analysis predicts response to anti-PD-1 immunotherapy. *Nat Med*. 2018 Feb;24(2):144-153. doi: 10.1038/nm.4466. Epub 2018 Jan 8.
17. Saltz J, Gupta R, Hou L, Kurc T, Singh P, Nguyen V, et al. Spatial Organization and Molecular Correlation of Tumor-Infiltrating Lymphocytes Using Deep Learning on Pathology Images. *Cell Rep*. 2018 Apr 3;23(1):181–7.
18. Ascierto PA, Agarwala SS, Ciliberto G, Demaria S, Dummer R, Duong CPM, Ferrone S, Formenti SC, Garbe C, Halaban R, Khleif S, Luke JJ, Mir LM, Overwijk WW, Postow M, Puzanov I, Sondel P, Taube JM, Thor Straten P, Stronck DF, Wargo JA, Zarour H, Thurin M. Future perspectives in melanoma research "Melanoma Bridge",

- Napoli, November 30th-3rd December 2016. *J Transl Med.* 2017 Nov 16;15(1):236. doi: 10.1186/s12967-017-1341-2.
19. Buggert M, Nguyen S, Salgado-Montes de Oca G, Bengsch B, Darko S, Ransier A, Roberts ER, Del Alcazar D, Brody IB, Vella LA, Beura L, Wijeyesinghe S, Herati RS, Del Rio Estrada PM, Ablanedo-Terrazas Y, Kuri-Cervantes L, Sada Japp A, Manne S, Vartanian S, Huffman A, Sandberg JK, Gostick E, Nadolski G, Silvestri G, Canaday DH, Price DA, Petrovas C, Su LF, Vahedi G, Dori Y, Frank I, Itkin MG, Wherry EJ, Deeks SG, Naji A, Reyes-Terán G, Masopust D, Douek DC, Betts MR. Identification and characterization of HIV-specific resident memory CD8+ T cells in human lymphoid tissue. *Sci Immunol.* 2018 Jun 1;3(24).
 20. Biology of single cells shines a light on collaboration. *Nature.* 2017 Jul 5;547(7661):5.
 21. Binnewies M, Roberts EW, Kersten K, Chan V, Fearon DF, Merad M, Coussens LM, Gabilovich DI, Ostrand-Rosenberg S, Hedrick CC, Vonderheide RH, Pittet MJ, Jain RK, Zou W, Howcroft TK, Woodhouse EC, Weinberg RA, Krummel MF. Understanding the tumor immune microenvironment (TIME) for effective therapy. *Nat Med.* 2018 May;24(5):541-550.
 22. Bolognesi MM, Manzoni M, Scalia CR, Zannella S, Bosisio FM, Faretta M, Cattoretto G. Multiplex Staining by Sequential Immunostaining and Antibody Removal on Routine Tissue Sections. *J Histochem Cytochem.* 2017 Aug;65(8):431-444.
 23. Botella-Estrada R, Traves V, Requena C, Guillen-Barona C, Nagore E. Correlation of histologic regression in primary melanoma with sentinel node status. *JAMA Dermatol.* 2014 Aug;150(8):828-35. doi: 10.1001/jamadermatol.2013.9856.
 24. Caicedo JC, Cooper S, Heigwer F, Warchal S, Qiu P, Molnar C, Vasilevich AS, Barry JD, Bansal HS, Kraus O, Wawer M, Paavolainen L, Herrmann MD, Rohban M, Hung J, Hennig H, Concannon J, Smith I, Clemons PA, Singh S, Rees P, Horvath P, Lington RG, Carpenter AE. Data-analysis strategies for image-based cell profiling. *Nat Methods.* 2017 Aug 31;14(9):849-863. doi: 10.1038/nmeth.4397.
 25. Chen H, Lau MC, Wong MT, Newell EW, Poidinger M, Chen J. Cytofkit: A Bioconductor Package for an Integrated Mass Cytometry Data Analysis Pipeline. Schneidman D, ed. *PLoS Computational Biology.* 2016;12(9):e1005112. doi:10.1371/journal.pcbi.1005112.
 26. Schapiro D, Jackson HW, Raghuraman S, Fischer JR, Zanotelli VRT, Schulz D, Giesen C, Catena R, Varga Z, Bodenmiller B. miCAT: A toolbox for analysis of cell phenotypes and interactions in multiplex image cytometry data. *Nature methods.* 2017;14(9):873-876. doi:10.1038/nmeth.4391.
 27. Chinello C, Cazzaniga M, De Sio G, Smith AJ, Grasso A, Rocco B, Signorini S, Grasso M, Bosari S, Zoppis I, Mauri G, Magni F. Tumor size, stage and grade alterations of urinary peptidome in RCC. *J Transl Med.* 2015 Oct 20;13:332
 28. Liu X, Chinello C, Musante L, Cazzaniga M, Tataruch D, Calzaferri G, James Smith A, De Sio G, Magni F, Zou H, Holthofer H. Intraluminal proteome and peptidome of human urinary extracellular vesicles. *Proteomics Clin Appl.* 2015 Jun;9(5-6):568-73. doi: 10.1002/prca.201400085
 29. *Nature Protocols* 2009; 4(1):44 & *Genome Biology* 2003; 4(5):P3
 30. Szklarczyk D, Franceschini A, Wyder S, Forslund K, Heller D, Huerta-Cepas J, Simonovic M, Roth A, Santos A, Tsafou KP, Kuhn M, Bork P, Jensen LJ, von Mering C. STRING v10: protein-protein interaction networks, integrated over the tree of life. *Nucleic Acids Res.* 2015 Jan;43(Database issue):D447-52.
 31. Alinikula J, Nera KP, Junttila S, Lassila O. Alternate pathways for Bcl6-mediated regulation of B cell to plasma cell differentiation. *Eur J Immunol.* 2011 Aug;41(8):2404-13.
 32. Gartrell RD, Marks DK, Hart TD, Li G, Davari DR, Wu A, Blake Z, Lu Y, Askin KN, Monod A, Esancy CL, Stack EC, Jia DT, Armenta PM, Fu Y, Izaki D, Taback B, Rabadan R, Kaufman HL, Drake CG, Horst BA, Saenger YM. Quantitative Analysis of Immune Infiltrates in Primary Melanoma. *Cancer Immunol Res.* 2018 Apr;6(4):481-493.
 33. Spranger S, Jason J. Luke, Riyue Bao, Yuanyuan Zha, Kyle M. Hernandez, Yan Li, Alexander P. Gajewski, Jorge Andrade, and Thomas F. Gajewski Density of immunogenic antigens does not explain the presence or absence of the T-cell-inflamed tumor microenvironment in melanoma. *Proc Natl Acad Sci U S A.* 2016 Nov 29;113(48):E7759-E7768. Epub 2016 Nov 11.
 34. Thorsson V, Gibbs DL, Brown SD, Wolf D, Bortone DS, Ou Yang TH, Porta-Pardo E, Gao GF, Plaisier CL, Eddy JA, Ziv E, Culhane AC, Paull EO, Sivakumar IKA, Gentles AJ, Malhotra R, Farshidfar F, Colaprico A, Parker JS, Mose

- LE, Vo NS, Liu J, Liu Y, Rader J, Dhankani V, Reynolds SM, Bowlby R, Califano A, Cherniack AD, Anastassiou D, Bedognetti D, Rao A, Chen K, Krasnitz A, Hu H, Malta TM, Noushmehr H, Pedamallu CS, Bullman S, Ojesina AI, Lamb A, Zhou W, Shen H, Choueiri TK, Weinstein JN, Guinney J, Saltz J, Holt RA, Rabkin CE; Cancer Genome Atlas Research Network, Lazar AJ, Serody JS, Demicco EG, Disis ML, Vincent BG, Shmulevich L. *The Immune Landscape of Cancer. Immunity.* 2018 Apr 17;48(4):812-830.e14. doi: 10.1016/j.immuni.2018.03.023. Epub 2018 Apr 5.
35. Simoni Y, Becht E, Fehlings M, Loh CY, Koo SL, Teng KWW, Yeong JPS, Nahar R, Zhang T, Kared H, Duan K, Ang N, Poidinger M, Lee YY, Larbi A, Khng AJ, Tan E, Fu C, Mathew R, Teo M, Lim WT, Toh CK, Ong BH, Koh T, Hillmer AM, Takano A, Lim TKH, Tan EH, Zhai W, Tan DSW, Tan IB, Newell EW. *Bystander CD8+ T cells are abundant and phenotypically distinct in human tumour infiltrates. Nature.* 2018 May 16 [Epub ahead of print]
 36. Bernsen MR, Diepstra JH, van Mil P, Punt CJ, Figdor CG, van Muijen GN, Adema GJ, Ruiter DJ. *Presence and localization of T-cell subsets in relation to melanocyte differentiation antigen expression and tumour regression as assessed by immunohistochemistry and molecular analysis of microdissected T cells. J Pathol.* 2004 Jan;202(1):70-9.
 37. Tirosh I, Izar B, Prakadan SM, Wadsworth MH 2nd, Treacy D, Trombetta JJ, Rotem A, Rodman C, Lian C, Murphy G, Fallahi-Sichani M, Dutton-Regester K, Lin JR, Cohen O, Shah P, Lu D, Genshaft AS, Hughes TK, Ziegler CG, Kazer SW, Gaillard A, Kolb KE, Villani AC, Johannessen CM, Andreev AY, Van Allen EM, Bertagnoli M, Sorger PK, Sullivan RJ, Flaherty KT, Frederick DT, Jané-Valbuena J, Yoon CH, Rozenblatt-Rosen O, Shalek AK, Regev A, Garraway LA. *Dissecting the multicellular ecosystem of metastatic melanoma by single-cell RNA-seq. Science.* 2016 Apr 8;352(6282):189-96.
 38. Wherry EJ. *T cell exhaustion. Nat Immunol.* 2011 Jun;12(6):492-9
 39. Pao W, Ooi CH, Birzele F, Ruefli-Brasse A, Cannarile MA, Reis B, Scharf SH, Schubert DA, Hatje K, Pelletier N, Spleiss O, Reed JC. *Tissue-Specific Immunoregulation: A Call for Better Understanding of the "Immunostat" in the Context of Cancer. Cancer Discov.* 2018 Apr;8(4):395-402.
 40. Weixler B, Cremonesi E, Sorge R, Muraro MG, Delko T, Nebiker CA, Däster S, Governa V, Amicarella F, Soysal SD, Kettelhack C, von Holzen UW, Eppenberger-Castori S, Spagnoli GC, Oertli D, Iezzi G, Terracciano L, Tornillo L, Sconocchia G, Droeser RA. *OX40 expression enhances the prognostic significance of CD8 positive lymphocyte infiltration in colorectal cancer. Oncotarget.* 2015 Nov 10;6(35):37588-99
 41. Ruea-Yea Huang, Cheryl Eppolito, Shashikant Lele, Protul Shrikant, Junko Matsuzaki, Kunle Odunsi. *LAG3 and PD1 co-inhibitory molecules collaborate to limit CD8+ T cell signaling and dampen antitumor immunity in a murine ovarian cancer model. Oncotarget.* 2015 Sep 29; 6(29): 27359–27377.
 42. Somasundaram R, Zhang G, Fukunaga-Kalabis M, Perego M, Krepler C, Xu X, Wagner C, Hristova D, Zhang J, Tian T, Wei Z, Liu Q, Garg K, Griss J, Hards R, Maurer M, Hafner C, Mayerhöfer M, Karanikas G, Jalili A, Bauer-Pohl V, Wehsengruber F, Rappersberger K, Koller J, Lang R, Hudgens C, Chen G, Tetzlaff M, Wu L, Frederick DT, Scolyer RA, Long GV, Damle M, Ellingsworth C, Grinman L, Choi H, Gavin BJ, Dunagin M, Raj A, Scholler N, Gross L, Beqiri M, Bennett K, Watson I, Schaidler H, Davies MA, Wargo J, Czerniecki BJ, Schuchter L, Herlyn D, Flaherty K, Herlyn M, Wagner SN. *Tumor-associated B-cells induce tumor heterogeneity and therapy resistance. Nat Commun.* 2017 Sep 19;8(1):607.
 43. Shalapour S, Font-Burgada J, Di Caro G, Zhong Z, Sanchez-Lopez E, Dhar D, Willimsky G, Ammirante M, Strasner A, Hansel DE, Jamieson C, Kane CJ, Klatte T, Birner P, Kenner L, Karin M. *Immunosuppressive plasma cells impede T-cell-dependent immunogenic chemotherapy. Nature.* 2015 May 7;521(7550):94-8.
 44. Barros MH, Hauck F, Dreyer JH, Kempkes B, Niedobitek G. *Macrophage polarisation: an immunohistochemical approach for identifying M1 and M2 macrophages. PLoS One.* 2013 Nov 15;8(11):e80908.
 45. Andrews LP, Marciscano AE, Drake CG, Vignali DA. *LAG3 (CD223) as a cancer immunotherapy target. Immunol Rev.* 2017 Mar;276(1):80-96.
 46. Azimi F, Scolyer RA, Rumcheva P, Moncrieff M, Murali R, McCarthy SW, Saw RP, Thompson JF. *Tumor-infiltrating lymphocyte grade is an independent predictor of sentinel lymph node status and survival in patients with cutaneous melanoma. J Clin Oncol.* 2012 Jul 20;30(21):2678-83

Supplementary materials

Marker	PC1	PC2	PC3	PC4
CD69	-0.6555	0.0444	-0.7505	-0.0699
OX40	-0.3153	0.7048	0.3656	-0.5197
LAG3	-0.1952	0.4764	0.1196	0.8488
TIM3	-0.6577	-0.5236	0.5372	0.0669



Supplementary Figure 1 The rotation matrix from the PCA shows that PC1 is capturing general expression of the initial markers (all the markers with the same sign). On the other hand, in PC2, TIM3 (exhaustion) has a different sign than the rest of the markers, and the same is true for PC3 and CD69 (activation). Therefore, PC2 and PC3 were used for the definition of the activation function.

The followed pipeline is detailed below:

- PC2 and PC3 are mapped into polar coordinates.

$$\rho = \sqrt{(PC_2)^2 + (PC_3)^2}$$

$$\varphi = \text{atan2}(PC_3, PC_2)$$

where PC2 and PC3 are calculated from the rotation matrix

$$PC_2 = 0.0444 \cdot CD69 + 0.7048 \cdot OX40 + 0.4764 \cdot LAG3 - 0.5236 \cdot TIM3$$

$$PC_3 = -0.7505 \cdot CD69 + 0.3656 \cdot OX40 + 0.1196 \cdot LAG3 + 0.5372 \cdot TIM3$$

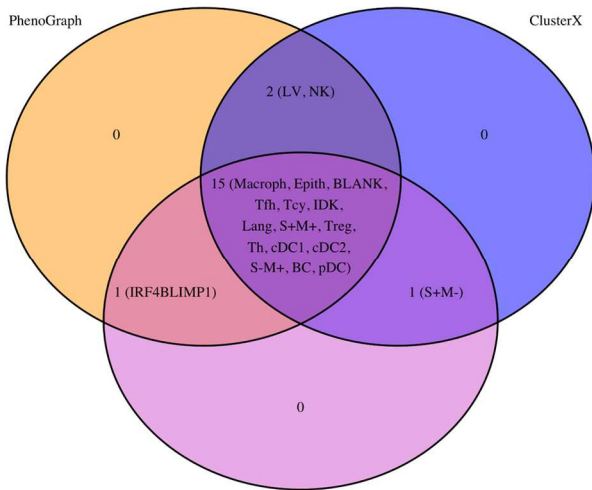
- The point of maximum activation (Activation = 1) was defined as the point where the projected value of CD69 in PCs 2 and 3 reaches a maximum (supplementary figure 1, point A). The angle corresponding to the multi-valued inverse tangent of the rotation vectors of PC3 and PC2 ($\text{atan2}(PC_3, PC_2)$) (φ_0) is added to φ .

$$\varphi' = \varphi + \varphi_0$$

- The point of maximum exhaustion (Activation = -1) was defined as the point where the projected value of TIM3 in PCs 2 and 3 reaches a maximum (supplementary figure 1, point B).
- The line of transition (Activation = 0) was defined as the bisector between the projected vectors of LAG3 and OX40 over PCs 2 and 3 (supplementary figure 1, Transition Line).
- The 4 resulting areas (supplementary figure 1, 1 to 4) do not cover the same range of φ . Each area was scaled so that it covers 90 degrees ($\pi/2$ rads).
- Finally, the value of activation of each cell was calculated as:

$$\text{Activation} = \rho \cdot \cos(\varphi')$$

where ρ is the radius and φ' the scaled angle.



KMeans

Cluster Intersection: PhenoGraph vs KMeans

PhenoGraph	ClusterX	Jaccard
BC	8457	14
BLANK	39164	304
cDC1	9717	45
cDC2	4095	26
Epith	8988	2
IRF4BLIMP1	2736	1
Lang	2295	4
Macroph	22383	243
pDC	5725	90
S-M+	23075	15
S-M-	11035	36
S-M+	43666	8
Tcy	11548	103
Tfh	23424	111
Th	15061	870
Treg	3280	3172
Total	5138	16707

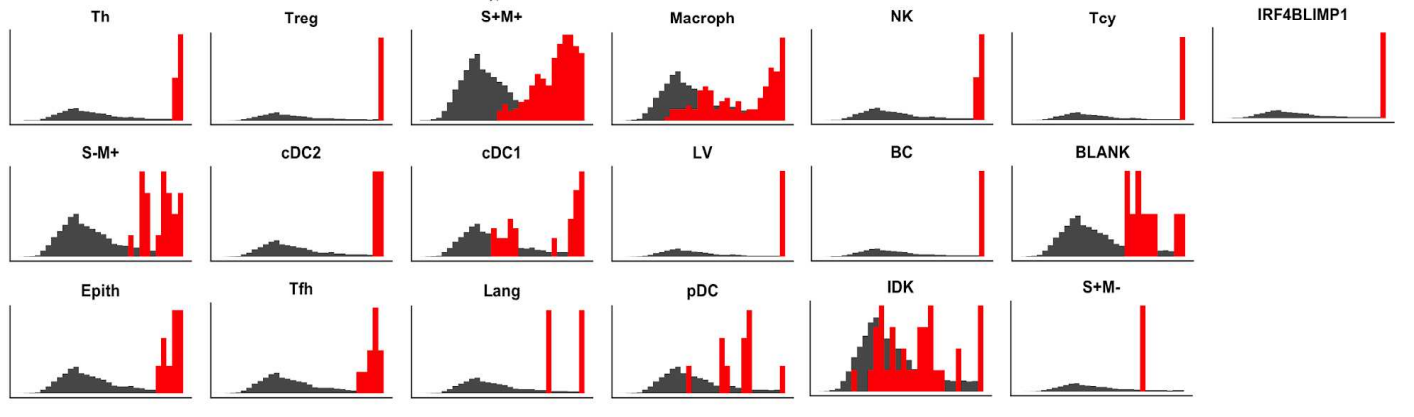
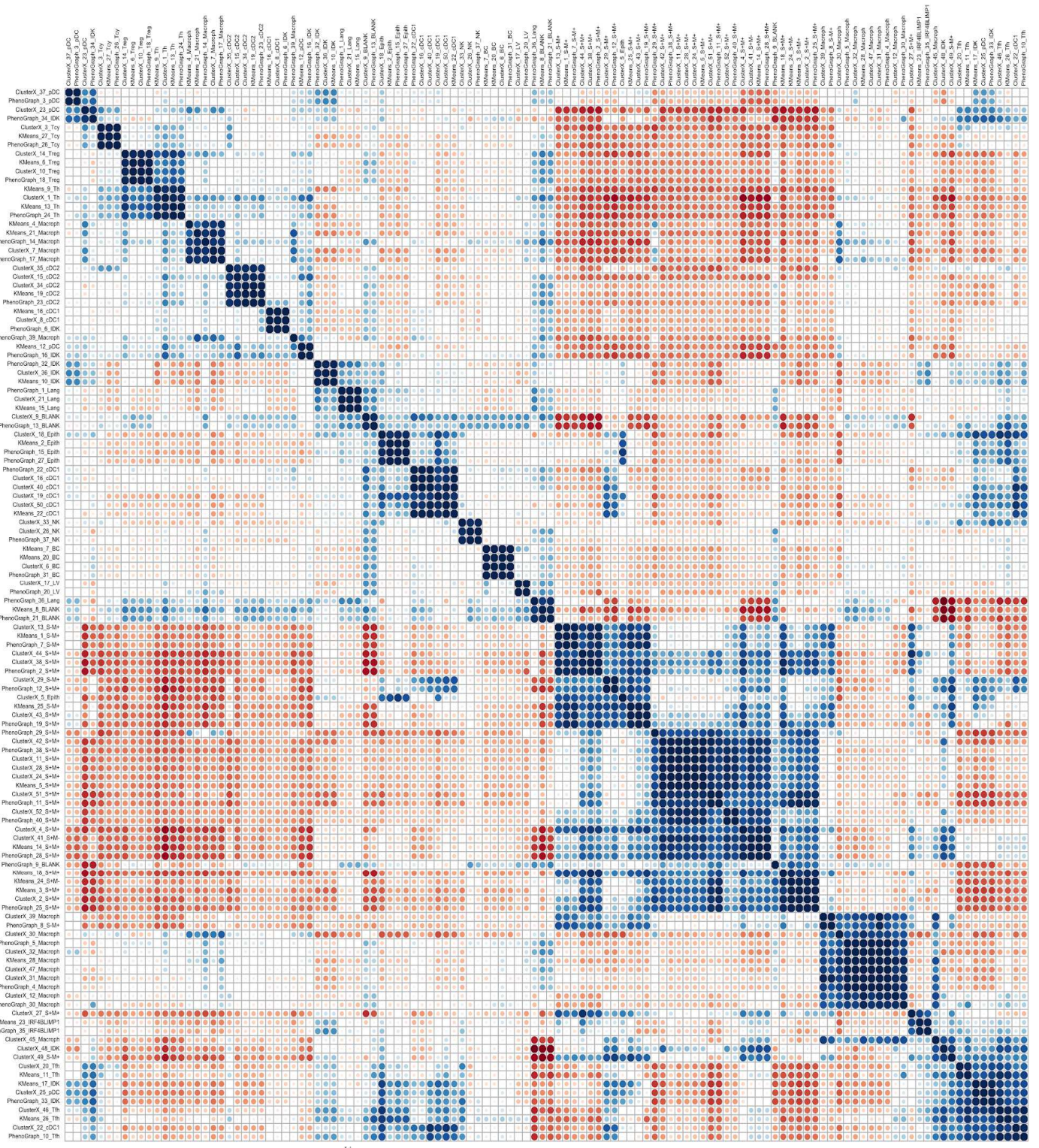
Cluster Intersection: PhenoGraph vs ClusterX

ClusterX	PhenoGraph	Jaccard
BC	10967	15
BLANK	11237	5
cDC1	8326	24
cDC2	3102	6
Epith	37583	4
IRF4BLIMP1	1629	0
Lang	4351	2
LIV	1290	0
Macroph	24425	38
SK	893	0
pDC	3021	17
S-M+	6190	0
S-M-	15602	0
S-M+	40229	22
Tcy	27123	165
Tfh	942	1
Th	40661	333
Treg	4653	58
Total	5138	16707

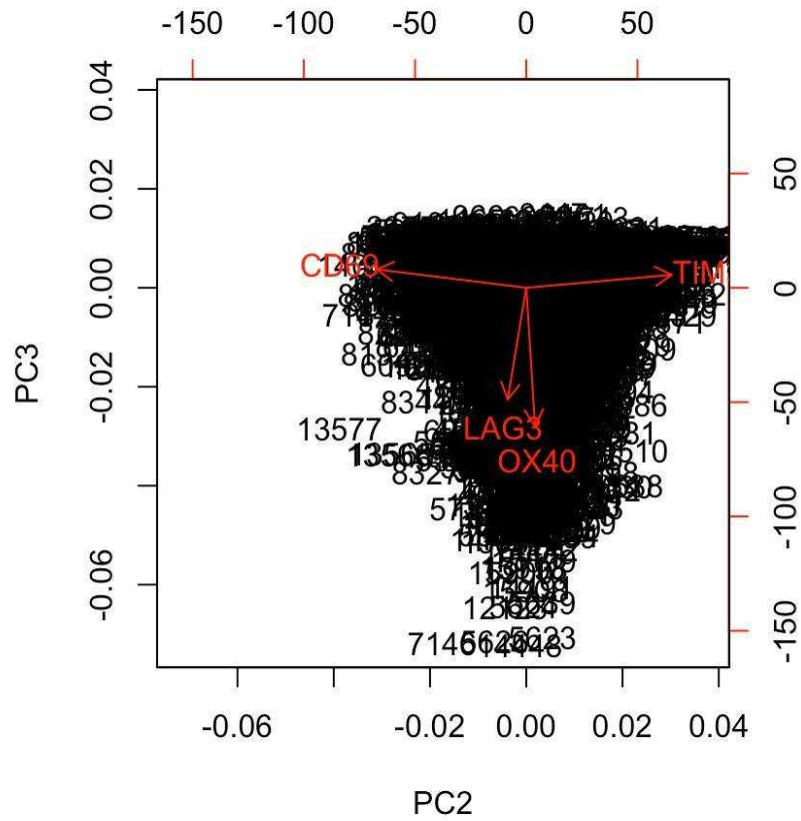
Cluster Intersection: ClusterX vs KMeans

ClusterX	KMeans	Jaccard
BC	8457	0
BLANK	39164	309
cDC1	9717	7
cDC2	4095	19
Epith	8988	0
IRF4BLIMP1	2736	1
Lang	2295	0
Macroph	22383	221
pDC	5725	91
S-M+	23075	4
S-M-	11035	23
S-M+	43666	7
Tcy	11548	10
Tfh	23424	79
Th	15061	750
Treg	3280	823
Total	4653	40661

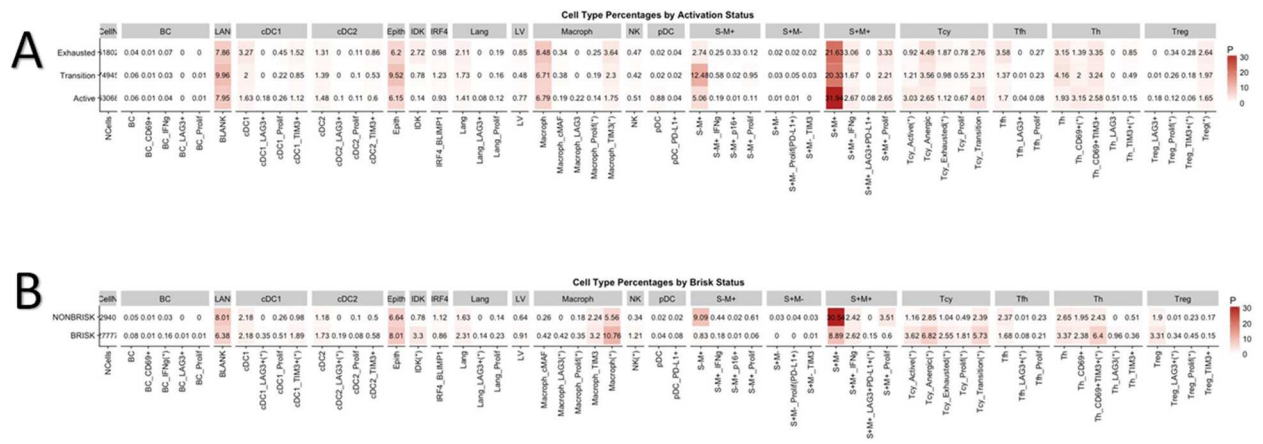
Supplementary Figure 2 Cluster stability. Venn Diagram showing the phenotypes identified by each clustering method, and contingency tables with the number of cells belonging to each cell phenotype for each clustering method pair (PhenoGraph vs Cluster X, PhenoGraph vs KMeans, and ClusterX vs KMeans, respectively). The tiles are colored by the jaccard similarity coefficient. PhenoGraph/ClusterX/KMeans identified 40/52/28 clusters that were mapped to 18/18/17 cell populations. There was no cell population identified by only one clustering method. Figure 1.B-D shows the contingency tables of cell populations for each pair of clustering methods (PhenoGraph vs ClusterX, PhenoGraph vs KMeans, and ClusterX vs KMeans, respectively). PhenoGraph and ClusterX showed a x% of agreement in phenotypic identification, while PhenoGraph and KMeans a y% and ClusterX and KMeans a z%. These results evidence the robustness of the clusters.



Supplementary Figure3 P-values Cluster stability. On top, correlation matrix between all the clusters for all the clustering methods for all the cells in the dataset (all cores), The Pearson correlation between the expression vector for each pair of clusters was calculated. The different clustering methods classified equally most of the cells. Below, histogram showing the distribution of all the correlation coefficients from the correlation matrix (grey) and taking only the correlation coefficients from those clusters that map to the same phenotype (red). These distributions were further evaluated for significance using one-tailed t tests. If we check the correlation coefficients between the clusters that were identified as the same cell type (red) and compare them with the distribution of all the clusters (grey), the red distributions are significantly different and higher than the grey one. Only S+M- shows a no-significant p-value and is because there are very few clusters that map to S+M-, and the t.test depends on the sample size.



Supplementary Figure 4 Biplot showing the projection of the Tcy cells over PCs 2 and 3. In order to compare the second dataset with the initial one (CD8+ mask), the same approach was repeated over T cytotoxic cells to evaluate if the initial set of cells could be recovered and if these showed the same structural behavior.



Supplementary Figure 5. Mean percentages of cell populations across the cores belonging to active, transition and exhausted cases (A), and brisk and non brisk cases (B). One-way Analysis of the Variance (ANOVA) tests were performed in order to find significant differences in the percentage of any of the cell subpopulations within the cores belonging to the different compared groups.

DISCUSSION AND FUTURE PERSPECTIVES

Three years ago, the idea to study some of the less known components of the immune response was driven by the explosion of interest toward immunotherapies, following the amazing survival advantage that they brought in melanoma (1) (2) (3). Most of the mechanisms influencing the success of checkpoint inhibitor were still to be discovered, but what was clear to every investigator was that the tumor microenvironment represented a complex system, dynamic in space and time, changing not only according to the body site (the so-called organ-related “immunostat”) (4), but also during melanoma progression due to immunoediting and immunomodulation processes (the so-called “immunome”) (5), and that every single component of this system has a potential role in influencing the response to these drugs.

An attempt to describe different types of microenvironments using a global approach was recently done on TCGA data, and 6 types of immune microenvironments, found across different types of cancer, were identified: C1 (“wound healing”, Th2-type of infiltrate, elevated expression of angiogenic genes, high proliferation rate), C2 (“IFN- γ dominant”, highest M1/M2 macrophage polarization, numerous CD8 with high TCR diversity), C3 (“inflammatory”, elevated Th17 and Th1 genes, low to moderate tumor cell proliferation, lower levels of aneuploidy and somatic copy variations), C4 (“lymphocyte depleted”, prominent macrophage signature, Th1 low and high M2 macrophage polarization), C5 (“immunologically quiet”, lowest lymphocyte, highest M2-unbalanced macrophage infiltrate), and C6 (“transforming growth factor- β (TGF- β) dominant”, TGF- β signature and abundant lymphocytic infiltrate)(6). Another recent review identified three classes of tumor microenvironments, based on human and mouse data: infiltrated–excluded, if containing an abundant immune infiltrate but poor in cytotoxic lymphocytes; infiltrated–inflamed, if containing abundant PD-1+ cytotoxic lymphocytes, and PD-L1+ leukocytes and melanoma cells; and infiltrated–inflamed with tertiary lymphoid structures, if containing in addition these ectopic lymphoid organs at the invasive tumor margin and in the stroma (7). The data from these papers are derived from bulk analysis and provide a rather low resolution picture of the tumor microenvironment. (5) To obtain a high resolution landscape of the tumor microenvironment one has to identify not only general categories of cancers with a similar inflammatory milieu, but to distinguish all the subclasses within these general categories, up to the possibility to characterize the tumor microenvironment of each single patient in order to achieve the goal of a personalized therapy. Moreover, high resolution means also to be able to characterize not only the heterogeneity of the immune infiltrate but also to define the spatial distribution and the function of each component within it (7). This doctoral project aimed to study the local immune response in melanoma by clarifying the possible role of individual inflammatory components in the tumor stroma of melanoma, and we started with two poorly studied cell types, i.e. plasma cells and melanophages.

The significance of **plasma cells** in melanoma had never been properly addressed in recent literature, and in general the role of B cells was controversial at the time we started the study, as stated in **Chapter I** of this thesis. Even though the two 30-yr-old papers addressing plasma cells in melanoma (8)(9) already pointed out a negative prognostic value for these cells, no clues that could explain this impact on survival were provided. Two new pieces of information came from our investigation: that the quantity of plasma cells influences the prognosis, and that the type of immunoglobulin produced could explain the impaired outcome with an immunosuppression-related mechanism. More evidence of the immunosuppressive role of B cells were reported in the years following the publication of our paper, some of them pointing out also their role in influencing the response to therapy. In particular, B cells were found to contribute to resistance to BRAF inhibitors (10) and to serve as biomarker for adverse reactions during immunotherapy (11), highlighting therefore their value not only as a prognostic marker but also as a marker for decision making in therapy.

Regarding the IgA that we found in the clusters of plasma cells in melanomas with poor outcome, it was shown that IgA⁺ plasma blasts in prostate cancer have an immunosuppressive role (12). Moreover, in the above-mentioned paper that identifies 6 types of immune microenvironment, C6 is characterized by an abundant lymphocytic infiltrate associated with a TGF- β -enriched microenvironment. Interestingly, TGF- β is known to favour IgA switching (13) and C6 is the type of microenvironment associated with the worst outcome (6). Hence, the clusters of IgA⁺ plasma cells, observed in thick melanomas, likely contribute to local immune suppression in melanoma, and thereby to their unfavourable prognosis. The sentinel lymph node, which is the first lymph node that drains the lymph derived from the area of the primary melanoma, has extensively been studied in melanoma, and has been found to represent an area undergoing immune suppression, either at the level of dendritic cells (14) (15), cytokine release (16) or activation status of lymphocytes (17). We have recently observed sentinel nodes from melanoma patients in which clusters of IgA⁺ plasma cells were found near the subcapsular sinus (Fig 1). In view of the immunosuppressive properties of IgA, we will conduct a retrospective study of the incidence and significance of IgA⁺ plasma cells in uninvolved and involved sentinel lymph nodes.

With **Chapter III** of the thesis we moved from a population-centered approach to a microenvironment-based approach. Recently, Johnson et al. identified MHC II positive melanomas as an immunotherapy-responsive phenotype (18). While the two mechanisms of MHC II expression, i.e. constitutive and IFN γ -induced, have been extensively elucidated (19), the data on the immunological context underlying MHC II positive melanoma areas is still controversial, being associated not only with the presence of TILs and better survival but also with TNF-producing CD4⁺ T cells that dampens cytotoxic T activation (20). In this chapter, we aimed to obtain a global view of the inflammatory milieu associated with HLA-DR expression using two “bulk” analysis approaches, next generation sequencing and multiplex ELISA. This approach allowed us to associate these HLA-DR⁺ areas with the humoral immune response, in particular the stage of maturation of the B cell after antigen presentation, a passage that takes normally place in the germinal center. The functional similarity of the HLA-DR-expressing areas with a germinal center has not been documented before, and this novel information therefore brings us one step closer to elucidating the biology behind response to checkpoint therapy. The expression of germinal center cytokines, in fact, could prevent primed dendritic cells and tumor infiltrating lymphocytes from re-circulating to the lymph node and from stimulating the arrival of waves of activated inflammatory cell at the tumor site. Moreover, tumor infiltrating lymphocytes that are prolongedly kept in HLA-DR positive areas would eventually become exhausted, but this may represent an advantage in case of start of PD-1 therapy, since those cells would be immediately available to be reactivated in loco against the tumor.

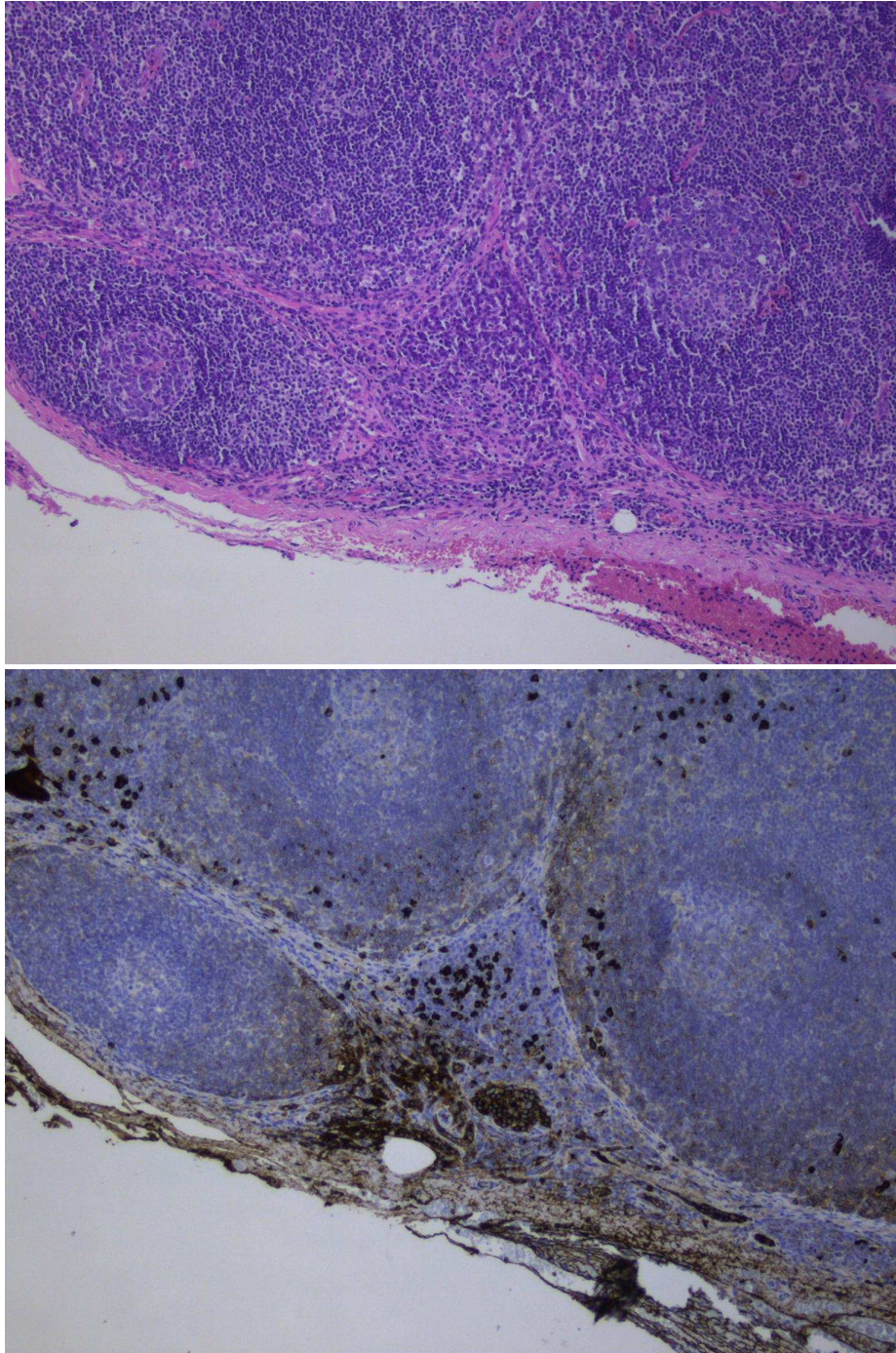


Figure 1. Clusters of plasma cells in the subcapsular sinus of a sentinel lymph node (upper image). Immunohistochemistry for IgA revealing these plasma cells as IgA-producing (lower image).

During the first years in which this doctorate was taking place, the development and widespread use of single cell technologies was so relevant that in July 2017 Nature published an issue focusing on the topic. While it was clear that bulk analysis produced data that were only the result of an average of the single cell data in the tissue, single cell analysis allows the characterization of the vast multitude of cells that forms that specific tissue (21). Most of the developed techniques focus on genomic analysis, the so-called single-cell sequencing. Single cell sequencing brought a revolution in the immunology field, allowing to identify numerous new subtypes of inflammatory cells (22). On the other hand, there are some delicate points to take into account regarding this technique. First, due to the small amount of RNA the data are produced with a higher background noise and have a much more enunciated batch effect. Second, the amount of data produced is so massive that the development of these techniques had to be followed by the parallel development of bioinformatic methods to analyze these data (23). Finally, for the study of immune cells, it was highly recommended that modifications of the state of the cells in the original tissue should be minimized, in order to mimic the reality and not to favour a specific cell type and losing information about other cell types (24). As said previously, high resolution will not only characterize the heterogeneity of the immune infiltrate but will also define the spatial distribution and the function of the cells involved. With single cell sequencing the spatial information is lost due to the dissociation of the cells in the tissue. Therefore, all the spatial relationships and the functional information that can be derived from it are lost. To overcome this problem, several tissue multiplex staining techniques, based on immunofluorescence or immunohistochemistry, were developed in the past few years. Different techniques have been developed that allow the detection of multiple markers on a single section in an amount that is adequate to give high throughput data. These include bleaching/quenching of the fluorochrome, cocktails of antibodies raised in different species or of different isotype that are delivered on the section serially or simultaneously without removing them or stripping of the antibodies from the slide. All these methods have pros and cons. Important problems are, for example, the loss of cells between the cycles for bleaching/quenching techniques (25), the steric hindrance between sequentially deposited antibodies that target nearby epitopes and that may mask the detection of the epitopes in later staining cycles when tyramide-based amplification methods are used (25) and the costs and difficulties for metal- or nucleotide-conjugated antibody techniques, that will reveal only regions of interest (and not the whole slide), that are burdened by long scanning times, that have a limited amount of validated pre-conjugated antibodies and, in case of homemade antibody conjugation, require reagents diluted in media without PBS; in addition, validating the panels of antibodies is not so straightforward as it may seem (based on personal experience of the author). For this reason, the multiplex staining used in this doctorate was performed jointly with the university of Milano-Bicocca, where important problems such as the development of an efficient stripping method (26), antigen retrieval method (27) and a technique to preserve the antigenicity of the tissue (28) were addressed and troubleshooted. A multiplex technique for high dimensional single cell analysis on tissue sections was developed, harboring the great advantage to use well characterized antibodies that are already widely used in the histopathology laboratory (29). Once the raw data from the staining of a tissue micro-array (TMA) with some 40 different immunological markers was obtained, a pipeline for Image Analysis was developed in collaboration with the university of Milano-Bicocca, and in collaboration with ProtAtOnce Ltd (Athens, Greece), we also developed an R-based bioinformatic pipeline for data analysis. At the end, we were able to obtain the high resolution picture we were aiming at in **Chapter IV** of the thesis, thereby accomplishing the aim of untangling the microenvironment in the “brisk” and “non brisk” morphologic categories of tumor infiltrating lymphocytes, not only quantitatively but also functionally through neighbour analysis. We obtained a functional classification of the T-cell infiltrates that could be considered more accurate than what was previously done in literature; indeed, instead of measuring the activation or exhaustion of T-cells through application of a single activation/inhibition marker per tissue section, we now analysed the simultaneous expression of the

4 activation/inhibition markers that we selected through principal component analysis, and thus were able to sense the fine tuning of activation/exhaustion in CD8+ cells.

Novel methods to analyse the tumor microenvironment (TME) are urgently needed to stratify melanoma patients for adjuvant immunotherapy. Tumor-infiltrating lymphocyte (TIL) analysis, by conventional pathologic methods, is predictive but is insufficiently precise for clinical application. Moreover, compared to other recent papers on the evaluation of the immune infiltrates in melanoma on tissue sections, our methods shows definitely a higher performance. Compared to Gartrell et al that performed a quantitative 6-plex immunofluorescence analysis based on the Opal™ System (Perkin Elmer, Waltham, Massachusetts, Stati Uniti) (30) our approach allowed to analyse many more markers, thereby giving a more global and in depth understanding of the heterogeneity and spatial relationships between different subtypes of inflammatory cells. Another study used a multispectral approach based on the Vectra Intelligent Slide Analysis System (PerkinElmer, Waltham, Massachusetts, Stati Uniti) (31), but their staining of the markers was carried out on serial tissue sections instead of the same section, therefore losing the single cell resolution. At this very moment, there are no other commercially available methods that can give a similar performance to the one applied in this thesis.

The **conclusion** that can be derived from our studies is that, in the perspective of building a multiplex panel of biomarkers in order to predict the response to immunotherapy, it will be necessary to take into account a deeper immune-profiling of both the T cells and B cells, including the evaluation of the functional status for the T-cells, and the type of immunoglobulin production and germinal center-related markers for the B-cells. Concerning the cells of myeloid lineage, melanophages should be included as potential immunosuppressive cells. Hence, when building a predictive panel of biomarkers, one will have to consider enough markers so to cover all players involved in the local immune response in melanoma. Some predictive markers associated with the response to checkpoint therapy have already been identified, i.e. a signature of 325 genes enriched in genes associated with the humoral and cellular immune response that predicts durable responses (32) and, on the contrary, a genetic signature that predicts resistance to checkpoint inhibition (33). Further predictive characteristics are the load of somatic gene mutations, responsible for sensitivity of cancer cells to T-cell-based immunotherapies (34); a heavy T cell infiltration as well as the T cell landscape (35), (31) (36) (37) (38); an increased number of circulating central memory T cells, NKT cells and activated T cells (39); relative/absolute lymphocyte, monocyte and eosinophil counts in peripheral blood (40); an imbalanced ratio between circulating T-cells and pretreatment disease burden (41); MHC II expression on melanoma cells (18); and PD-L1 positivity, even if it is still highly debated (42) (43) (44) (45) (46). The source of these markers is highly variable: some are taken from blood, some from the genetic landscape of the tumor, and some from proteins expressed by the tumor tissue. The association of data collected from the tumoral tissue can benefit from the association of data collected from the peripheral blood, in view of the known interconnection between the tumor tissue and the systemic immune response through cytokines and growth factor secretion (7). Therefore, to guarantee the best predictive power, different parameters depicting different aspects of the immune response (tumoral burden, mutational burden, amount and function of the inflammatory cell subtypes, T and B cell clonality, etc.) need to be integrated, as anticipated already in the concept of the “cancer immunogram” described in the introduction of this thesis (47). In my personal view, the evaluation of the immune response done directly on tissue section from the patient through an high-dimensional multiplex technique should be integrated with the evaluation of other predictive parameters derived from peripheral blood, as well as with markers obtained with other methods, i.e. genomic and epigenomic evaluations. In the effort to include as many significant parameters together as possible, an “Immunogram 2.0” will be obtained that depicts the complexity of the immune microenvironment and that should reach a

satisfactory predictive power in clinical practice. The aim of this Immunogram 2.0, that currently is merely centered on predicting the response to immunotherapy, should evolve in the future to represent a tool to decide which type of treatment the patient should receive. By applying it not only at the beginning of the therapeutic path of the patient but also during the course of the treatment, it will represent a tool to follow the evolving tumoral landscape and it will allow to closely monitor response of the patient to the therapeutic protocols, thereby fulfilling the need for a completely personalized therapy for the patient.

References

1. Ribas A, Flaherty KT. Gauging the Long-Term Benefits of Ipilimumab in Melanoma. *J Clin Oncol*. 2015 Jun 10;33[17]:1865-6.
2. Ribas A, Hamid O, Daud A, Hodi FS, Wolchok JD, Kefford R, Joshua AM, Patnaik A, Hwu WJ, Weber JS, Gangadhar TC, Hersey P, Dronca R, Joseph RW, Zarour H, Chmielowski B, Lawrence DP, Algazi A, Rizvi NA, Hoffner B, Mateus C7, Gergich K, Lindia JA, Giannotti M, Li XN, Ebbinghaus S, Kang SP, Robert C. Association of Pembrolizumab With Tumor Response and Survival Among Patients With Advanced Melanoma. *JAMA*. 2016 Apr 19;315[15]:1600-9.
3. Robert C, Long GV, Brady B, Dutriaux C, Maio M, Mortier L, Hassel JC, Rutkowski P, McNeil C, Kalinka-Warzocho E, Savage KJ, Hernberg MM, Lebbé C, Charles J, Mihalcioiu C, Chiarion-Sileni V, Mauch C, Cognetti F, Arance A, Schmidt H, Schadendorf D, Gogas H, Lundgren-Eriksson L, Horak C, Sharkey B, Waxman IM, Atkinson V, Ascierto PA. Nivolumab in previously untreated melanoma without BRAF mutation. *N Engl J Med*. 2015 Jan 22;372[4]:320-30.
4. Pao W, Ooi CH, Birzele F, Ruefli-Brasse A, Cannarile MA, Reis B, Scharf SH, Schubert DA, Hatje K, Pelletier N, Spleiss O, Reed JC. Tissue-Specific Immunoregulation: A Call for Better Understanding of the "Immunostat" in the Context of Cancer. *Cancer Discov*. 2018 Apr;8(4):395-402.
5. Bindea G, Mlecnik B, Tosolini M, Kirilovsky A, Waldner M, Obenaus AC, Angell H, Fredriksen T, Lafontaine L, Berger A, Bruneval P, Fridman WH, Becker C, Pagès F, Speicher MR, Trajanoski Z, Galon J. Spatiotemporal dynamics of intratumoral immune cells reveal the immune landscape in human cancer. *Immunity*. 2013 Oct 17;39[4]:782-95.
6. Thorsson V, Gibbs DL, Brown SD, Wolf D, Bortone DS, Ou Yang TH, Porta-Pardo E, Gao GF, Plaisier CL, Eddy JA, Ziv E, Culhane AC, Paull EO, Sivakumar IKA, Gentles AJ, Malhotra R, Farshidfar F, Colaprico A, Parker JS, Mose LE, Vo NS, Liu J, Liu Y, Rader J, Dhankani V, Reynolds SM, Bowlby R, Califano A, Cherniack AD, Anastassiou D, Bedognetti D, Rao A, Chen K, Krasnitz A, Hu H, Malta TM, Noushmehr H, Pedamallu CS, Bullman S, Ojesina AI, Lamb A, Zhou W, Shen H, Choueiri TK, Weinstein JN, Guinney J, Saltz J, Holt RA, Rabkin CE; Cancer Genome Atlas Research Network, Lazar AJ, Serody JS, Demicco EG, Disis ML, Vincent BG, Shmulevich L. The Immune Landscape of Cancer. *Immunity*. 2018 Apr 17;48(4):812-830.e14.
7. Binnewies M, Roberts EW, Kersten K, Chan V, Fearon DF, Merad M, Coussens LM, Gaborilovich DI, Ostrand-Rosenberg S, Hedrick CC, Vonderheide RH, Pittet MJ, Jain RK, Zou W, Howcroft TK, Woodhouse EC, Weinberg RA, Krummel MF. Understanding the tumor immune microenvironment (TIME) for effective therapy. *Nat Med*. 2018 May;24(5):541-550.
8. Weissmann A, Roses DF, Harris MN, Dubin N. Prediction of lymph node metastases from the histologic features of primary cutaneous malignant melanomas. *Am J Dermatopathol*. 1984;6:35-41.
9. Mascaro JM, Molgo M, Castel T, Castro J. Plasma cells within the infiltrate of primary cutaneous malignant melanoma of the skin. A confirmation of its histoprosthetic value. *Am J Dermatopathol*. 1987;9:497-9.
10. Somasundaram R, Zhang G, Fukunaga-Kalabis M, Perego M, Krepler C, Xu X, Wagner C, Hristova D, Zhang J, Tian T, Wei Z, Liu Q, Garg K, Griss J, Hards R, Maurer M, Hafner C, Mayerhöfer M, Karanikas G, Jalili A, Bauer-Pohl V, Wehsegruber F, Rappersberger K, Koller J, Lang R, Hudgens C, Chen G, Tetzlaff M, Wu L, Frederick DT, Scolyer RA, Long GV, Damle M, Ellingsworth C, Grinman L, Choi H, Gavin BJ, Dunagin M, Raj A, Scholler N, Gross L, Beqiri M, Bennett K, Watson I, Schaidler H, Davies MA, Wargo J, Czerniecki BJ, Schuchter L, Herlyn D, Flaherty K, Herlyn M, Wagner SN. Tumor-associated B-cells induce tumor heterogeneity and therapy resistance. *Nat Commun*. 2017 Sep 19;8(1):607.
11. Liudahl SM, Coussens LM. B cells as biomarkers: predicting immune checkpoint therapy adverse events. *J Clin Invest*. 2018 Feb 1;128(2):577-579.
12. Shalpour S, Font-Burgada J, Di Caro G, et al. Immunosuppressive plasma cells impede T-cell-dependent immunogenic chemotherapy. *Nature*. 2015;521:94-8.
13. Vale AM, Schroeder HW Jr. Clinical consequences of defects in B-cell development. *J Allergy Clin Immunol*. 2010;125:778-87.
14. van den Hout MFCM, Koster BD, Sluijter BJR, Molenkamp BG, van de Ven R, van den Eertwegh AJM, Scheper RJ, van Leeuwen PAM, van den Tol MP, de Gruijl TD. Melanoma Sequentially Suppresses Different DC Subsets in

- the Sentinel Lymph Node, Affecting Disease Spread and Recurrence. Cancer Immunol Res.* 2017 Nov;5(11):969-977.
15. Ito M, Minamiya Y, Kawai H, Saito S, Saito H, Nakagawa T, Imai K, Hirokawa M, Ogawa J. Tumor-derived TGFbeta-1 induces dendritic cell apoptosis in the sentinel lymph node. *J Immunol.* 2006 May 1;176(9):5637-43.
 16. Lee N, Zakka LR, Mihm MC Jr, Schatton T. Tumour-infiltrating lymphocytes in melanoma prognosis and cancer immunotherapy. *Pathology.* 2016 Feb;48[2]:177-87.
 17. Barbour AH, Coventry BJ. Dendritic cell density and activation status of tumour-infiltrating lymphocytes in metastatic human melanoma: possible implications for sentinel node metastases. *Melanoma Res.* 2003 Jun;13(3):263-9.
 18. Johnson DB, Estrada MV, Salgado R, Sanchez V, Doxie DB, Opalenik SR, Vilgelm AE, Feld E, Johnson AS, Greenplate AR, Sanders ME, Lovly CM, Frederick DT, Kelley MC, Richmond A, Irish JM, Shyr Y, Sullivan RJ, Puzanov I, Sosman JA, Balko JM. Melanoma-specific MHC-II expression represents a tumour-autonomous phenotype and predicts response to anti-PD-1/PD-L1 therapy. *Nat Commun.* 2016 Jan 29;7:10582.
 19. Degenhardt Y, Huang J, Greshock J, Horiates G, Nathanson K, Yang X, Herlyn M, Weber B. Distinct MHC gene expression patterns during progression of melanoma. *Genes Chromosomes Cancer.* 2010 Feb;49(2):144-54.
 20. Donia M, Kjeldsen JW, Svane IM. The controversial role of TNF in melanoma. *Oncoimmunology.* 2015 Oct 29;5[4]:e1107699
 21. *Biology of single cells shines a light on collaboration. Nature.* 2017 Jul 5;547(7661):5.
 22. Giladi A, Amit I. Immunology, one cell at a time. *Nature.* 2017 Jul 3;547(7661):27-29.
 23. Perkel JM. Single-cell sequencing made simple. *Nature.* 2017 Jul 3;547(7661):125-126.
 24. Sood A, Miller AM, Brogi E, Sui Y, Armenia J, McDonough E, Santamaria-Pang A, Carlin S, Stamper A, Campos C, Pang Z, Li Q, Port E, Graeber TG, Schultz N, Ginty F, Larson SM, Mellinghoff IK. Multiplexed immunofluorescence delineates proteomic cancer cell states associated with metabolism. *JCI Insight.* 2016 May 5;1(6). pii: e87030.
 25. Tóth ZE, Mezey E. Simultaneous visualization of multiple antigens with tyramide signal amplification using antibodies from the same species. *J Histochem Cytochem.* 2007 Jun;55(6):545-54.
 26. Gendusa R, Scalia CR, Buscone S, Cattoretti G. Elution of High-affinity (>10⁹ KD) Antibodies from Tissue Sections: Clues to the Molecular Mechanism and Use in Sequential Immunostaining. *J Histochem Cytochem.* 2014 Jul;62(7):519-31.
 27. Scalia CR, Gendusa R, Cattoretti G. A 2-Step Laemmli and Antigen Retrieval Method Improves Immunodetection. *Appl Immunohistochem Mol Morphol.* 2016 Jul;24(6):436-46.
 28. Boi G, Scalia CR, Gendusa R, Ronchi S, Cattoretti G. Disaccharides Protect Antigens from Drying-Induced Damage in Routinely Processed Tissue Sections. *J Histochem Cytochem.* 2016 Jan;64(1):18-31.
 29. Bolognesi MM, Manzoni M, Scalia CR, Zannella S, Bosisio FM, Faretta M, Cattoretti G. Multiplex Staining by Sequential Immunostaining and Antibody Removal on Routine Tissue Sections. *J Histochem Cytochem.* 2017 Aug;65(8):431-444.
 30. Gartrell RD, Marks DK, Hart TD, Li G, Davari DR, Wu A, Blake Z, Lu Y, Askin KN, Monod A, Esancy CL, Stack EC, Jia DT, Armenta PM, Fu Y, Izaki D, Taback B, Rabadan R, Kaufman HL, Drake CG, Horst BA, Saenger YM. Quantitative Analysis of Immune Infiltrates in Primary Melanoma. *Cancer Immunol Res.* 2018 Apr;6(4):481-493.
 31. Vasaturo A, Di Blasio S, Verweij D, Blokx WA, van Krieken JH, de Vries IJ, Figdor CG. Multispectral imaging for highly accurate analysis of tumour-infiltrating lymphocytes in primary melanoma. *Histopathology.* 2017 Mar;70(4):643-649.
 32. Seremet T, Koch A, Jansen Y, Schreuer M, Wilgenhof S, Del Marmol V, Liènard D, Thielemans K, Schats K, Kockx M, Van Criekinge W, Coulie PG, De Meyer T, van Baren N, Neyns B. Molecular and epigenetic features of melanomas and tumor immune microenvironment linked to durable remission to ipilimumab-based immunotherapy in metastatic patients. *J Transl Med.* 2016 Aug 2;14(1):232.
 33. Hugo W, Zaretsky JM, Sun L et al. Genomic and Transcriptomic Features of Response to Anti-PD-1 Therapy in Metastatic Melanoma. *Cell* 2016; 165: 35-44. [2016].
 34. Patel SJ, Sanjana NE, Kishton RJ, Eidizadeh A, Vodnala SK, Cam M, Gartner JJ, Jia L, Steinberg SM, Yamamoto TN, Merchant AS, Mehta GU, Chichura A, Shalem O, Tran E, Eil R, Sukumar M, Gujjarro EP, Day CP, Robbins P,

- Feldman S, Merlino G, Zhang F, Restifo NP. Identification of essential genes for cancer immunotherapy. *Nature*. 2017 Aug 31;548(7669):537-542.
35. Vasaturo A, Halilovic A, Bol KF, Verweij DJ, Blokx WA, Punt CJ, Groenen PJ, van Krieken HJ, Textor J, de Vries IJ, Figdor CG. T cell landscape in a primary melanoma predicts the survival of patients with metastatic disease after their treatment with dendritic cell vaccines. *Cancer Res*. 2016 Apr 11.
 36. Loo K, Daud A. Emerging biomarkers as predictors to anti-PD1/PD-L1 therapies in advanced melanoma. *Immunotherapy*. 2016 Jun;8[7]:775-84.
 37. Koguchi Y, Hoen HM, Bambina SA, Rynning MD, Fuerstenberg RK, Curti BD, Urba WJ, Milburn C, Bahjat FR, Korman AJ, Bahjat KS. Serum Immunoregulatory Proteins as Predictors of Overall Survival of Metastatic Melanoma Patients Treated with Ipilimumab. *Cancer Res*. 2015 Dec 1;75[23]:5084-92.
 38. Krieg C, Nowicka M, Guglietta S, Schindler S, Hartmann FJ, Weber LM, Dummer R, Robinson MD, Levesque MP, Becher B. High-dimensional single-cell analysis predicts response to anti-PD-1 immunotherapy. *Nat Med*. 2018 Feb;24(2):144-153.
 39. Saltz J, Gupta R, Hou L, Kurc T, Singh P, Nguyen V, et al. Spatial Organization and Molecular Correlation of Tumor-Infiltrating Lymphocytes Using Deep Learning on Pathology Images. *Cell Rep*. 2018 Apr 3;23(1):181–7.
 40. Ascierto PA, Agarwala SS, Ciliberto G, Demaria S, Dummer R, Duong CPM, Ferrone S, Formenti SC, Garbe C, Halaban R, Khleif S, Luke JJ, Mir LM, Overwijk WW, Postow M, Puzanov I, Sondel P, Taube JM, Thor Straten P, Stroncek DF, Wargo JA, Zarour H, Thurin M. Future perspectives in melanoma research "Melanoma Bridge", Napoli, November 30th-3rd December 2016. *J Transl Med*. 2017 Nov 16;15(1):236.
 41. Huang AC, Postow MA, Orlowski RJ, Mick R, Bengsch B, Manne S, Xu W, Harmon S, Giles JR, Wenz B, Adamow M, Kuk D, Panageas KS, Carrera C, Wong P, Quagliarello F, Wubbenhorst B, D'Andrea K, Pauken KE, Herati RS, Staupé RP, Schenkel JM, McGettigan S, Kothari S, George SM, Vonderheide RH, Amaravadi RK, Karakousis GC, Schuchter LM, Xu X, Nathanson KL, Wolchok JD, Gangadhar TC, Wherry EJ. T-cell invigoration to tumour burden ratio associated with anti-PD-1 response. *Nature*. 2017 May 4;545(7652):60-65.
 42. Teng MW, Ngiow SF, Ribas A, Smyth MJ. Classifying Cancers Based on T-cell Infiltration and PD-L1. *Cancer Res*. 2015 Jun 1;75[11]:2139-45.
 43. Compton LA, Murphy GF, Lian CG. Diagnostic Immunohistochemistry in Cutaneous Neoplasia: An Update. *Dermatopathology [Basel]*. 2015 Apr 8;2[1]:15-42.
 44. Tumei PC, Harview CL, Yearley JH, Shintaku IP, Taylor EJ, Robert L, Chmielowski B, Spasic M, Henry G, Ciobanu V, West AN, Carmona M, Kivork C, Seja E, Cherry G, Gutierrez AJ, Grogan TR, Mateus C, Tomasic G, Glaspy JA, Emerson RO, Robins H, Pierce RH, Elashoff DA, Robert C, Ribas A. PD-1 blockade induces responses by inhibiting adaptive immune resistance. *Nature* 2014 Nov 27;515(7528):568-71
 45. Herbst RS, Soria JC, Kowanetz M, Fine GD, Hamid O, Gordon MS, Sosman JA, McDermott DF, Powderly JD, Gettinger SN, Kohrt HE, Horn L, Lawrence DP, Rost S, Leabman M, Xiao Y, Mokatriin A, Koeppen H, Hegde PS, Mellman I, Chen DS, Hodi FS. Predictive correlates of response to the anti-PD-L1 antibody MPDL3280A in cancer patients. *Nature*. 2014 Nov 27;515(7528):563-7).
 46. Knol AC, Nguyen JM, Pandolfino MC, Denis MG, Khammari A, Dréno B. PD-L1 expression by tumor cell-lines: a predictive marker in melanoma. *Exp Dermatol*. 2018 Mar 5.
 47. Blank CU, Haanen JB, Ribas A, Schumacher TN. CANCER IMMUNOLOGY. The "cancer immunogram". *Science*. 2016 May 6;352[6286]:658-60.

ACKNOWLEDGEMENT, PERSONAL CONTRIBUTION AND CONFLICT OF INTEREST

Personal contribution

I actively discussed, planned and modified the doctoral plan with my supervisor and co-supervisors. I reviewed the literature for each topic. I personally performed almost all the experiments in this thesis (selection of the cases, immunohistochemistry stainings and evaluation, microdissection, RNA extraction, qPCR, statistical analysis, macrophage cell culture, ELISA, flow cytometry, viability assay, phagocytic assay, pathway analysis, TMA design and construction, image pre-processing, image analysis). I presented as posters and oral presentations these works at around 6 national and international congresses per year. I wrote all the manuscripts.

Conflict of interest statement

I was funded by the MEL-PLEX research training programme ("Exploiting MELanoma disease compLEXity to address European research training needs in translational cancer systems biology and cancer systems medicine", Grant agreement no: 642295, MSCA-ITN-2014-ETN, Project Horizon 2020, in the framework of the MARIE SKŁODOWSKA-CURIE ACTIONS).

Scientific acknowledgements

KU LEUVEN

Prof. Joost van den Oord gave a huge amount of research ideas to work on and reviewed every paper, abstract or presentation that I prepared during these years.

Jasper Wouters taught me all the molecular lab techniques I used in chapter I, III and IV.

Nathalie Volders performed all the immunohistochemical stainings with the automatic immunostainer from Chapter I and taught me how to use the autostainer and how to do manual immunostainings.

Marguerite Stas performed all the melanomas excisions of the Leuven material used in this thesis.

Prof. Stein Aerts did the NGS experiment in his laboratory and discussed the research ideas of chapter III, giving great inputs on how to interpret the NGS results.

Zeynep Kalender Atak performed the first part of the bioinformatics analysis (before the multiplex) of Chapter III of the thesis.

UNIVERSITÀ DI MILANO-BICOCCA

Prof. Cattoretti Giorgio invented and optimized the multiplex staining-stripping technique, bought part of the antibodies and all the reagents for it and reviewed the paper in chapter IV.

Maddalena Maria Bolognesi developed a pipeline for image pre-processing and image analysis and reviewed the paper in chapter IV.

Prof. Fulvio Magni and Clizia Chinello discussed and performed the proteomic part of chapter IV and reviewed the paper.

UC LOUVAIN

Prof. Nicolas van Baren contributed to chapter I and III, giving precious inputs, hosting me in his lab to do the gene scan analysis and the sequencing of the plasma cells and reviewing the paper.

Marjorie Mercier taught me and executed the Gene Scan Analysis and part of the topocloning of the plasma cells.

UNIVERSITY COLLEGE OF DUBLIN/ONCOMARK Ltd

Prof. William Gallagher discussed and gave essential inputs regarding chapter II.

Arman Rahman taught me cell culture, viability assay, phagocytic assay, and ELISA, giving me a great and efficient supervision, and reviewed the paper in chapter II.

Prof. Alfonso Blanco gave me an amazing theoretical and practical training course on flow cytometry, discussed the flow cytometry part and reviewed the paper in chapter II.

Esther Peralbo tutored me at the flow cytometer machine, being there when I was most lost.

Louise Elliott contributed to Chapter II, teaching me CD14+ monocytic peripheral blood cells separation.

Elizabeth Ryan discussed thoroughly the macrophage polarization concept giving me essential direction while planning and performing the experiments in Chapter II, and reviewed the paper.

PROTATONCE

Prof. Leonidas G Alexopoulos discussed the project of chapter II and III giving essential supervision that I had all the necessary material to complete these two chapters of my thesis

Angeliki Minia and Vicky Pliaka and Jan Roznac practically executed, explained me and supervised me for all the multiplex ELISA assay experiments with the Luminex in chapters II and III.

Asier Antoranz performed the multiplex-related part of the bioinformatic analysis in chapters II and III and all the bioinformatic analysis in chapter IV, explaining patiently to me every step and continuously discussing and exchanging ideas for the analysis, that brought the whole chapter to another level.

VARIOUS

James S Wilmott, Willeke AM Blokx, Daniela Massi, John F. Thompson and Richard A. Scolyer contributed with melanoma cases and review of the paper in chapter I.

Personal acknowledgement

The first *bedankt!* goes to my promotor **Prof. Joost van den Oord**, an outstanding dermatopathologist, researcher and human being, who welcomed me in Leuven for my thesis as a pathologist, offered me the best PhD that I could ever get, and then lured me to stay in Leuven forever just copying and paste the section “5- and 10-years career plans” from my personal career development plan into his job offer. His contribution to my PhD was enormous. Not only he is an explosive source of research ideas (first task learnt as a PhD student: manage the tsunami of “why don’t we do this...?!?” coming from my PI), he has an extensive research knowledge and experience, he taught me as much as I could learn in 3 years, he encouraged me to go to as many congresses as I could (paying for my “expensive 7 stars hotels”, as he liked to remember me) and he was always available for any PhD-related urgent task, but also he came in the lab almost every day to check regularly how I was doing, more than what I was doing, making me the most envied PhD student in the lab and making me spend 3 years of a really happy and careless PhD. Plus, he took care of teaching me some of the most sophisticated and elegant but also old-style and useless words in dutch while I was learning Nederlands. “Best promoter ever!”, they said. I agree. There is no best promotor than the one the leaves you his place upon retirement, even if it will not be possible for me to fill the gap that he is going to leave. *Hartelijke bedankt.*

I would like to thank all the members of my thesis committee that took time in reviewing and commenting my thesis, starting with **Prof. Lorenzo Cerroni**, that took a very special place in my career path, since he was my first, encouraging experience abroad and above all taught me the *real* meaning of dermatopathology. I would have been a “blind” dermatopathologist without the training in Graz, and he has always been extremely supporting allowing me to come back to Graz whenever I felt the need to refresh my dermatopathology background in a period in which I mainly focused on research. I am extremely thankful that he agreed to participate in the thesis defense, closing my “higher education” training path when it started, in Graz. Thanks to my co-promoters, **Dr. Nicolas van Baren**, **Dr. Jasper Wouters**, and **Prof. Cattoretti Giorgio**. They all helped me a lot at the very beginning, when I was starting to understand how science looked like, prof. Cattoretti first, a man with special foresight that saw something in my “*brain*” and put me on the path of research when I didn’t even know yet that I wanted to start an academic career. Then, prof. van Baren, welcoming me in his lab when I couldn’t do anything yet but giving me the best support theoretically, with his deep knowledge in immunology, and technically, through the teaching of the amazing **Marjorie Mercier**, that baby-sittered me in topo-cloning and sequencing. And finally Jasper, that taught me how to move in the lab and have fun with RNA extraction, qPCR and continuous jokes on how murderous Italian people can be. Thanks also to my PhD supervisors, **Prof. Patrizia Agostinis** (and **Dr. Enrico Redaelli** before prof. Agostinis stepped in) and **Prof. Patrick Matthys**, that gave very interesting comments, suggestions and guidance at every milestone achievement during the PhD process, and to **Prof. Biagio Eugenio Leone** and **Prof. Fulvio Magni** for taking time for being part of the committee. Prof. Magni tutored me together with **Dr. Clizia Chinello** in my first steps in the world of proteomic, offering me great supervision and expertise. There are not enough words to thank Prof. Leone, my mentor in pathology for exactly 10 years now. It was 2008 when I first asked him an internship that ended up in him teaching me my broad and solid base in pathology during endless days at the microscope. I also learnt from him how to approach adversities with solid calm and elegant resilience, that it’s not easy for someone with my temperament. He never opposed to my innate predilection for dermatopathology, showing me challenging cases and giving me skin biopsies in big amount since the beginning. Thanks to him I also learnt how to construct TMAs and to microdissect, two very important skills that gave me an advantage at the beginning of my PhD. But, most importantly, he gave me 10 years of priceless support.

My first arrival in Leuven was made special and very busy by finding myself in what I now call “the OLD TCWO lab”: everyone was Belgian, so I soon became the “foreign weirdo” of the lab. How to forget how noisy the OLD lab was! And how to forget amazing things like the weekly sport day (Volleyball? Handball? Basketball? Beach Volley? Football? Can do!), the Harry Potter Drinking Club, the venetian murder dinner and, above all, the terrible Gotcha game... So thanks to the best first impact with Belgian people that I could have, **An, An-Katrien, Annelies, Bart, Emilie, Gijs, Julie, Juan, Kathleen, Linde, Marcella, Nathalie, Olivier, Sarah, Sofie and Wilfried!** Then, I left for one year of secondments abroad, and when I came back everyone had finished the PhD and new people had come in the lab: the NEW TCWO! It’s a strange sensation when you do not know almost anyone in your own lab, where you are supposed to be a senior PhD student... but enthusiasm quickly kicked in and we started doing team building! Actually, we never finished to have a team building, since after the first one we decided to have weekly team buildings! So, **Annelies, Dena, Emanuela, Eef, Lien, Lukas, Marleen, Matthias, Pieter-Jan, Steffi, Veerle,** thanks for the lively atmosphere in the lab and all the good comfort food (and comfort evenings!) that we spend together!!! Thanks also in particular to the new PI that I found in the lab, **prof. Frederik De Smet**, who with a combination of high competence and intense enthusiasm for research is giving me a great model of how a young PI should be.

I had two very special experiences abroad during my PhD that I terribly enjoyed, mainly because I met outstanding researchers and entrepreneurs but above all incredibly lovely people. My first stop were 6 months in Dublin, a secondment for which I am very grateful because I had the occasion of discover the whole, beautiful Ireland, and to receive the guidance of the brilliant **Prof. William Gallagher**, who made sure I could get the best training in Oncomark and offered me the possibility to attend several congresses, in one of which I had the opportunity to be rewarded with a prize for the best poster. During my stay he put me under the guidance of **Dr. Arman Rahman**, a highly competent researcher and an amazing person that taught me efficiently a lot of different techniques, never letting me down when all my ELISA assays were failing at the beginning (what a patience!). Moreover, he put me in contact with **Prof. Elizabeth Ryan**, who taught me a lot on macrophages and put me in the hands of **Louise Elliott**, who spent with me a long afternoon and night, till 2 am, separating CD14+ monocytic cells from peripheral blood until we got ‘em all; and **Prof. Alfonso Blanco**, a renowned flow cytometry expert and talented teacher, but above all a very pleasant person to talk to, that offered me the opportunity to attend his flow cytometry course and to use the machines in the Flow Cytometry Core, thank God under the supervision of **Esther Peralbo**, who was very kind and always available to help. But it was the company, the support and the help of all the people of the lab that really made the difference on a everyday life basis, so thank you from the top of my heart to **Alex, Bo, Charles, Claire, Emer, Fiona, Nebras, Niamh, Romina, Ruth and Seodhna** (in particular Alex and Romina, our weekend in Athens was so fun and I enjoyed so much living with Romina for one month in Leuven!!!). And then I move to Athens, and there are not enough words to express how wonderful this second secondment was. There I spent 3 months in the company of another successful interpreneur, **Prof. Leonidas G Alexopoulos**, who put me in the conditions to be able to finishing 3 projects thanks to his technology and his amazing employees, **Angeliki Minia, Asier Antoranz, Jan Roznac and Vicky Pliaka**. They all became more than colleagues: me and Angeliki discovered how many wonderful things can a Slytherin and a Ravenclaw achieve if left alone in the lab with the right “machine”. And in particular Asier, who brought a revolution with his “bioinformatics magic” in my projects and, consequently, in my life.

But my PhD would have never been so successful and brilliant if I didn’t have the opportunity to join the most awesome Marie-Curie ITN ever, the **MEL-PLEX**. I am very grateful to prof. **Markus Morrison**, prof. **Dagmar Kulms**, prof. **Thomas Sauter**, prof. **Martin Leverkus**, prof. **Patrizia Agostinis**, prof. **Leonidas Alexopoulos**, prof. **Francesco Cecconi**, prof. **William Gallagher**, prof. **Walter Kolch**, prof. **Zvia Agur**, prof.

Hans-Uwe Simon and **Dr. Isabela Aparicio** for the incredible guidance, thorough teaching and good atmosphere that they infused in the project, and above all to my companions in the MEL-PLEX journey, **Vesna, Greta, Marco, Biswajit, Anna, Laura, Nicole, Sebastien, Jan, Valerie, Cristiano, Katja, Romina, Alba, Estefi, Neta** and **Ziva**, all of them very special, smart, easy-going, cheerful and somehow rightfully mad, (yes yes, I know that you want also to read “childish”) for the great harmony that was present since the first day we met. I will miss our great meetings.

I left for last my closest friends, because they know that I am a little bit of a weirdo, and I like to play it cool with them rather than tell them how important they are to me. So, now that *I really have to*, I want to thank what was known as the temible *Zumba Crew*. **Jasmine**, the last one standing of the Zumba crew, always ready for a gin tonic (and for a moving, a nice, relaxing, enjoyable moving!) and a very caring and sensible person; **Nicole**, oh God, how much I would have to say, starting from “Piacere di conoscerti, tu dormi a destra o a sinistra del letto?” and ending with “Dimmelo se non torni a dormire”, and in the middle terrific nights out, tons psychological support and laughter, and all the best tours of Leuven that have ever been made. And, least but not last, my doppelganger and my curse, same name, same middle name, 20 years knowing each other that means high school, university and PhD together; one neuron in sharing, one letter to distinguish us, no way to have us look normal when we are together; thanks, **Francesca Maria R**, for dragging me here shaping my destiny and for a lively co-abitation in Leuven! BDM, always.